Thermal Aging Time-temperature Effects on Low Voltage EPR/XLPE Insulated Cables

by

Farhana Hossain Priana

A thesis
presented to the University of Waterloo
in fulfillment of the
thesis requirement for the degree of
Master of Applied Science
in
Electrical and Computer Engineering

Waterloo, Ontario, Canada, 2022

Author's Declaration

I hereby declare that I am the sole author of this thesis. This is a true copy of the thesis, including any required final revisions, as accepted by my examiners.

I understand that my thesis may be made electronically available to the public.

Abstract

Low-voltage (LV) insulated cables are widely used in nuclear power plant environments in critical applications such as power transmission, control of equipment and instrumentation, and signal and data communication. Since the majority of nuclear power plants are nearing reaching their end-of-life, extending their operating life by up to 40 years is critical. As a result, assessing the health of LV cables has become a critical issue, as this is typically accomplished through destructive techniques.

Most cables are made with polymer insulation and jacket materials, which can become brittle, crack, or degrade over time due to exposure to harsh environmental conditions such as high temperatures, moisture, and radiation. Degradation of the properties of these materials, particularly the insulation, can result in a significant decrease in the overall health and performance of the cable, eventually leading to failure. Aging assessments are performed on cable polymers exposed to harsh conditions in service to identify and quantify the severity of degradation and determine when they will reach their end of life.

Cross-linked polyethylene (XLPE) and ethylene propylene rubber (EPR) insulated cables are among the most commonly used in the industry, and their use is continuing to increase. A variety of cable samples are thermally aged at 130 °C for different periods of time in this paper. These samples are subjected to frequency-domain dielectric spectroscopy (FDS) and polarization/depolarization current (PDC) measurements. The dielectric response characteristics of FDS and PDC are examined, and a variety of diagnostic "metrics" derived from variable frequency dielectric response and polarization and depolarization current data have been trended as a function of aging time.

Acknowledgements

I'd like to thank Professor Sheshakamal Jayaram for her unwavering support as a supervisor and for her invaluable advice along the way. I'd also like to thank Amin Gorji and Sarajit Banerjee for their unwavering support and guidance throughout my laboratory research. I'd like to thank my parents and my sister for patience, and support throughout my master's journey. A special thanks to my husband for always pushing and motivating me during my highs and lows.

Dedication

This is dedicated to my husband Shahriar Real, my parents, sister, friends, roommates who have continuously supported me during my research.

Table of Contents

List of Figures

List of Tables

Chapter 1

Introduction

Global population growth, combined with rapid development and urbanization, has increased energy demand, which is predicted to increase significantly in the decades ahead. In the future, this will significantly increase the world's supply of energy, particularly cleanly produced energy. Nuclear power generates about 10% of global electricity, according to the World Nuclear Association. According to studies, because nuclear energy is a low-emitting and low-carbon source of power generation, this could play a growing role in future energy supply as an eco-friendly way of generating reliable electricity on a large scale. As a result, existing and new nuclear power plants are critical to the global energy market. [4] Despite being a clean source of energy, nuclear power plants raise some concerns. A major environmental concern is the creation of radioactive waste, which can remain radioactive and hazardous to human health for long periods of time. As a result, in order to protect human health and the environment, radioactive wastes are subject to special rules concerning their handling and disposal. Nuclear waste's radioactivity decreases over time, and it is commonly temporarily stored before disposal. The majority of the waste is radioactively low. Spent reactor fuel, which is the used fuel that is no longer useful for generating electricity, is highly radioactive. It must be handled carefully when stored for disposal as the world currently lacks a permanent disposal infrastructure and a working waste management method for high-level nuclear waste.[5]

Nuclear power plants are expected to operate for longer periods of time in the future,

and more countries will build nuclear power plants as there is a growing demand for sustainable energy. Currently, there are several nuclear power plants operating around the world, and for supply of a reliable, affordable and low carbon emission energy, a high level of reliability and integrity is required for smooth and long-term operation. This is dependent not only on advances in waste disposal, reactor designs, and fuels, but also on the ability to maintain and monitor structures, systems, and components such as cables.

Nuclear power plants use a variety of cable types, including low, medium, and high voltage power cables, instrumentation and control (IC) cables, special cables, and general service cables. Depending on their location and application, these cables are exposed to a range of stresses as well as environmental factors throughout their nominal operating lifetime, including electrical, mechanical, thermal, radiation, and humidity. Among various thermal stressors, temperature and radiation are dominant and cables, particularly the insulation, can degrade as a result of these stresses. Furthermore, when cables are located in nuclear plant containments, they are subjected to much harsher environmental conditions, as the normal temperature and radiation levels inside the containment are higher than those in the rest of the facility. A containment is an enclosure that is typically built around a nuclear reactor to confine fission products that would otherwise be released into the atmosphere in the event of an accident. The containment building is the most distinguishing feature of a nuclear power plant.[6] Polymers are widely used as primary cable insulation and because these cables traverse long distances in power plants and are also deployed in confined areas they are subjected to further harsh conditions and stresses. [7][8]

Thermal aging occurs when cable materials are exposed to both normal and extreme thermal conditions. The majority of industrial sites have an ambient room temperature that causes the materials used for cable insulation and jackets to deteriorate over time. Localized high temperatures, radiating heat from nearby sources, or insufficient airflow, on the other hand, can cause significant damage rather quickly. In general, material aging causes a partial or complete loss of material ductility, making the material brittle and increasing the likelihood of cracking under mechanical pressures. In practice, mechanical integrity loss has been the leading factor that causes low-voltage cable failure, culminating in electrical integrity loss.

As such, polymeric-insulated cables, particularly cross-linked polyethylene (XLPE) and ethylene propylene rubber (EPR) cables, are widely used in power transmission and distribution networks in power plants, and cable failure can result in lengthy outages and significant financial loss for electrical utilities, as a result, cable function is essential in directly supporting safe operation. Therefore, insulation degradation is, without a doubt, one of the most common causes of cable failure over time, and it is a critical area of study and research as harsh conditions like high temperature and gamma-radiations can cause accelerated aging.[9]

Many nuclear power plants in operation today have used up their 40-year operating licenses and are approaching the end of their useful lives. Several studies have concluded that operating nuclear power plants beyond their expected lifespan while retaining stability and security is technically feasible. The majority of them have currently been given permission to extend their operating licences by 20 years and the possibility of further extending the duration to 80 years will greatly benefit the regulators and plant operators.[10] [11] Hence it is crucial that all safety-related components of the nuclear plants can operate under both normal and abnormal operating conditions. As a result, the aging-related degradation of power plant components is of great importance for the power industry.[10, 11, 12, 13, 14]

The following sections will provide a literature review, and background research for this thesis study on thermal aging time-temperature effects on low-voltage power cables. The areas discussed will include power cables overview, degradation and qualification techniques.

1.1 Power Cables Overview

Power cables can be classified based on materials and design such as oil impregnated cables, extruded solid cables and gas insulated cables. In oil impregnated cables the insulation used is oil impregnated paper or fluid filled paper. The first oil-paper insulated cable was invented by Ferranti for electric power transmission in 1891, and it was widely used for many years until the early 1960s. These cables are well established technology, and their service life has been well studied and understood and have been used in the industry for a long time. They provide excellent reliable economic insulation due to the combination of the electrical and mechanical characteristics of the liquid and paper. However, since core of the paper is filled with liquid, as compared to extruded cables where there are small cavities which give rise to discharge activities. In early 1960s when polymeric insulation, notably Polyethylene (PE) and Cross-linked polyethylene (XLPE), was introduced and oil-impregnated cables became less popular. Polymers are widely used as primary cable insulation and jacketing for long-term operation where rubber and plastic are the two most common types of insulation used in the industry. Plastic insulation can be further subdivided into Polyethylene (PE), Polyvinyl chloride (PVC), and Cross-linked polyethylene (XLPE), etc. and rubber insulation into Ethylene propylene rubber (EPR), Silicone, etc. Based on the studies in high voltage engineering and insulating dielectrics, there has been considerable technological advancement and extruded cables use solid insulation such as EPR and XLPE instead of oil insulation and they have similar structure to oil impregnated cables.[15]

Generally power cables are made up of a conductor, which is usually made of copper or aluminium, and an insulation layer. Copper is commonly used in cables due to its durability and electrical conductivity. Power cables are also classified according to their intended application, conductor material and insulation material. Low-voltage (LV), medium-voltage (MV), and high-voltage (HV) cables are the three types of electrical power cables based on their voltage levels. Low-voltage cables are typically designed for systems with voltage $\leq$ 1 kV. Medium-voltage cables, on the other hand, are intended for use in systems with voltages range of 5-45 kV and are most commonly identified by their insulation type, which is primarily XLPE and EPR. High-voltage cables, like medium-voltage cables, are

Figure 1.1: The structure of underground cables: 1, Insulation shield, 2, Insulation, 3, Conductor, 4, Jacket, 5, Conductor shield, 6, Metallic shield

made of XLPE and EPR and have voltage range of 45-150kV in North America. In utility applications, such as power plant to substation connections, high-voltage cables are used. Common cable components include a conductor, insulation, jacket and field limiting layers which is typically made of semiconducting materials. For corrosion protection, they can also have metallic coatings and outer coverings. The conductor is typically made of copper or aluminium, with polyethylene or cross-linked polyethylene insulation. The cable's protective jacket shields it from physical damage, electrical interference, and corrosion. As a result, underground power cables are durable and dependable.

1.2 MV and HV Cables Overview

A cross-section of two main types of MV cables is shown in Fig 1.1, on the left is a 15kV tree-retardant cross-linked polyethylene (TR-XLPE) and on the right is a 15 kV pristine MV ethylene propylene rubber (EPR) insulated cable. The following components can be identified in the structure of the cables: conductor core, semi-conductor screen on the conductor (conductor shield), insulation, semi-conductive screen on insulation (insulation shield), metallic screen, and jacket or sheath.

The cable conductors are typically either compacted stranded or solid construction. Stranded conductors can be made up of several layers of spiral wound wires that have been compacted together. In order to prevent electrical short circuits, insulation must be provided around the conductor. Today, XLPE is the most used material, whereas EPR is more flexible than XLPE but not as effective at reducing circuit losses as XLPE. Cables for medium and high voltages typically require three layers of extruded material to form the insulation system, according to various standards. These layers are the conductor screen, insulation, and insulation screen.

The conductor screen is made up of a layer of black semi-conductive cross–linked compound that is typically less than 1.0mm thick. It also serves as the interface between the conductor and the insulation. Because the conductor's external surfaces may not be smooth, especially for stranded conductors, this layer provides a smooth surface at the same potential as the conductor to keep the electric field consistent all the way around the surface. Without this layer, any small peaks or troughs could cause electrical energy concentrations, resulting in small arcs that could erode the insulation layer and cause cable failure over time.

After the conductor screen, comes the insulation layer, which insulates the conductor at a voltage from the outer screens, which are at ground potential. The insulation is thick enough to withstand the electric field under rated and transient operating conditions. The insulation is surrounded by a semi-conductive screen which plays the role of offering smooth transition from the insulating medium to the grounded metallic screen. This is a layer of black cross linked semi conductive compound of approximately 1mm thickness and can be fully bonded to the insulation layer.

The metallic screen's primary function is to cancel out the electric field outside of the cable. It also acts as a radial barrier to prevent humidity from penetrating the cable insulation system, as strong electric fields, if present, can deteriorate the insulation, a process known as "water-treeing."

The outermost layer jacket protects the metal components from corrosion and humidity, insulates the metallic screen from the ground, and shields the cable from mechanical stresses.

1.3 Low-Voltage Cables Overview

Most low-voltage cables are unshielded and multipolar, and they are typically housed in metallic cable trays. Figures 1.2a and 1.2b depict cross-section of commonly utilized cables in nuclear power plants.To allow for flexibility during installation, conductors are typically made of strands. Like MV and HV cables, their conductor material is copper, and it is frequently coated with tin-lead alloy, pure lead, nickel, or silver to reduce oxidation and allow operation at higher conductor temperatures. A jacket is also included to protect against mechanical damage during installation as well as any stresses that may occur during operation. The most commonly used insulation materials in LVs are XLPE and EPR.[16]

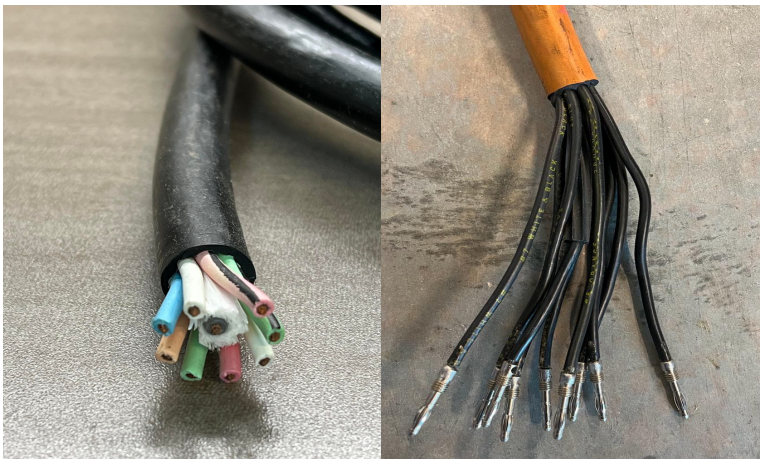

(a) 9/C XLPE Cable (b) 9/C EPR Cable

Figure 1.2: 600V LV cables

Electrical cables, as is well known from various works, use polymers for insulation and jackets, with polyethylene (PE), ethylene-propylene copolymer (EPR), and silicone rubber (SR) being the most commonly used materials for insulation bases, and chlorosulfonated polyethylene (CSPE) and polyvinylchloride (PVC) being the most commonly used materials for jackets (PVC)[17]

Cable manufacturers employ formulations to enhance polymers used in nuclear power

facilities fire resistance. They are created by combining the basic polymer with additive which are specific chemicals, fillers, antioxidants, retardants, plasticizers, accelerators, dyes, and vulcanizing agents for heat and radiation stability to improve their electrical and physical properties. During the formation of polymeric materials, additives such as brominated and chlorinated compounds and antioxidants are used. Brominated and chlorinated compounds provide fire resistance properties and slow their rate of combustion. Antioxidants, on the other hand, are used because of their ability to delay the onset of polymer degradation and greatly extend polymer service life.[18, 19]

The additives utilised may deplete from the polymer, meaning from the insulation layer to the environment, due to chemical reactions. As a result, the oxidation process is accelerated, leading to alterations in the macromolecular structures. Electrical, mechanical, physical, and chemical properties will deteriorate as a result and the aging characteristics of insulating materials are heavily influenced.[7]

The chemical composition of insulation includes an extensive number of constituents of varied natures and concentrations due to the addition of several components. Cable producers may select the most appropriate compounds from a wide range of additives by taking into account their properties in terms of stability and compatibility. Hence, insulation exhibits the most substantial degradation and is directly subject to the thermal aging of all the sub-components of low-voltage cables utilised inside the containment at nuclear power plants.

1.4 Degradation and Qualification Techniques

Material aging is defined as the irreversible change in at least one property of a material exposed to its surroundings during its operational life, which is always induced by a change in the physicochemical structure. The principal aging mechanism is the degradation of polymer chains, which has a direct impact on the material's service performance. Key factors that contribute to polymer breakdown are changes in the chemical structure of the polymer sample, which produce early chemical degradation, physical changes in the polymer, and the presence of traces of unstable structures such as impurities and additives.

The common mechanical, thermal, and electrical property indicators for aging are as follows: elongation at break and tensile strength for mechanical; oxidation induction, degree of crystallinity, and infrared spectrum for thermal; and space charge quantity and dielectric strength for electrical properties.

The nuclear cable industry relies heavily on manufacturers' qualification data to assess cable performance and with nuclear power plants and extensions underway, researchers are looking for new ways to monitor cable health. To effectively measure cable health one single technique is not sufficient rather a few techniques can better provide an indication of and degree of cable degradation. Cable condition monitoring can be divided into two methods: destructive and non-destructive., which can include physical, mechanical, chemical and electrical tests.

1.5 Destructive Condition Monitoring Techniques

1.5.1 Tensile Testing

Tensile testing is one of the most often used mechanical tests. Tensile tests offer critical mechanical parameters such as elongation, stiffness, breakpoint strength, and others. Polymer degradation due to aging creates structural changes that threaten embrittlement and physical structure integrity concerns. Tensile testing, specifically elongation at breakpoint, is a generally established technique.

Elongation at break (EaB), commonly known as fracture strain, is the ratio of the test sample's modified length to its initial length following breakage. It displays the capacity to withstand shape changes without cracking. The acceptable end-of-life criterion is 50% of the absolute value of the EaB and is usually the primary indicator of aging degradation. However, it was observed in various works that the EaB degraded faster than other measurable properties and for most polymers it tends to decrease gradually with degradation time, hence in many studies only a slight change was observed in the initial stages of aging compared to the last quarter of the total life. With techniques like this it is not possible to monitor regularly and detect early defects as it is a destructive and intrusive method and generally requires larger sample sizes.[20, 21, 22]

In [23] XLPE samples were studied under accelerated electrical-thermal aging in different aging stages at 90, 103, 114 and 135°C. The cable samples were extracted in five phases based on aging time and tested for breaking elongation, as well as tensile strength, dielectric constant, and dielectric loss. The results showed that the breaking elongation values in the final stage at 103, 114, and 135°C differed little from the values before aging. Similar research on the physical properties of XLPE insulation material during thermal aging revealed a trend of reduction following a minor increase as aging progressed.[24]

Important test factors such as sample size, tensile test speed, and temperature might lead to misleading or inconsistent test findings. As a result, it is critical to specify the test methodology and maintain track of these characteristics in order to allow for test reproducibility. Another essential step that might affect tensile testing results is sample preparation; for example, extracting the conductor from a cable sample can harm the insulation, particularly the most seriously damaged.[22]

1.5.2 Oxidation Induction Time

The oxidation induction time (OIT) is a widely used measure for determining polymer heat stability. In OIT, samples are heated at a steady rate under the influence of inert gas to a predetermined temperature before being exposed to oxygen. Finally, the material is kept at a steady temperature until the oxidation reaction occurs. The OIT value is the time elapsed between the first oxygen exposure and the commencement of oxidation. Fig. 1.3

depicts the progression of a standardised OIT time measurement using the DSC method. Oxidation is observed as an exothermic peak and in most OIT studies, just the onset of the peak is recorded. Although OIT is a destructive test, it only requires a little amount of sample, i.e. 10 mg. However, several factors may influence OIT outcomes, including gas atmosphere, test temperature, static OIT time, sample size, and surface area in contact with the sample pan. [25, 26]

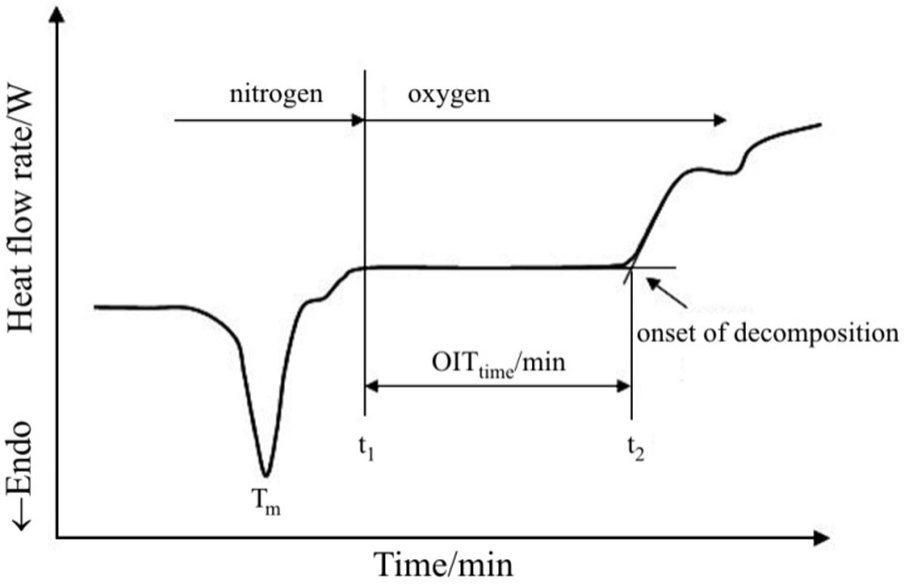

Figure 1.3: Schematic of OIT sequence [1]

1.5.3 Oxidation Induction Temperature

Oxidation Induction Temperature is similar to that for OIT, the sample is heated with oxygen, and oxidation is characterised by an increase in exothermic heat flow, which accelerates as the temperature rises. The OITP normally falls as the extent of degradation increases. Fig. 1.4 depicts the standard sequence for an OITP test.

Because the OIT and OITP are connected to antioxidant concentration, they may be useful indicators for monitoring cable insulation degradation. However, because OIT

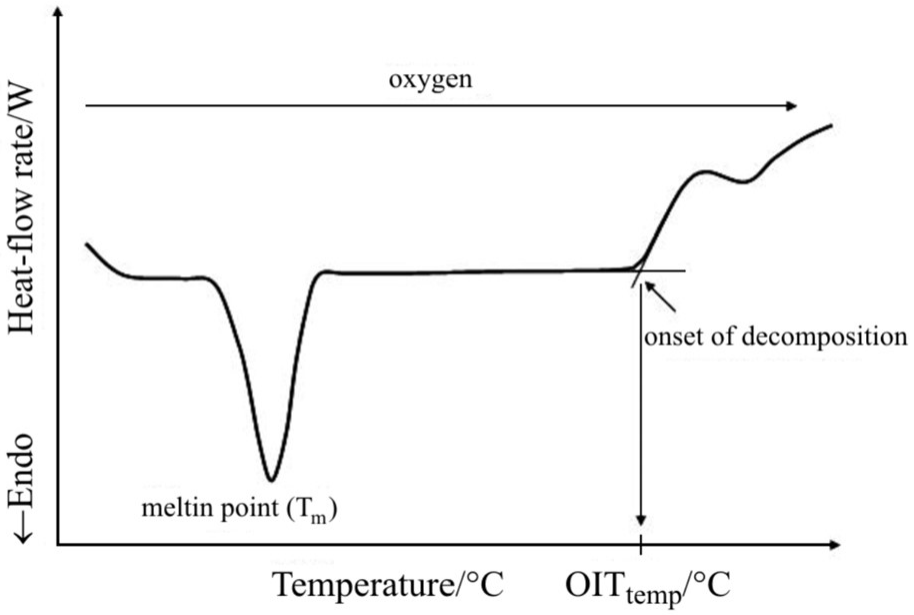

Figure 1.4: Schematic of OITP sequence [1]

measurement does not provide an absolute indicator of cable condition, the end-of-life cannot be specified. As a result, the OIT values for cable insulation that have been subjected to aging monitoring have been associated to elongation at break using correlation curves. [26, 1, 27]

In [26], OIT measurements from DSC and elongation at break measurements from tensile tests were performed, and a correlation curve depicting the dependence of OIT vs. elongation at break was produced, which can later be utilised to analyse the real state of already placed cables.

1.6 Non-Destructive Condition Monitoring Techniques

1.6.1 Fourier Transform Infrared Spectroscopy (FTIR)

Fourier Transform Infrared Spectroscopy (FTIR) is a well-known technique for studying the molecular structure of materials that detects chemical bond vibrations. Infrared radiation is directed towards the target sample in order to determine the wavelengths at which the material absorbs the radiation as well as the intensity of absorption. The wavelengths absorbed by the sample are typical of the chemical groups present, and the intensity reflects the concentration of the chemical group responsible for absorption. This technique requires a high level of ability, experience, and knowledge in the operation and analysis of FTIR spectroscopy, and polymer chemistry.[28]

In studies like XLPE and EPR, cables have been successfully characterised, providing useful understanding of deterioration mechanisms. Based on FTIR analysis of pristine and aged XLPE insulation cables, it was clear that aging caused more significant oxidation. This method has the benefit of allowing samples to be acquired from extremely small portions of cable, making it a non-destructive technique. Because different manufacturers utilise different polymer compositions, the results obtained will differ. As a result, for each material or sample, absorption or transmittance data at specified relevant peak wavelengths can be used as a baseline to analyse the effect of aging. However, under extreme environmental circumstances, an oxidation gradient may form at the sample surface, causing the spectroscope to detect more oxidation than the average bulk value. [29, 30]

1.6.2 Insulation Resistance (IR)

Insulation Resistance (IR) testing is a typical troubleshooting technique to localize issues by assessing electrical parameters. A short DC voltage is applied to the test cable, and the DC current is measured. The insulation resistance is given by the ratio of the applied voltage to the measured current. A shortcoming of this method is it cannot detect insulation damage or any other degradation until a very severe damage or deterioration occurs. These tests better serve as a pass-fail indicator of functionality. [31]

1.6.3 Space Charge Measurement

XLPE and EPR are dielectric polymers which can be polarised by an applied electric field from their equilibrium position. In their energy band, they have various depth traps to capture space charges. As a result, a lot of space charge which is essentially free charge might build up in the traps. Under high voltage DC electric charges can be injected into the insulation and can be trapped, this may lead to space charge accumulation in the insulation that is dependent on the depth of the traps present in the material. Measurement of space charge accumulation in the polymeric material is a non-destructive approach and can be carried out in different ways.

Researchers have commonly used isothermal relaxation current (IRC) and thermally stimulated depolarization current (TSDC) to measure trap charge density and depth as de-trapping current can be used to calculate the density of the trapped charge as well as the trap depth. The TSDC approach necessitates increasing the temperature of the sample over a wide range and the complete test system is difficult to adapt to the actual size of the cable. The IRC approach has mostly been utilised to separate the depletion current from the dipole relaxation current.

This method is often used for high-voltage and medium-voltage cable insulation, which is subjected to high fields and where space charge accumulation might produce electric field distortion in the insulation bulk. In [32] a 10kV XLPE-insulated cable was subjected to combined electrical-thermal stress at an AC voltage of 26.1 kV and three temperatures: 103°C, 114°C, and 135°C, and changes in mechanical, physiochemical, and dielectric strength were examined at various stages of aging. Because the chemical bonds of the cable insulation material are broken down as the XLPE cable ages, the experimental results revealed a decreasing trend in mechanical strength and oxidation induction time. The AC space charge, on the other hand, exhibited a gradual accumulation trend with aging time.

Space charge accumulation, on the other hand, does not constitute a problem for low voltage cable insulation. This method, however, can be utilised in both circumstances to detect morphological changes in a material induced by aging.[32, 33, 34, 35]

1.6.4 Dielectric Spectroscopy

Dielectric spectroscopy is another most popular technique among researchers to study the dielectric properties of insulating materials as a function of time and frequency based on the interaction of electric field with the material. Material responds to electric fields by dispersing its component charges to some extent. Positive charges are drawn to the negative electrode and vice versa. This is referred to as polarization. The real dielectric constant, also known as the real part of complex permittivity, is a measure of the material's polarization, whereas the imaginary relative permittivity is a measure of dielectric losses. The main electrical parameter is the complex permittivity which accounts for the polarization and is an important property of dielectric materials, depending on the frequency of the field applied, humidity, temperature and is correlated to dielectric loss. The dielectric loss tangent represents the quantitative dissipation of electrical energy caused by physical processes such as electrical conduction, dielectric relaxation, dielectric resonance, and loss from non-linear processes.

Dielectric spectroscopy, like space charge measurements, can indicate bulk degradation caused by thermal and electrical aging which can cause variations in the material's polarization properties, particularly the imaginary part of permittivity, which is correlated to dielectric losses. Measurements of dielectric spectroscopy can be performed on any type of insulation system and in the case of multipolar non-shielded cables, the measurement can be accomplished by treating each couple of conductors as electrodes.

Polarization-Depolarization Current (PDC) and Frequency Domain Spectroscopy (FDS) are two most used dielectric spectroscopy methods. Generally, capacitance and dielectric loss are measured as a function of frequency and polarization and depolarization currents measured as a function of time.[36]

Polarization-Depolarization Current (PDC)

The PDC method is commonly used for non-destructive insulation condition detection of cables and oil-filled transformers. It is one of the widely used dielectric methods based on the notion that the charge in the trap is more likely to transfer to the conduction band in

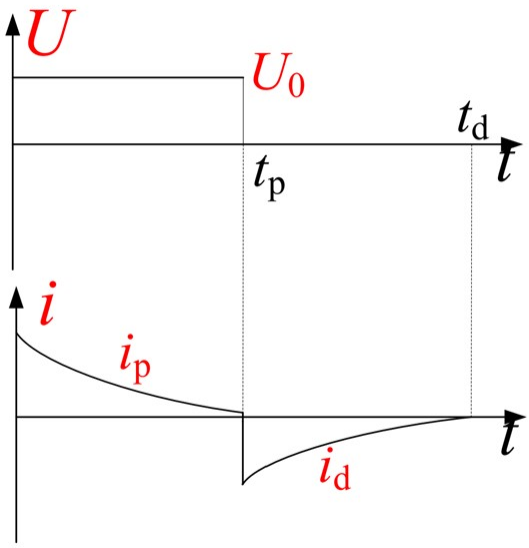

Figure 1.5: Ideal polarization and depolarization currents under DC voltage [2]

the presence of a DC electric field. Polarization current is the current measured by applying a DC voltage to the insulating material and once steady state is reached the DC voltage is taken off and the value of the depolarization current is recorded until it reaches negligible values. Fig. 1.5 shows the principle behind PDC measurements where DC voltage (U_0) is applied, and polarization current i_p and depolarization current i_d is measured to analyze the insulation conditions.

Polarization current is made up of conductive current caused by the material's inherent conductivity and current caused by polarization processes such as electronic polarization, dipolar polarization, and interfacial polarization. There is no conductive current in the depolarization current and taking the influence of the power source into account, the polarization current and the first 10 seconds of depolarization current are often ignored. [37]

PDC has been employed in MV and HV cables, and studies have shown that a considerable change in depolarization current indicated progressing insulation damage, which could imply an increased likelihood of failure. [38, 39, 40] An accelerated aging experiment was carried out [39], and tests were carried out to evaluate the aging of the cable subjected

to water tree at various aging durations using the PDC method. Water tree is one of the primary causes of MV and HV XLPE cable insulation deterioration. When the charging time is long enough, the polarization and depolarization currents can be used to compute the conductivity of the cable sample. The measured conductivity increased gradually with the passage of time.

Frequency Domain Spectroscopy(FDS)

In general, frequency domain spectroscopy (FDS) involves measuring capacitance, real permittivity, and dissipation factor, or the dielectric loss as a function of frequency. FDS measurements can be used to assess dielectric loss (tanδ) at low and high frequencies. This technique is based on the fact that dielectric loss is a dimensionless property of a dielectric that is determined by the structure of the insulator. As a result, structural changes caused by aging should have an effect on dielectric loss.

In [41] XLPE cables were thermally aged and studied using FDS, which included measurements of capacitance, real permittivity, and dielectric loss. The findings of this research indicate that dielectric loss increased significantly with aging time, and capacitance showed a slight increase while the real permittivity was almost constant when frequency was greater than 1Hz.

It was also discovered that the real component of permittivity increases with increasing test temperature at frequencies less than 1 Hz. Hence, the dielectric loss will also increase as the test temperature rises. Meanwhile, as the test temperature was raised, the minimum dielectric loss value shifted to a high frequency region.

It was also shown that capacitance and the real part of permittivity were more susceptible to temperature variation, implying that temperature is an important aspect to consider when utilising the FDS method to diagnose cable insulation.

During the investigation in this study, it was found that some test findings were irregular due to unforeseen damage during sample preparation or nonuniform heating inside the oven. In this experiment, aluminium tape was applied to cover the cable surface as a measuring electrode, and Vaseline was used as an adhesive. The experiment employed a

three-electrode test device, and the cables were aged for a total of 120 hours and 240 hours. Because the XLPE cables had significant hysteresis, the samples were short-circuited prior to the experiments. As a result, it is critical to repeat the measurement numerous times and to carefully prepare the samples.

Several studies concluded that dielectric spectroscopy is useful and practical for assessing the aging of XLPE and EPR cables. A study identical to [41] was carried out in [42], where 20mm MV XLPE cables were examined. With increasing aging time, a similar trend in dielectric loss and actual permittivity was observed. Furthermore, it was revealed that the dielectric loss and real permittivity displayed good regularity in high frequency areas, however the regularity of these curves varied in low frequency areas.

1.7 Research Objectives

The previous discussions evaluated current knowledge on cable monitoring approaches for nuclear power reactors, namely XLPE and EPR cables. Currently, the nuclear industry relies heavily on manufacturers' qualification data to ensure adequate cable performance, and very little testing is done to ensure that cables remain reliable for long-term service, with the exception of cable troubleshooting to locate and solve problems in conductors, connectors, and end devices. With attempts to extend plant life presently underway, cable monitoring techniques are taking centre stage at utilities and regulatory bodies alike. Significant research has been conducted in connection with plant life management and plant life extension to address the aging of the reactor vessel and its internals, pipes, and civil structures. As cables are essential for maintaining and extending plant life, it is imperative to monitor how they are aging so that they may be replaced before reaching the end of their useful life.

As insulated cables used in nuclear power plant environments in critical applications have been and continue to be subjected to qualification and research accelerated thermal aging projects in which mechanical 'end-of-life' conditions for different aging time-temperature combinations are determined, these experiments enable the determination of estimated remaining and absolute physical life spans for cables aged at various temperatures by evaluating 'Arrhenius' relationships, as described in standards such as IEC 60216. The significance of such information gives vital information for cable manufacturers and clients to calculate and meet standards for a minimum "qualified life" for cables provided for use in critical end-use applications with specified or known environmental operating temperatures. Furthermore, when combined with operating temperature information, it can be utilized for the aging evaluation of in-situ field-aged cables, which can be selectively removed and subjected to destructive physical mechanical testing such as tensile strength in some circumstances.

Variations in dielectric characteristics using advanced dielectrical diagnostic tests such as Low Frequency Dielectric Spectroscopy (LFDS) and PDC measurements have been tracked with respect to varying rates of accelerated thermal aging in very few published investigations. Such data would be a starting point for determining Arrhenius relationships

and estimating remaining life from in-situ field aged cables, which inherently age at varying temperatures, using non-destructive electrical measurements such as LFDS and PDC, which do not require sample removal for destructive testing and can represent global cable insulation rather than localised areas. The research would thus contribute significantly to increasing the value of applying LFDS and PDC-based techniques to the condition monitoring of in-situ LV cables, particularly in critical environments such as nuclear power plants, which are regarded as a highly valuable source of meeting carbon-free emission targets and thus life extension in most jurisdictions.

Cable specimens will be aged to estimated 'end-of-life' conditions based on published parameters from accelerated aging tests typically performed as part of insulation qualification. The experimental results will be used to create time-temperature condition monitoring curves for various LV cable EPR/XLPE insulation types, utilizing selected LFDS and PDC parameters.

1.8 Scope of Research

The following items summarize the scope of this research:

- Small 10" single core pieces are extracted from 2 types of EPR and 1 type of XLPE multi-conductor unshielded low-voltage cables utilized in existing nuclear generation plants.
- The samples are shielded and prepared for three-terminal electrical dielectric characterization tests in accordance with ASTM D150.
- Un-aged samples from each type will be initially characterized using AC low frequency dielectric spectroscopy (LFDS) and DC polarization / depolarization current measurement (PDC) using a Dielectric Response Analyzer
- Key electrical parameters such as real permittivity(C'/ϵ'), complex permittivity (C"/ϵ''), and dielectric loss (Tanδ) are extracted from these measurements, with respect to frequency (or time).
- The baseline sample measurements are repeated at multiple environmental / ambient temperatures between 25 - 80°C, representing average and elevated temperature environments within operating plants.
- Samples were aged at 130°C in thermal aging oven, representing a common accelerated aging temperature utilized in cable manufacturer environmental qualification and/or published or ongoing research studies.
- At 10 intervals during the aging process, samples were extracted from each insulation type, prepared for three-terminal dielectric characterization tests as described above, and subjected to the dielectric measurements utilized during the baselining process described above at ambient temperature.

1.9 Thesis Outline

The thesis is organized as follows:

- Chapter 1 reviews cable condition monitoring techniques and thermal aging time-temperature effects on power cables
- Chapter 2 covers the experimental setup and materials used and preparation of the test samples.
- Chapter 3 presents the frequency domain and time domain results - FDS and PDC
- Chapter 4 discusses the experimental results, and its implications to low-voltage cable for different aging intervals
- Chapter 5 gives a summary of the research, conclusions, and suggestions for future work in the area of application of advanced electrical diagnostic tests for monitoring thermal aging of cable insulation

Chapter 2

Experimental Setup and Sample Preparation

2.1 Accelerated Aging

Accelerated aging is a mechanism that uses aggravated circumstances such as heat, humidity, oxygen, radiation, and, etc. to accelerate the typical aging processes of test objects or materials. Because normal operating conditions would take a long time to age insulating materials and it is impractical to acquire aged samples from the field for evaluation and assessment, the researchers used accelerated aging techniques to simulate the stresses and environmental factors that the cables are most likely to experience while in service. Accelerated aging is also commonly associated with the application of increased electrical stress (voltage), as well as an increase in temperature. Accelerated aging at elevated temperatures is most typically used to artificially speed up the aging process in order to evaluate the impact of various strains on XLPE and EPR power cables.

2.1.1 Convection Oven

The research conducted is based on accelerated aging to simulate stresses identical to real life exposure. Samples of XLPE and EPR low voltage cables were placed inside a

mechanical convection oven for thermal exposure and were hung from a tray in the oven allowing ample space for uniform air circulation.

Figure 2.1: VWR 1370 FM Convection Oven

A mechanical convection oven is also known as a forced air oven which works by forcing warm air around the oven chamber with the assistance of a blower fan. Hot air travels through a duct system creating a uniform distribution of warm air within the chamber and is insulated from outside. Fig. 2.1 shows the VWR Signature Horizontal Airflow 1370 FM convection oven used for aging in this study which offers excellent temperature uniformity with the true horizontal airflow design, heated air is directed into the ductwork on the right side of the oven. The slightly pressurized air escapes through the small perforations

Table 2.1: Convection Oven Specifications

Model	**Rated Voltage (V)**	**Temperature Range (°C)**	**Uniformity (°C)**
VWR 1370FM	110V	40°C to 240°C	± 1.5°C @ 150°C

in the chamber wall, flows across each shelf picking up moisture, and is gently suctioned through large openings on the opposite chamber wall. The built-in microprocessor control that ensures stable accurate temperature control without temperature overshoot. It also has a digital electronic timer that has the capability of automatically turning off the oven at the end of an application cycle. It also has the ability of holding temperature and time set points. The model can be used for three main purposes: drying, baking and curing. By positioning the damper on the exhaust port accordingly, the three types of applications can be achieved. The exhaust port is 3-inches in diameter, further aiding in drying time. Table. 2.1 contains the specification of the oven used.

2.1.2 Aging Specifications

Aging temperatures ranging from 90 - 130°C, represent a range of common accelerated aging temperatures utilized in cable manufacturer environmental qualification and/or published or ongoing research studies [43]. The aging temperature was set at 130°C with a tolerance of ± 2°C and between 100 and 200 volumetric air changes per hour, which was ensured by positioning the damper on the top exhaust port. The temperature was recorded by inserting the measuring probe in the oven from the top exhaust of the oven. Fig.2.2 shows the temperature variations recorded during continuous aging and it was found to be consistent and within the tolerance of ± 2°C.

The aging was interrupted at regular intervals to extract samples from each insulation type to perform electrical testing of the cables and remove samples for material and electrical characterization. The intent of aging was not to relate accelerated aging to actual life in the plants but to achieve information at different levels of thermal degradation.

Figure 2.2: Temperature Variations

Table 2.2: Aging interval and test durations

Interval	Aging Hours
1	100
2	200
3	300
4	400
5	600
6	800
7	1000
8	1200
9	1400
10	1600

Samples were extracted at 10 spaced intervals during the aging as depicted in Table 2.2 with respective hours.

Fig.2.3 shows sample cables extracted from whole cables and prepared for aging to be placed in the oven. The following gives an overview of number of insulation, samples and aging intervals and total number of cables aged and extracted. At the end of each aging interval 15 cables were extracted.

- Insulation types = 5
- Aging intervals = 10
- Sample number for each Insulation type & interval = 3
- Total number of samples aged =150

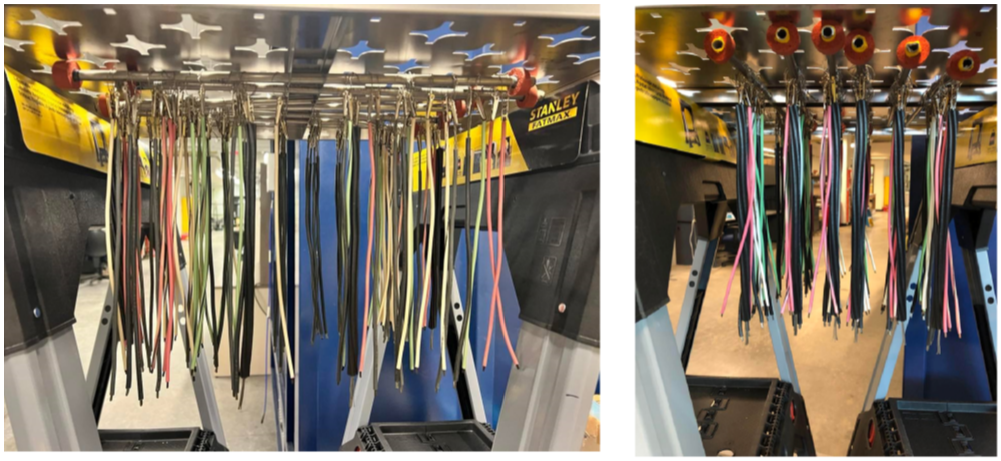

Figure 2.3: Arrangement of cable samples for aging

2.2 Materials and Sample Preparation

2.2.1 Cable Specimens

The selection of cables presents a wide range of different cable types used in power plants. Experimental studies have been carried out on cable specimens that were extracted from cables used in the industry.

Ethylene-Propylene Rubber (EPR)

Two types of EPR specimens have been extracted from the following LV cables:

- **OKONITE 9/C 12 AWG 600V EPR HYPALON/CSPE**: A 9/C cable manufactured in 1980 and rated 600V. Its construction includes 9 conductors #12AWG (3.31mm2), ethylene-propylene rubber (EPR) layer insulation (OKONITE-OKO) and Hypalon CSPE jacket. Fig.2.4 shows the cross-sectional view of the cable used to extract the specimens and in the later sections these samples will be called **EPR-OKO**.

Figure 2.4: Cross-Section of 9/C EPR OKO Cable

- **KERITE 15/C 12 AWG 600V FR-FR**: A 15/C cable manufactured in 1977 and rated 600V. Its construction includes 15 conductors #12AWG (3.31mm2), ethylene-propylene rubber (EPR) layer insulation (KERITE-KER) and Fire-Resistant jacket. Fig.2.5 shows the cross-sectional view of the cable used to extract the specimens and in the later sections these samples will be called **EPR-KER**.

Figure 2.5: Cross-Section of 15/C EPR KER Cable

Cross-Linked Polyethylene (XLPE)

The three types of XLPE specimens were extracted from a control cable, multi-conductor, overall shield low-voltage cable:

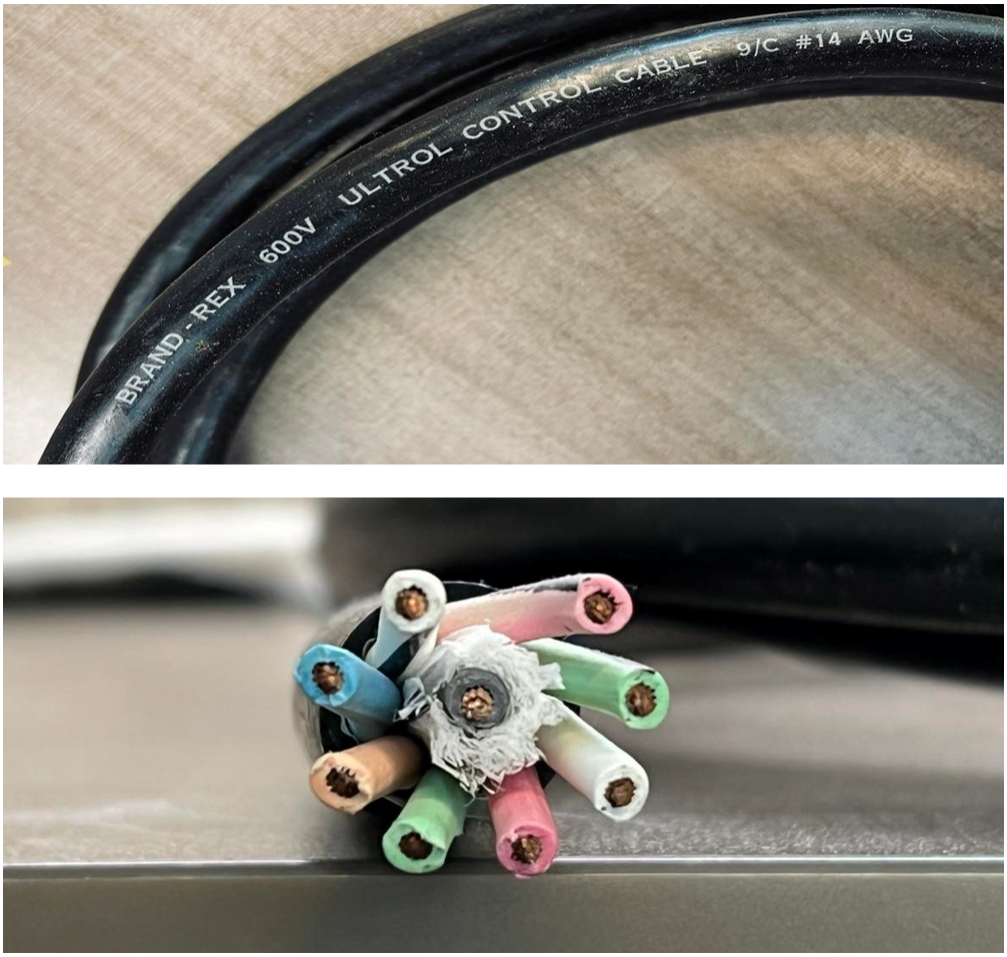

Figure 2.6: Cross-Section of 9/C XLPE Cable

- **Brand Rex 600V Ultrol Control Cable 9/C #14 AWG**:A 9/C cable rated 600V. Its construction includes 9 conductors #14AWG (2.08 mm2), Cross-Linked

Polyethylene (XLPE) layer insulation and jacket. Fig.2.6 shows the cross-sectional view of the cable used to extract the specimens of XLPE samples. In the later sections these samples will be called **XLPE-RED, XLPE-GREEN, XLPE-WHITE**.

2.2.2 Three-terminal Sample Preparation

This section contains the detailed sample preparation method for short LV cables in accordance with ASTM D150 [3]. Small approximately 0.254m single core samples are cut from the above mentioned EPR and XLPE unshielded low-voltage cables. After precisely procuring the samples, they were cleaned vigorously with alcohol to remove any organic residual, dirt, stain and oil, followed by wiping the cable surface with distilled water. The cables were then pat dry with paper towel and further left to air dry naturally. This ensure there is no residual alcohol on the cables surface that would later cause interferences in the dielectric characterization. To prepare the sample for three-terminal tests it is important to prepare them carefully and precisely as they will be placed in an Enclosure Box and make connections with the measuring instrument for accurate characterization.

The ends of the cleaned cables were then stripped for approximately 5mm on both the ends to expose the core which would later be connected to the high voltage output of the instrument.

To create the path for the return current electrode copper tape was cut according to the following equation: Length of Copper Tape = Length of Cable – 0.0381m. Therefore, for our samples copper tape of length 0.2159m was wrapped around the cable by leaving 19.05mm on both ends, dedicated for the guards. The width of the 0.2159m copper tape is such that it covers the entire diameter of the insulation jacket leaving no exposed insulation. At this point it is important to make sure that the copper tape is in contact with the cable surface properly leaving no air bubble which could later cause leakage current, and the length of the 0.2159m copper tape on the cable surface is fine-tuned cautiously to create a constant and precise length of return current for all samples for consistency. Fig.2.7 shows the picture of a cable at this stage of preparation.

A 6.35mm wide teflon sealant tape was wrapped around the cable jacket right after the end of the return current electrode for about 3 to 5 turns so that is within the height of the

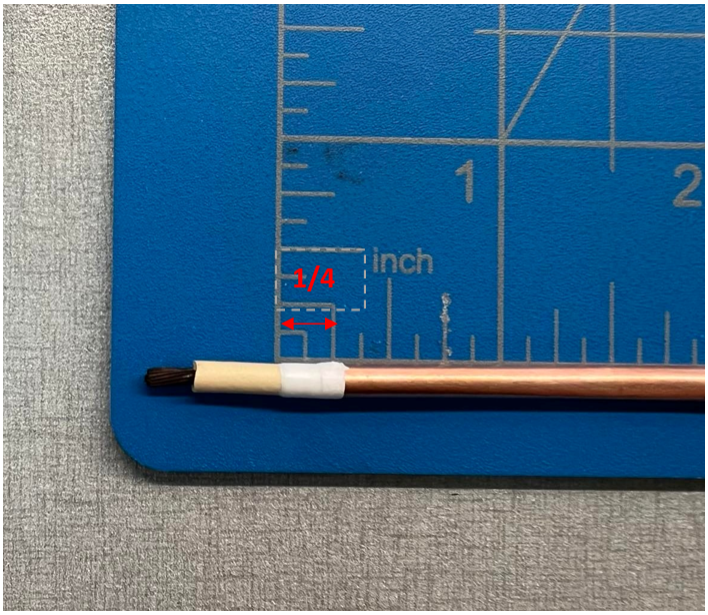

Figure 2.7: Teflon Sealant Tape wrapped around right after the end of the Return Current Electrode

copper tape. In Fig.2.7 the cable with the teflon wrap can be found which slightly overlaps the copper tape. The width of the teflon tape determines the gap between the return current electrode and the guard and guarantees a secure and tight contact between the tape and the cable jacket and leaving no air gap between the layers to produce a reliable and repeatable guard from sample to sample.

At this stage, approximately 50.8mm wide adhesive teflon tape is aligned with the non-adhesive Teflon tape of the previous stage and wrapped around for 2 to 3 times. Fig.2.8 shows a depiction of wrapping the adhesive teflon tape over the cable where it is aligned with the previously wrapped teflon sealant tape and the left end lies over the return current electrode.

A 6.35mm wide copper tape is cut according to the diameter of the sample cable and tightly wrapped around the cable jacket again for 2 to 3 turns right after the end of the adhesive Teflon tape. This should leave an approximately 25.4mm gap between the end of

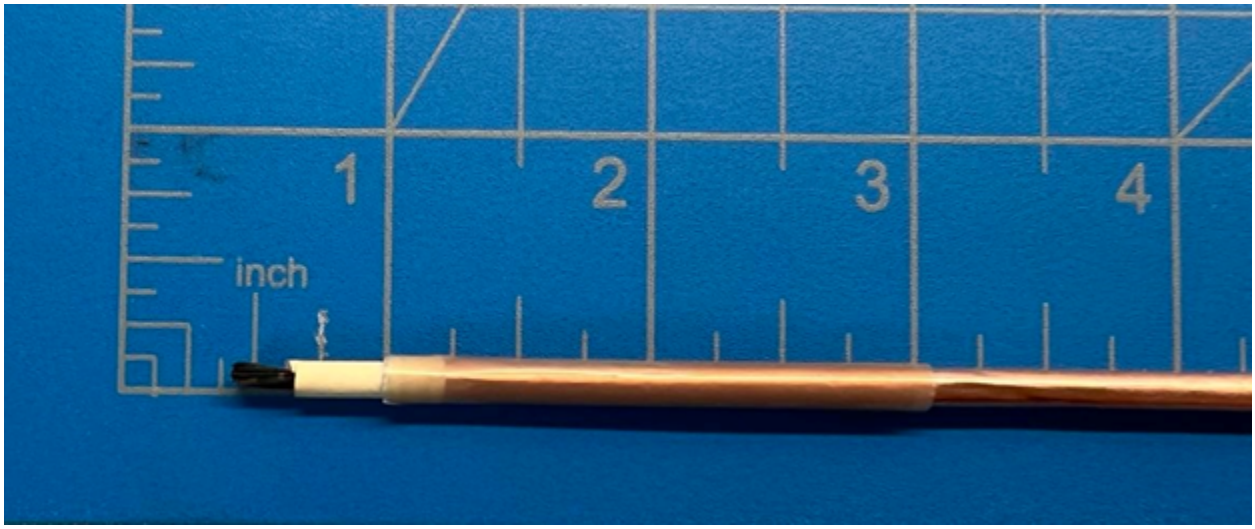

Figure 2.8: Adhesive Teflon Tape wrapped over the cable

the copper strip and end of the cable jacket. Fig.2.9 shows the remaining gap at the end of cable after wrapping the 6.35mm wide copper tape.

At the end, on top of this, a 0.0254m wide and long copper tape is aligned with the cable end of the 6.35mm wide copper tape and wrapped around which should cover the 6.35mm wide copper tape and some part of the adhesive teflon tape. Fig.2.10 shows a clear picture of wrapping a 0.0254m wide copper strip which produces our desired guard.

Fig.2.11 shows the final prepared cable ready for dielectric characterization test which much rest for a minimum of 12 hrs to let the adhesive teflon settle to minimize the uncertainties in capacitance measurements which may happen due to these chemical compounds over time. Fig.2.12 shows a cross-sectional graphical representation of the shielded prepared three-terminal cable.

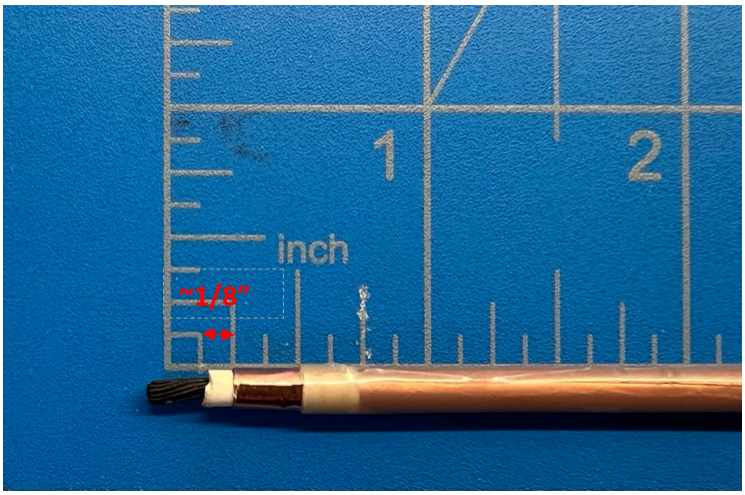

Figure 2.9: 1/4" wide copper tape strip wrapped around the cable jacket

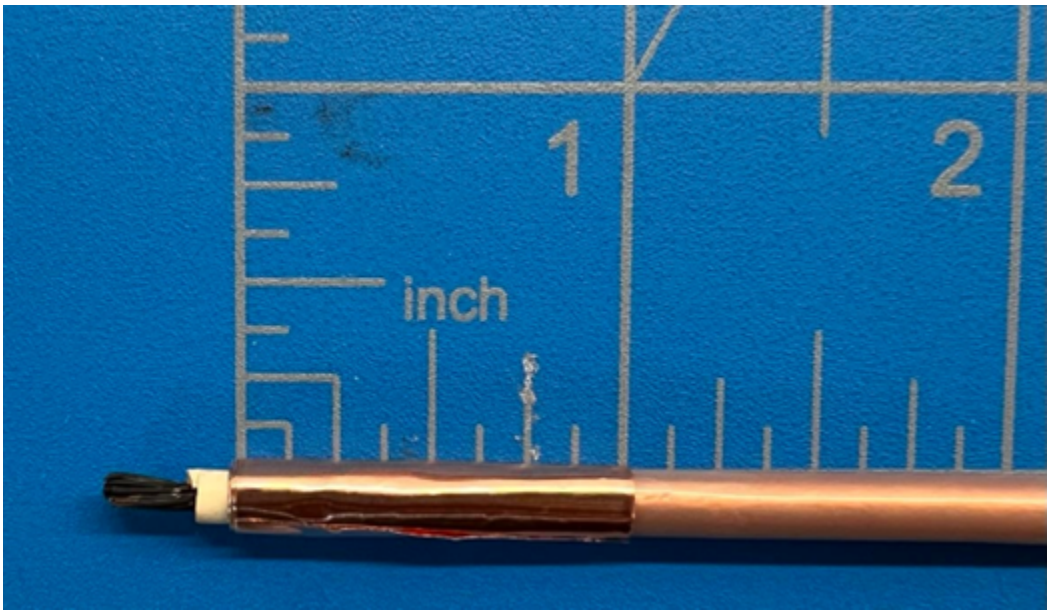

Figure 2.10: 1" wide copper tape strip wrapped around the cable

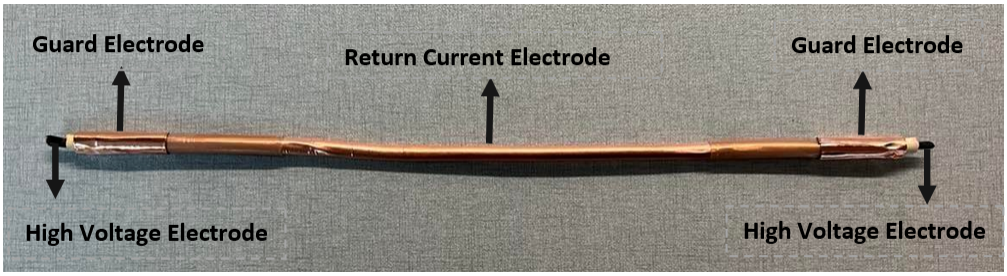

Figure 2.11: Final prepared cable

Figure 2.12: Graphical representation of three-terminal shielded cable[3]

2.3 Experimental Setup

The following sections present the experimental setup for dielectric spectroscopy and polarization-depolarization current measurements.

2.3.1 LFDS and PDC

The primary goal of the study is to investigate the electrical aging markers such as dielectric loss. This is due to the fact that the analysis does not necessitate knowledge of the actual dimensions of the cables for determining real and imaginary permittivities, which can be challenging in the case of standard multicore cables. As a result, the data of short cable samples can be extrapolated to considerably longer cable sections. [44]

OMICRON DIRANA which is a dielectric insulation analyzer was used to perform frequency domain spectroscopy (FDS) as well as polarization and depolarization current (PDC) measurements. However, while dielectric frequency response measurements over a wide frequency range allow for the determination of crucial parameters without the drawbacks of conventional approaches, the measurement period can be rather long and can take many hours. FDS entails applying a variable frequency AC voltage to the cable under test in order to determine capacitance (C') and tangent delta (C"/C') versus frequency. As the frequency decreases, the time required for an AC waveform to complete one cycle increases. Measuring using a frequency range that is too small results in faster measurement times but may result in inaccurate readings, whereas measuring with a frequency range that is too broad results in unnecessary long measurement periods. The OMICRON DIRANA offers an advanced, much faster approach that uses both frequency and time domain measurements to provide information for the needed frequency range in a shorter period of time. The DIRANA combines the benefits of both dielectric measurement techniques—frequency domain spectroscopy (FDS) and polarisation depolarization current (PDC), as observed dielectric properties in specific frequency or time ranges can be transformed into each other when conducted correctly. The measurement sequence is FDS followed by PDC. The advantage of time domain measurements is that a single measurement can be used to estimate dielectric properties at many frequencies, saving time. To obtain data in frequency

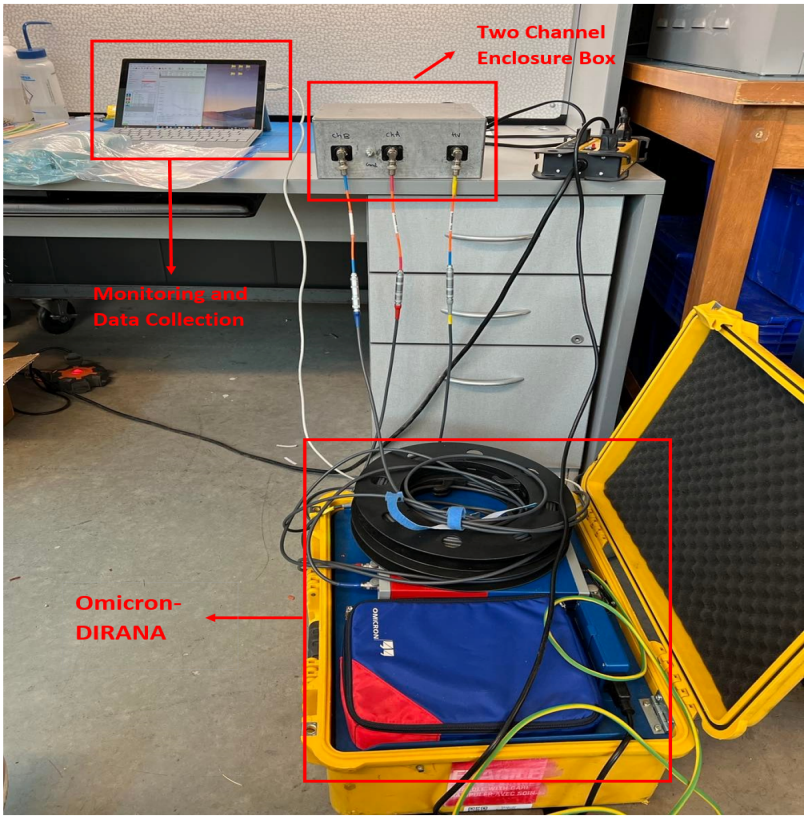

Figure 2.13: Laboratory setup for the experiment

domain, measurements in time domain taken over a finite interval of time are transformed to frequency domain.[45]

The experiment's equipment and laboratory test setup are depicted in Fig.2.13. The experiment was carried out separately for each cable sample. The test time was reduced even further by employing a dual-channel enclosure box shown in Fig.2.14, which permitted parallel testing of two cables at the same time without producing interference. Because they have been exposed to the same environment, it is anticipated that their ageing circumstances will be similar, and this will be studied in the results section.

The FDS and PDC studies were conducted with the following configuration:

- Output voltage: 200 V
- Frequency range: 1 mHz- 1 kHz
- PDC to FDS conversion is employed for frequencies below 100 mHz
- Polarization and Depolarization time: 1000s
- Temperature: Ambient

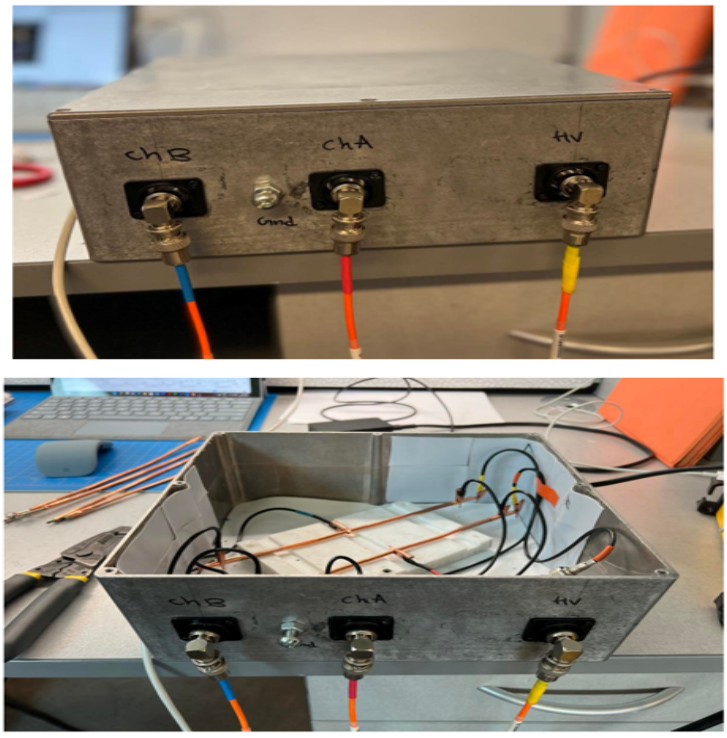

Figure 2.14: Dual-Channel Enclosure Box

2.3.2 Instrument Connection to Dual-Channel Enclosure Box

The connection of DIRANA to Dual-Channel Enclosure Box is shown in Fig.2.15 and Fig.2.16. Three pieces of coaxial cables with corresponding adaptors for DIRANA were

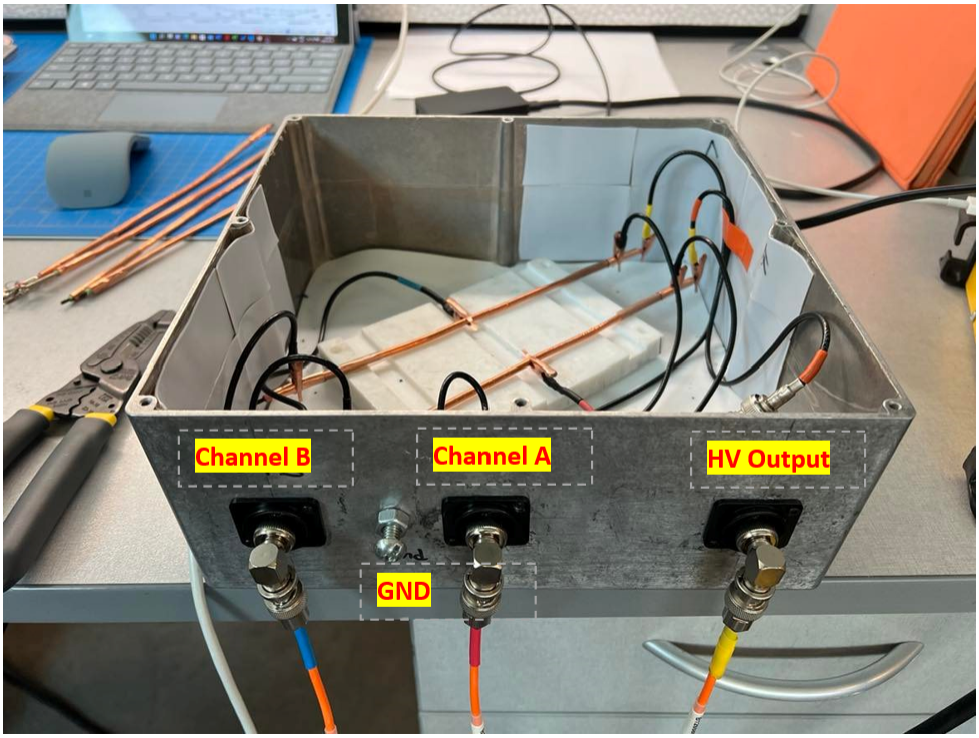

Figure 2.15: Enclosure Box connection

connected to the Box. The High Voltage Output can be connected to either side (left/right) of the cable cores. Channel A and Channel B inputs are connected to the Return Current Electrodes of the respective cables and Ground is connected to the Guard Electrodes at both ends.

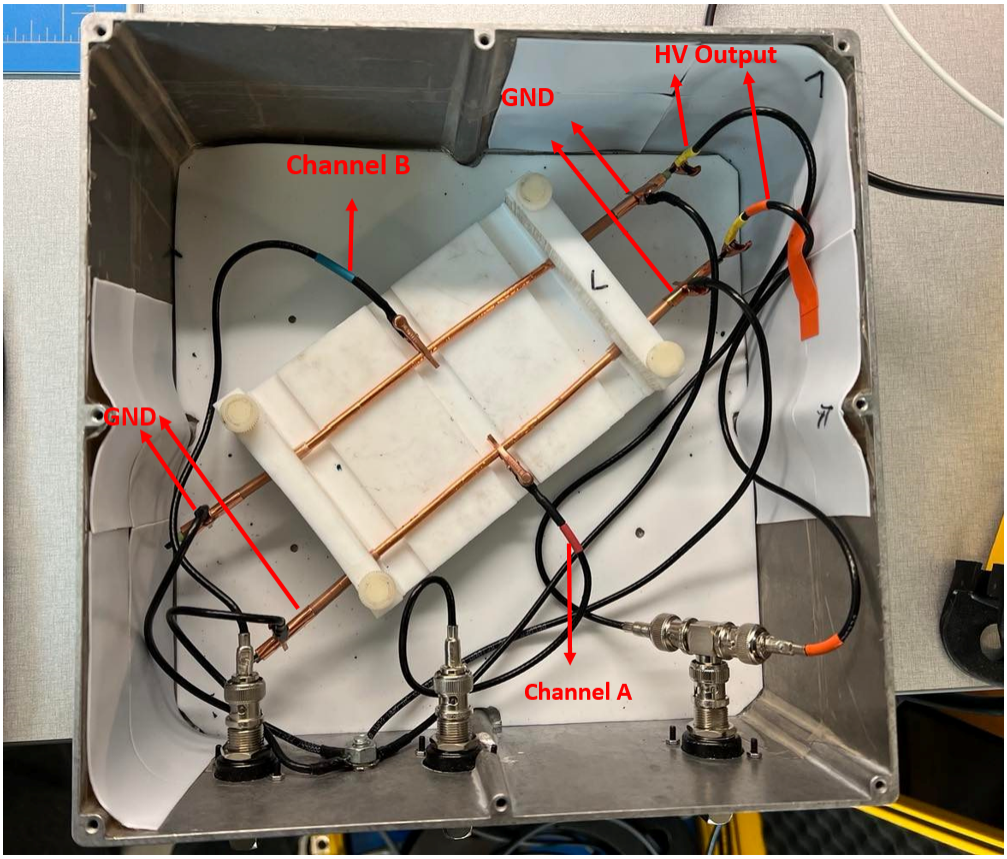

Figure 2.16: Dual channel connection with the cables and DIRANA

Chapter 3

Experimental Results and Analysis

Dielectric spectroscopy is very valuable for insulating materials, especially at very low frequencies where FDS results become sensitive to the aging level of the insulation being tested. The dielectric response of test samples extracted from low-voltage cables with various insulations was investigated over a wide frequency range using the techniques described in sections 2.2 and 2.3 This study looked into the effects of thermal aging on electrical properties. Test samples of various insulating materials were taken in both their pristine and aged stages in order to study at how aging affects their properties. Due to the fact that temperature is an important factor in the electrical characteristics of insulating cables, temperature dependence was also examined for all baseline tests. Four temperatures—ambient, 40°C, 60°C, and 80°C—were ued to examine the cables for comparison. The operational temperature of insulating cables can be met at these temperatures without the cable samples melting.

Using a dielectric spectroscopy experimental setup with DIRANA, this chapter presents and examines the specimen measurement data. The effects of test temperature on pristine sample FDS and PDC results are demonstrated in Sections 3.1 and 3.2, respectively.In order to determine the effects of thermal aging, the measurement results of pristine and aged samples are presented in Sections 3.3 and 3.4.

3.1 Influence of test temperature on FDS results of Pristine Cables

Figures 3.1, 3.2, 3.3, 3.4 and 3.5 show the dielectric losses (tanδ) of **XLPE-RED**, **XLPE-GREEN**, **XLPE-WHITE**, **EPR-KER** and **EPR-OKO** at four different temperatures (ambient, 40°C, 60°C and 80°C).

These findings show a clear temperature dependence of tanδ for all five different insulation types. The tanδ grows progressively with increasing temperature, with the increase being particularly pronounced at low frequencies. It is clear that XLPE samples exhibit a peak in their responses when comparing the XLPE and EPR responses at room temperature. The reactions of EPR-OKO did, however, show peaks as the temperature was increased. The dipolar relaxation peak can also be compared to an increase in temperature, which reveals a shift in the peak frequency of XLPEs and EPR-OKO from the low to the high range.

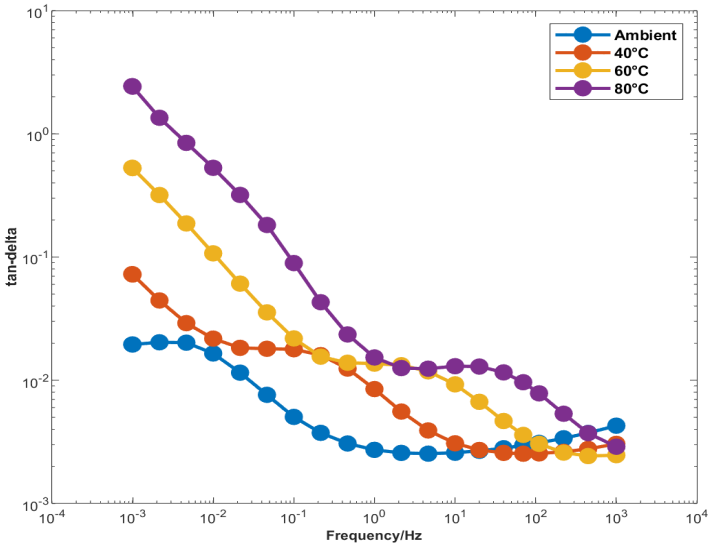

Figure 3.1: tan-delta of XLPE-RED at various temperatures

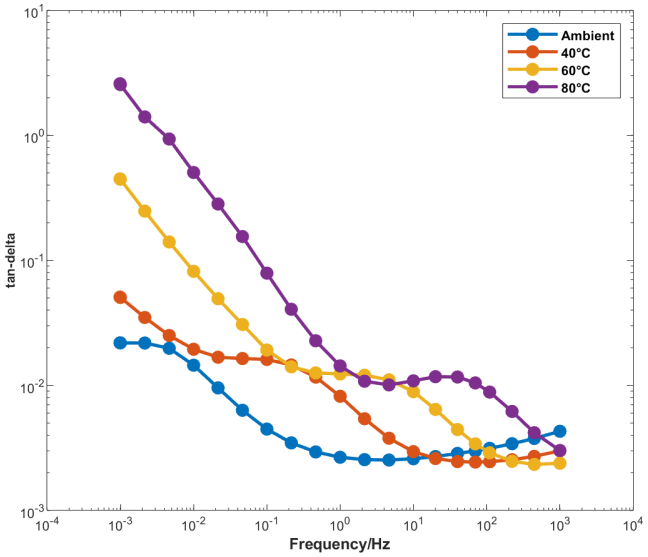

Figure 3.2: tan-delta of XLPE-GREEN at various temperatures

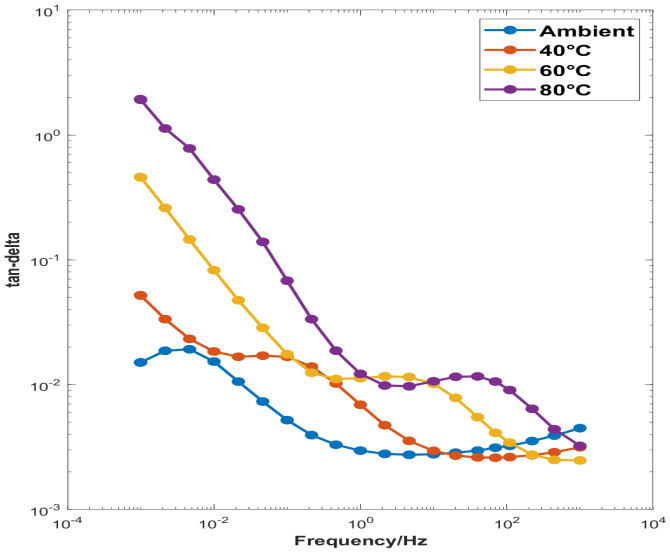

Figure 3.3: tan-delta of XLPE-WHITE at various temperatures

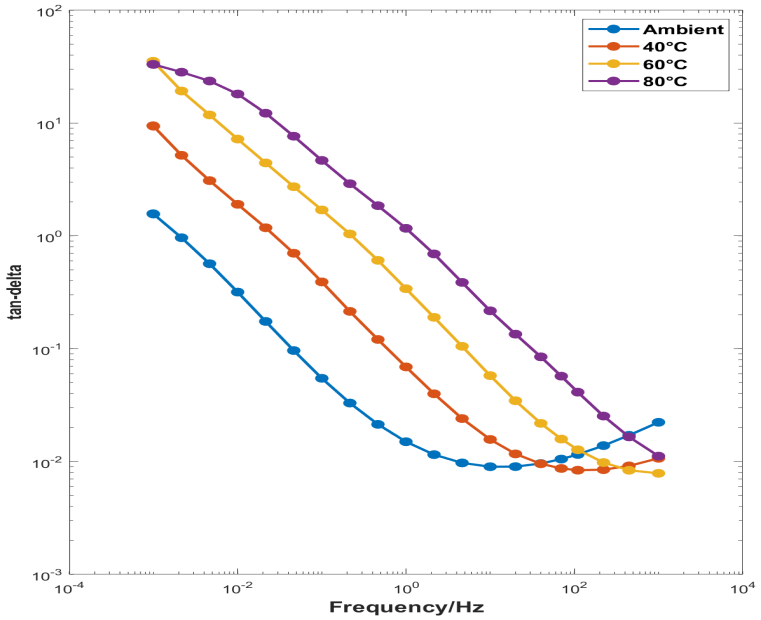

Figure 3.4: tan-delta of EPR-KER at various temperatures

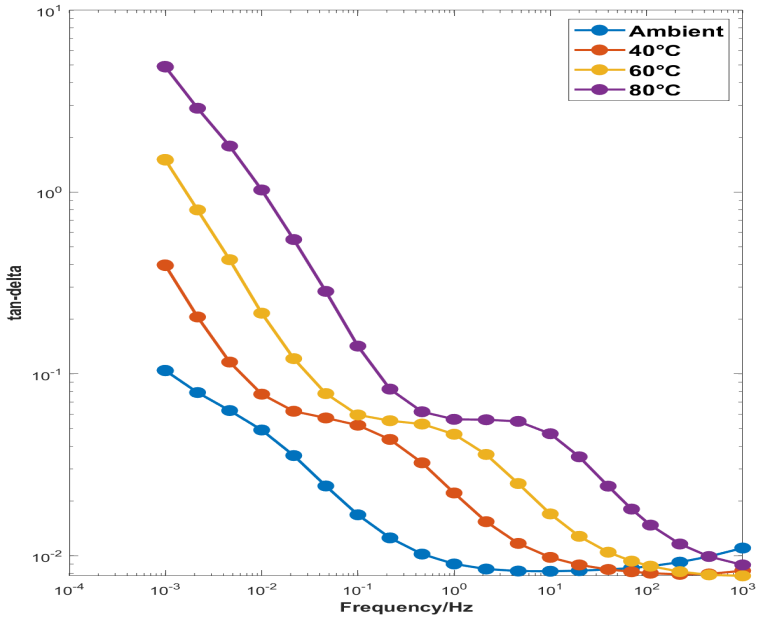

Figure 3.5: tan-delta of EPR-OKO at various temperatures

3.2 Influence of test temperature on Polarization and Depolarization Current of Pristine Cables

PDC testing was carried out on five different types of specimens with increasing test temperatures, and similar effects were observed for all samples.

Figures 3.6, 3.7, 3.8, 3.9 and 3.10 show polarization data for XLPE-RED, XLPE-GREEN, XLPE-WHITE, EPR-KER, and EPR-OKO, respectively. These results show changes as the temperature rises. More specifically, the polarization current response exhibits curve shifts across the entire time range of 10 to 1000s, with the effects most noticeable between 12s and 1000s that were consistent across all specimens studied in this study. It should be noted that after 100 seconds at room temperature, the polarization current becomes noisy, with XLPE-WHITE exhibiting the worst behaviour.

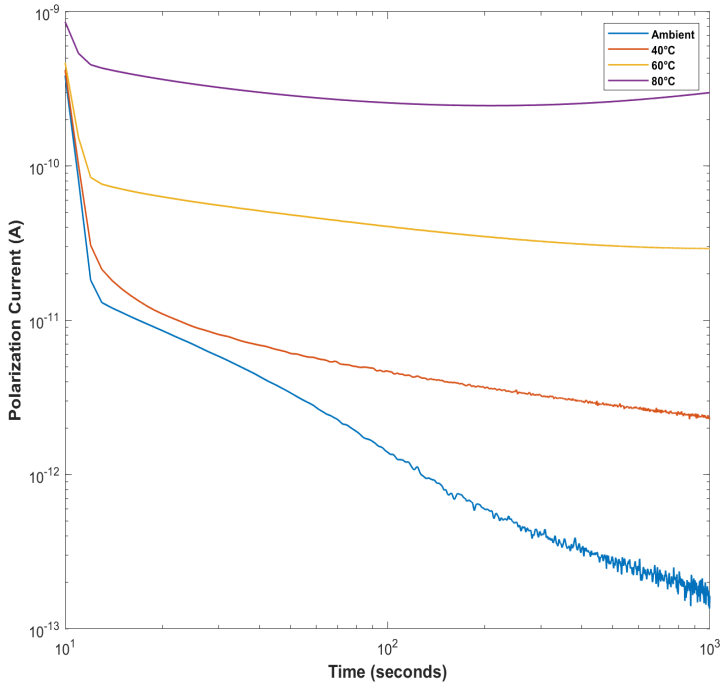

Figure 3.6: Polarization current of XLPE-RED from 10s to 1000s

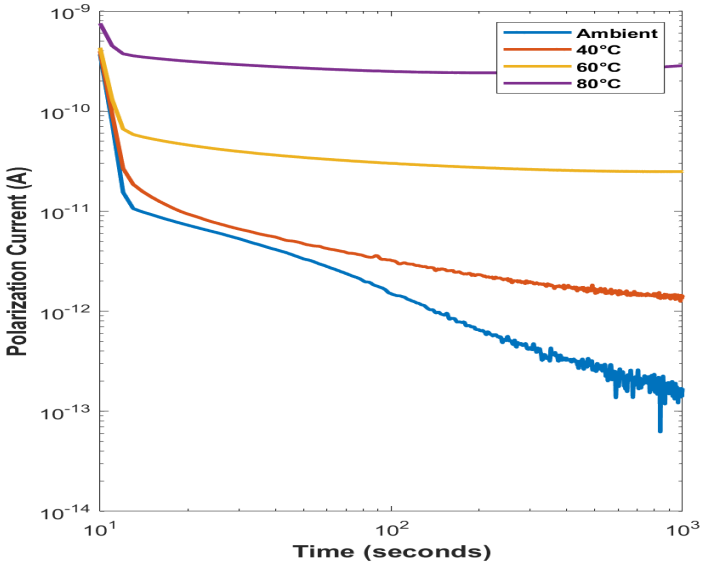

Figure 3.7: Polarization current of XLPE-GREEN from 10s to 1000s

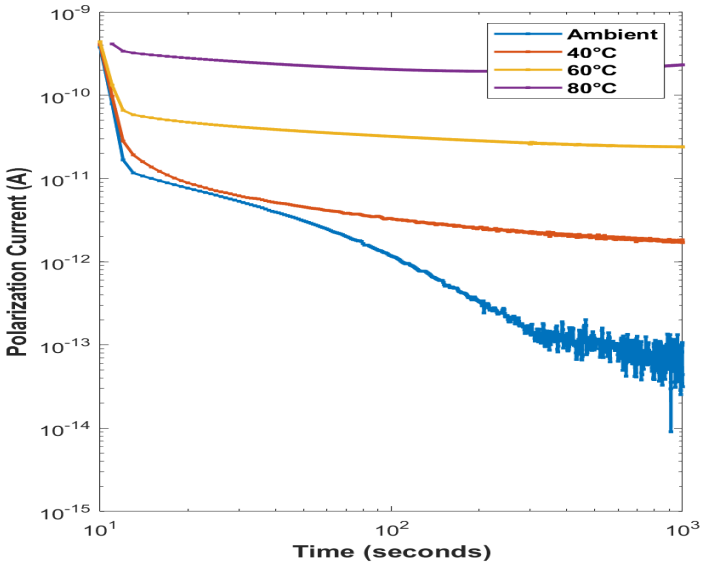

Figure 3.8: Polarization current of XLPE-WHITE from 10s to 1000s

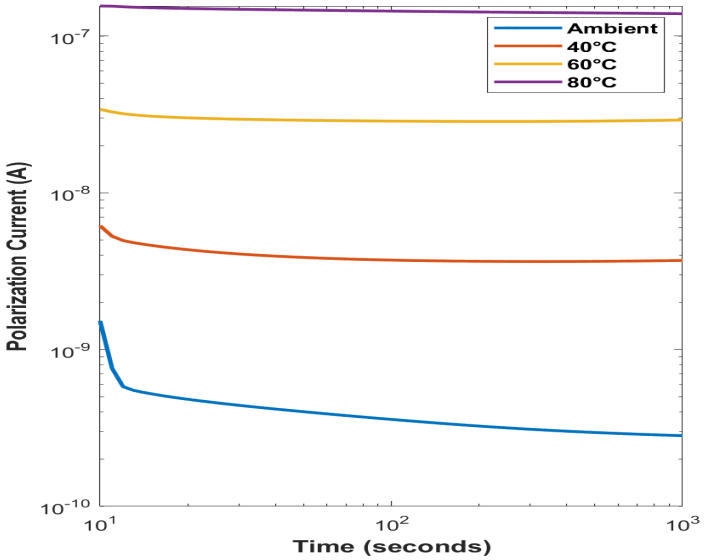

Figure 3.9: Polarization current of EPR-KER from 10s to 1000s

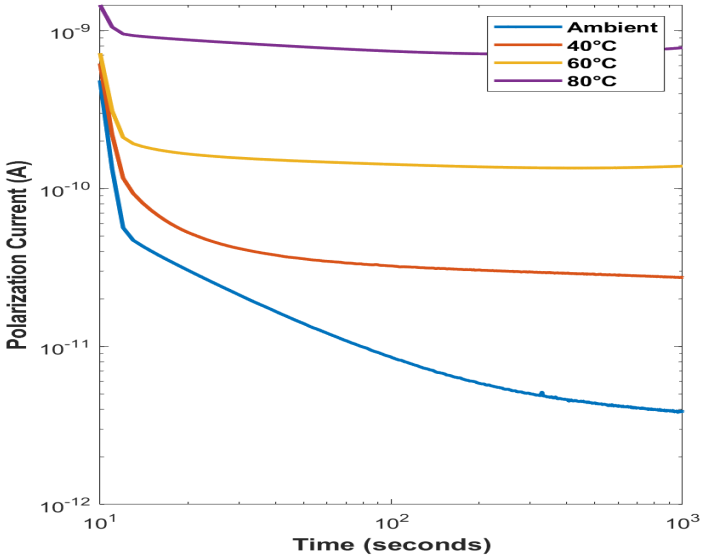

Figure 3.10: Polarization current of EPR-OKO from 10s to 1000s

The depolarization current exhibits similar curve shifts, as represented in Figures 3.11, 3.12, 3.13, 3.14 and 3.15, most notable for temperatures 60°C and 80°C with ambient temperature as reference. For ease of comparison, the polarity of the depolarization current values has been changed to positive. As a result, it was determined that temperature influences the magnitude and slope of the current data. Simialr to polarization current, depolarization current for XLPE samples demonstrated noisy behaviour after 100s mostly at ambient temperature..

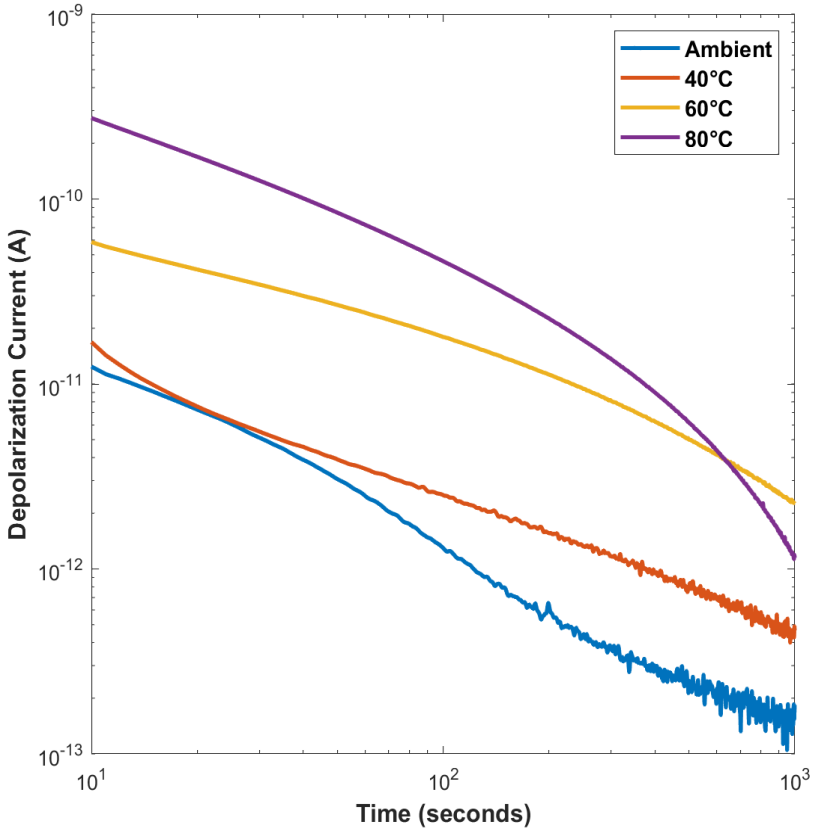

Figure 3.11: Depolarization current of XLPE-RED from 10s to 1000s

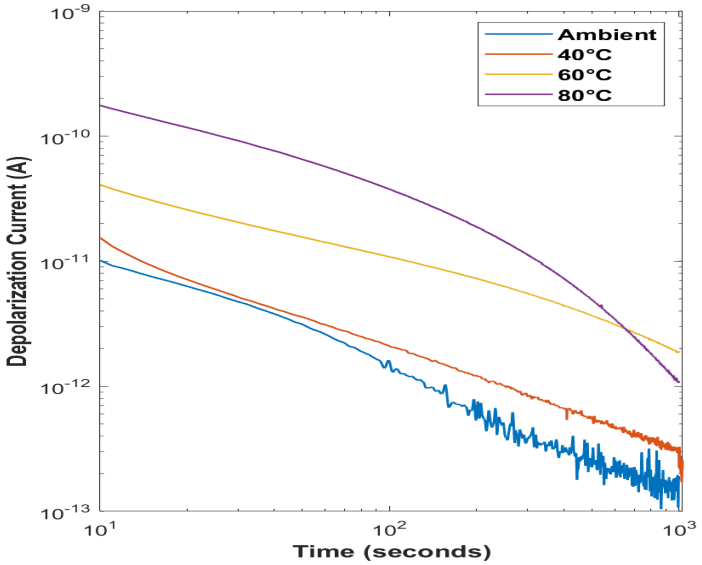

Figure 3.12: Depolarization current of XLPE-GREEN from 10s to 1000s

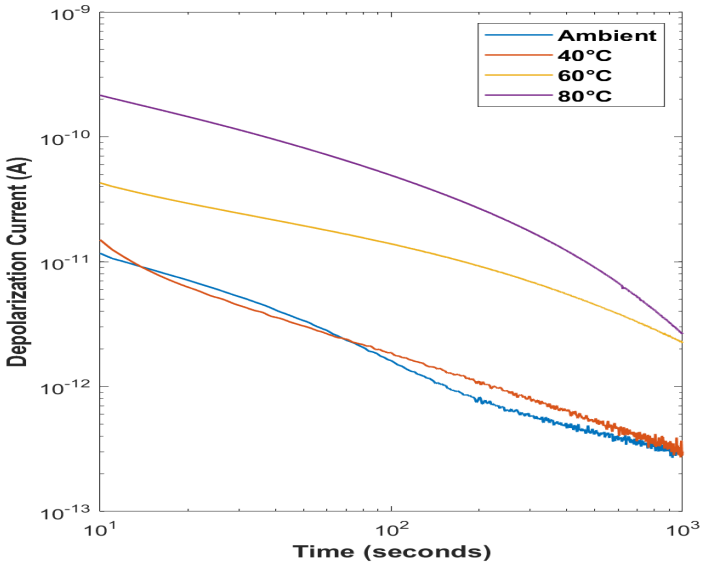

Figure 3.13: Depolarization current of XLPE-WHITE from 10s to 1000s

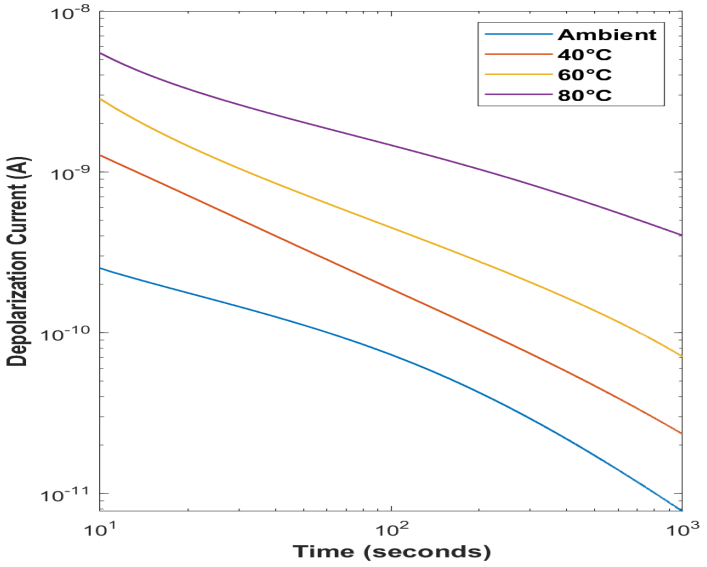

Figure 3.14: Depolarization current of EPR-KER from 10s to 1000s

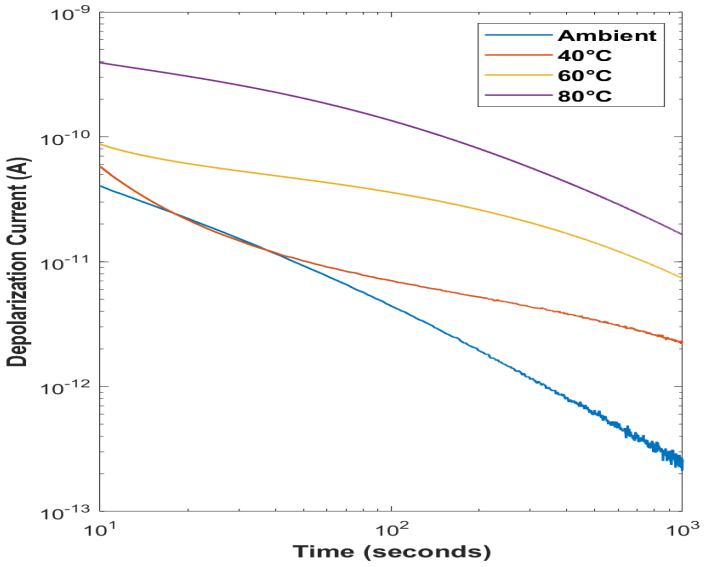

Figure 3.15: Depolarization current of EPR-OKO from 10s to 1000s

3.3 Aging Effects on FDS results

3.3.1 XLPE-RED

Test results of XLPE-RED are presented in Figures 3.16 and 3.17 for C' and C", respectively, for all the aging intervals. The FDS data exhibited very clear changes in dielectric frequency response with thermal aging. Specifically, the C' data showed variation over the whole frequency range between 0.001 to 1kHz in the form of vertical shift, although the effects are most clearly visible between 0.001 to 10Hz.

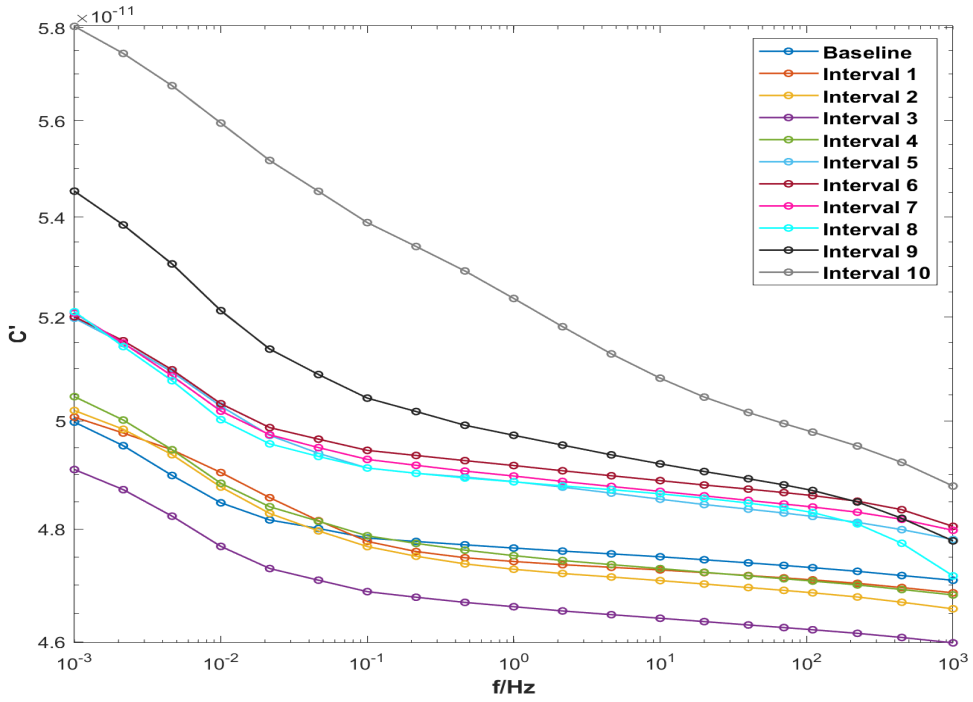

Figure 3.16: C' of XLPE-RED vs. thermal aging

It can also be observed that after certain hours of aging the responses nearly saturate for a while. An increasing trend is visible with respect to interval 1 (hundred hours aging) particularly at lower frequency portion (i.e. conductivity) with an exception of interval 3

which demonstrates anomalous response where it is well below the baseline as well.

An increasing trend is also observed in C" with increasing aging hours with respect to interval 1. The C" showed a variation in the polarization peak as well, visible in the low frequency region of 0.001 to 0.1 Hz. The polarization peak was found to shift towards the lower frequency zone for increasing aging hours. It was also noted that the C" for interval 10, had two peaks in it's response.

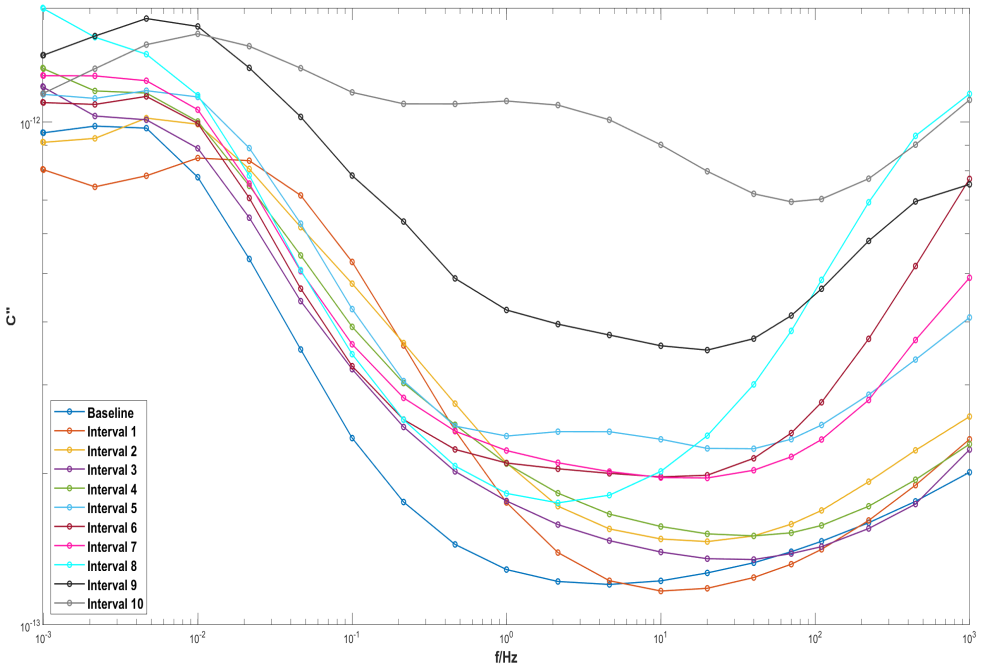

Figure 3.17: C" of XLPE-RED vs. thermal aging

The tanδ(C”/C’) data shown in Fig.3.18, reflected similar characteristics observed in the C”, albeit with C” values orders of magnitude smaller.

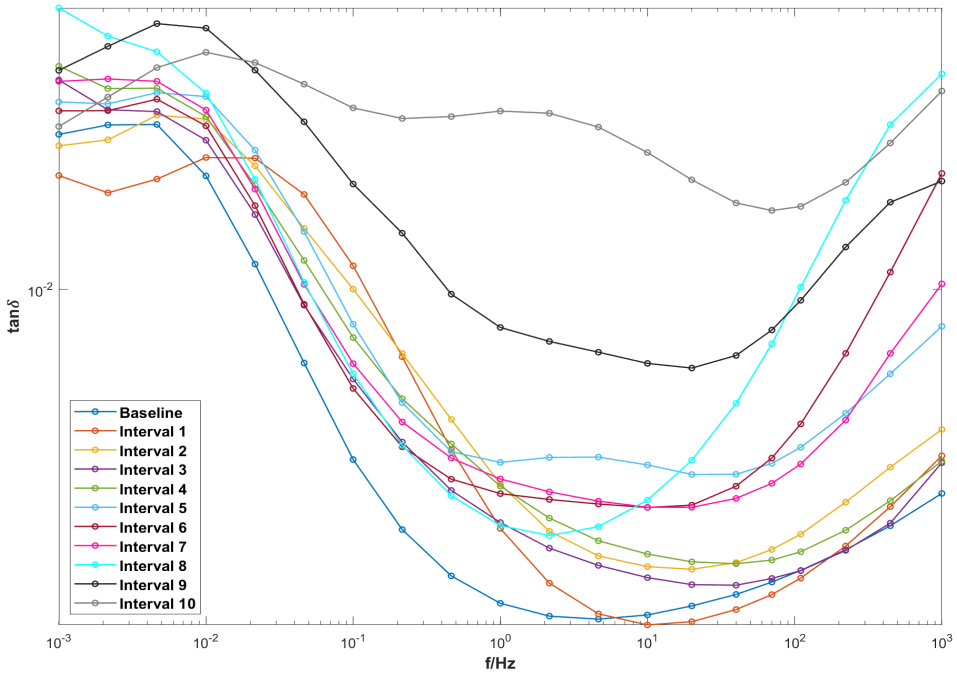

Figure 3.18: tan-delta of XLPE-RED vs. thermal aging

3.3.2 XLPE-GREEN

Test results of XLPE-GREEN are presented in Figures 3.19 and 3.20 for C' and tanδ, respectively, for all the aging intervals. Since C" and tanδ demonstrate similar response, only tanδ will be displayed. Similar to the XLPE-RED FDS results, thermal aging caused noticeable changes in dielectric frequency response. The C' data showed good variation in the form of a vertical shift across the entire frequency range between 0.001 and 1 kHz, with the most visible effects between 0.001 and 10 Hz.

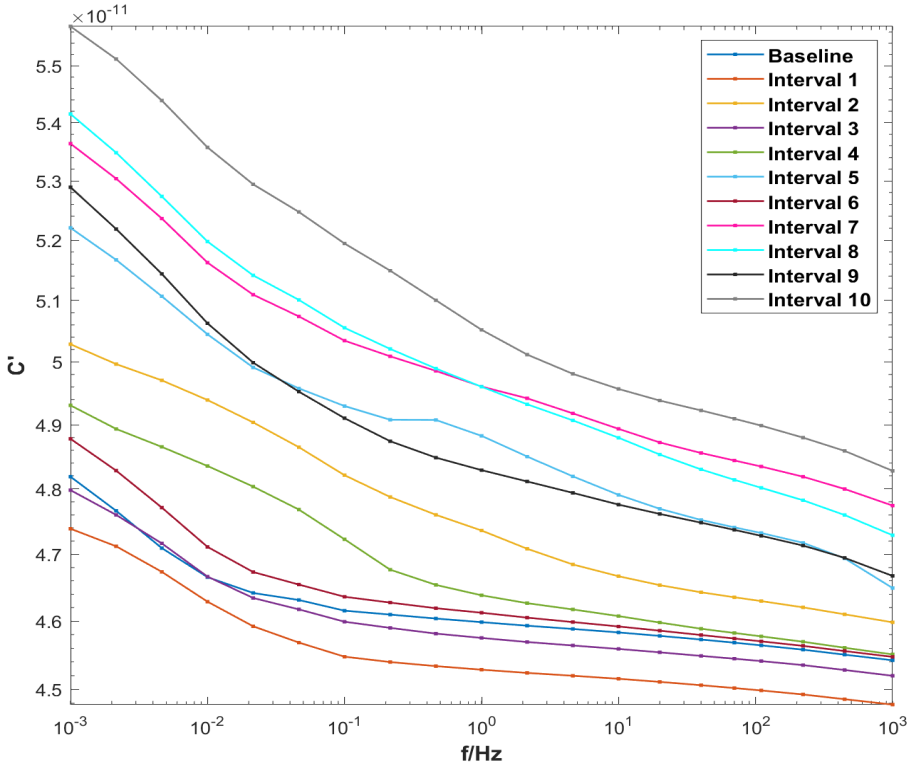

Figure 3.19: C' of XLPE-GREEN vs. thermal aging

Overall, an increasing trend with aging over the entire frequency range was observed in C' with respect to interval 1. However, C' at intervals 3, 4, and 6 dropped with respect to interval 2. It was also noted that C' at interval 9 demonstrated a similar result to 5.

An overall increasing trend is also observed in tanδ with increasing aging hours with respect to interval 1. However, there were inconsistencies in the trend of increasing aging hours interval. Tanδ response curve for intervals 1, 3, and 6 can be seen to show a similar nature and trend in the response. On the other hand, intervals 7–10 that have a similar trend can be grouped together. It can also be noticed that intervals 2, 5, 7, 8, and 10 had two polarization peaks.

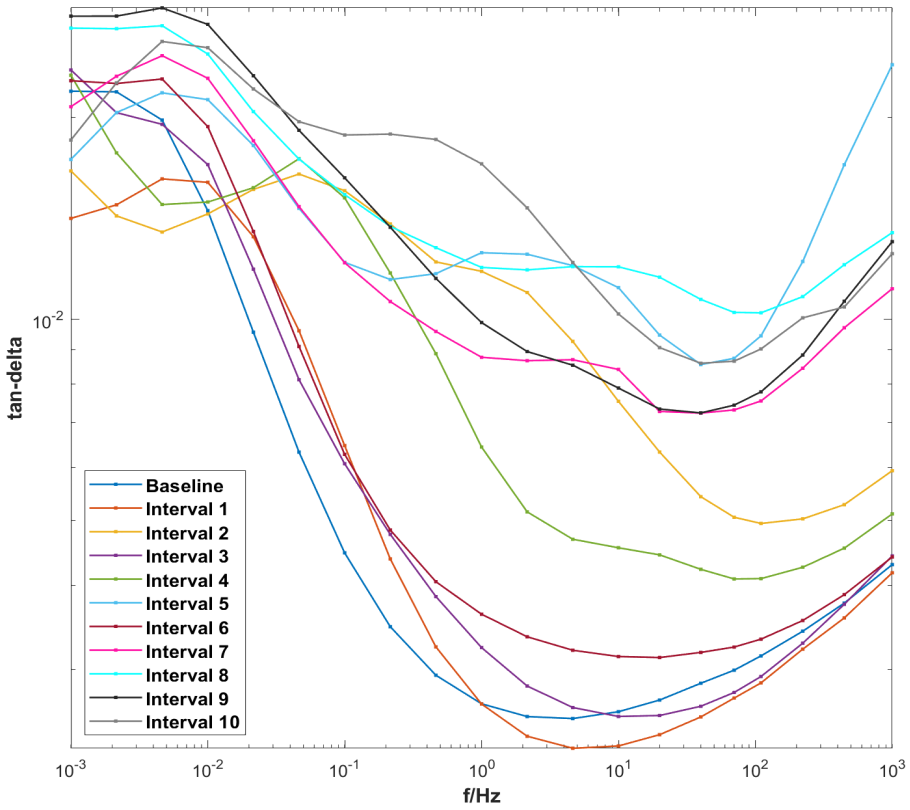

Figure 3.20: tan-delta of XLPE-GREEN vs. thermal aging

3.3.3 XLPE-WHITE

Figures 3.21 and 3.22 depict the behavior of the real part of permittivity (C') and tanδ vs. frequency, at different aging times. Noticeable changes in C' with thermal aging were observed, especially noticeable in the lower frequency region (0.001 to 0.1 Hz).

C' demonstrated a decreasing trend until interval 3 with respect to interval 1, and an increasing trend from interval 5 with respect to interval 1. An overall good trend was observed for C' with some anomalous behaviour at intervals 4 and 8.

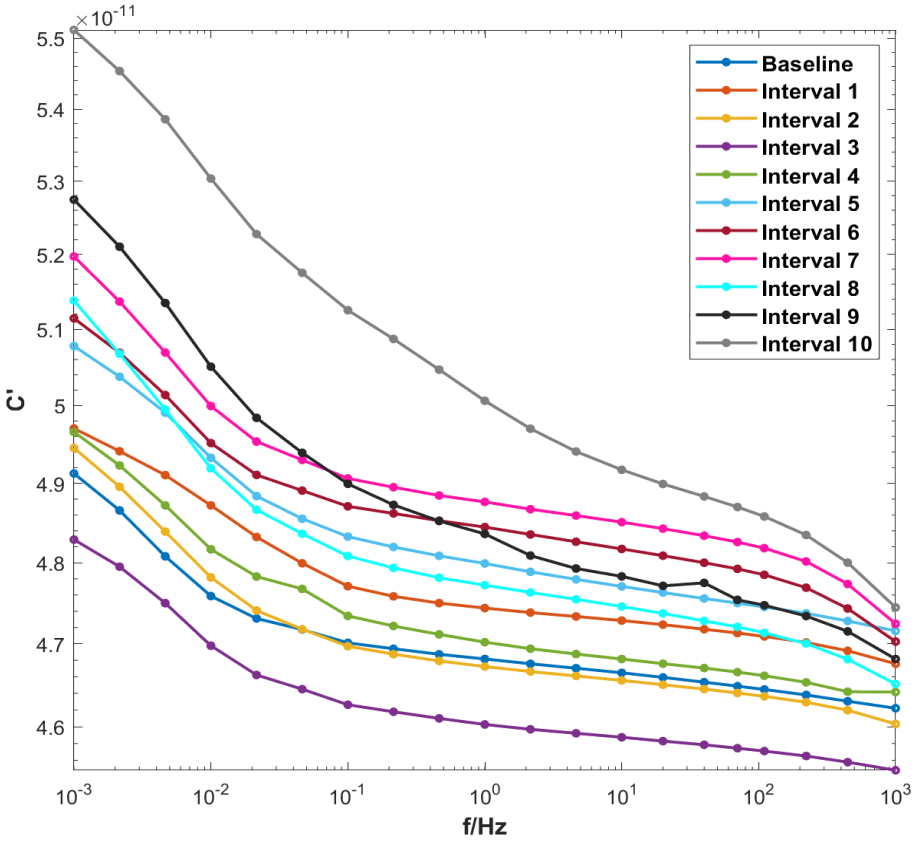

Figure 3.21: C' of XLPE-WHITE vs. thermal aging

Tanδ showed an increasing trend with increasing aging hours in comparison to interval 1 and a variation in the polarization peak, which was visible in the low-frequency region of 0.001 to 0.01 Hz. The polarization peak was found to shift slightly towards the lower frequency zone for most increasing intervals. It was also noted that interval 10 had two peaks in its response.

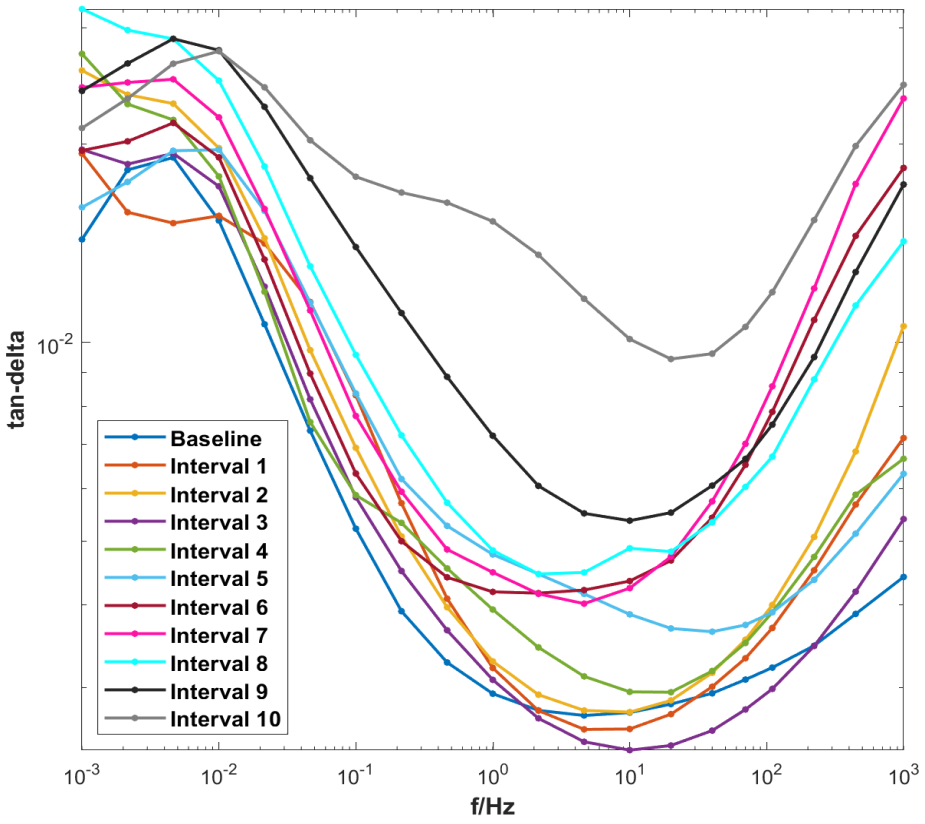

Figure 3.22: tan-delta of XLPE-WHITE vs. thermal aging

3.3.4 EPR-KER

Figures 3.23 and 3.24 depict the behavior of the real (C') part of permittivity and tanδ vs. frequency, at increasing aging times. Changes in c' over the whole frequency range are clearly visible below 10 Hz. An increasing trend is observed up to interval 5 with respect to interval 1. On the other hand, C' had a decreasing trend from interval 6 onwards until interval 10 with respect to interval 5.

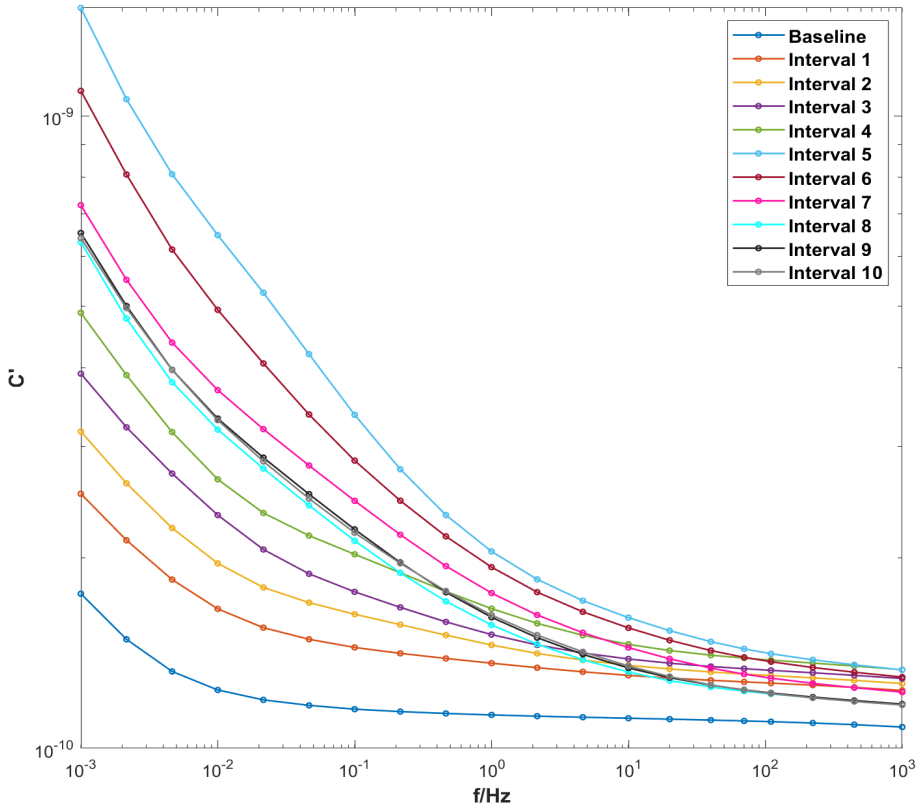

Figure 3.23: C' of EPR-KER vs. thermal aging

While for tanδ, the effect of aging appears over the entire frequency range. Similar to its C' response, an increasing trend is observed until interval 5 with respect to interval 1, and a decreasing trend from interval 6 to interval 10 with respect to interval 5. Also, there is no visible polarization peak in the tan-delta behavior.

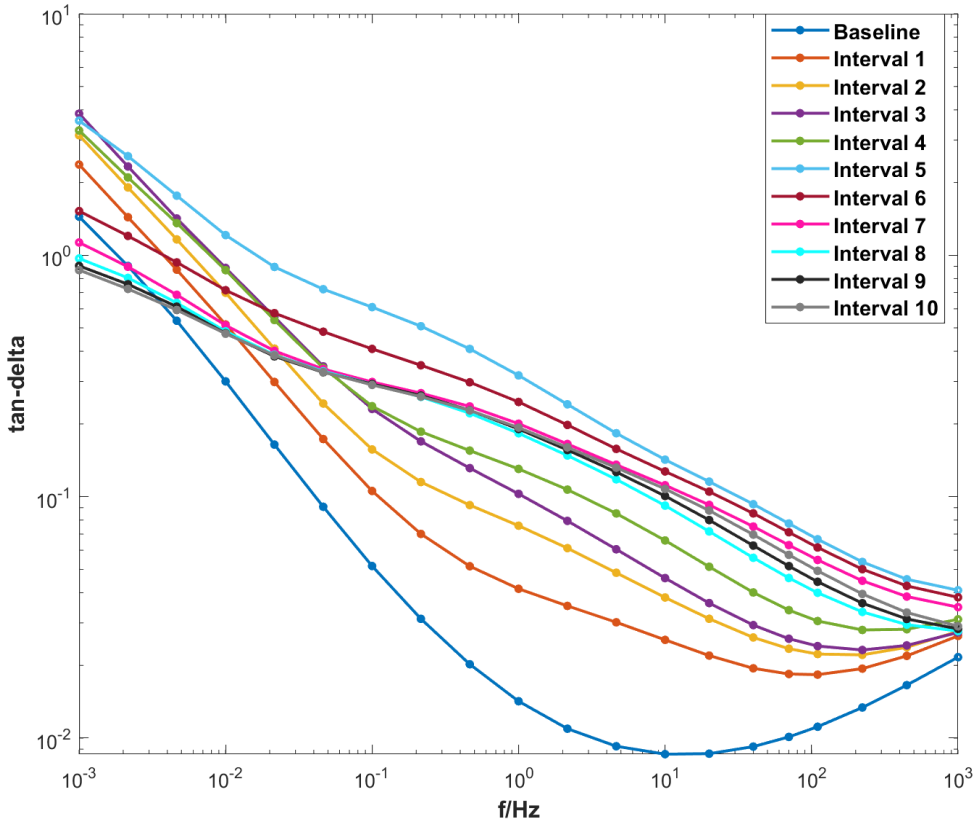

Figure 3.24: tan-delta of EPR-KER vs. thermal aging

3.3.5 EPR-OKO

C' of EPR-OKO showed a good trend over the entire frequency range, as can be seen in Fig.3.25. It increases significantly until interval 7 with respect to interval 1. Interval 8-9 had very much the same response and decreased after interval 7, whereas interval 10 showed a response similar to interval 7.

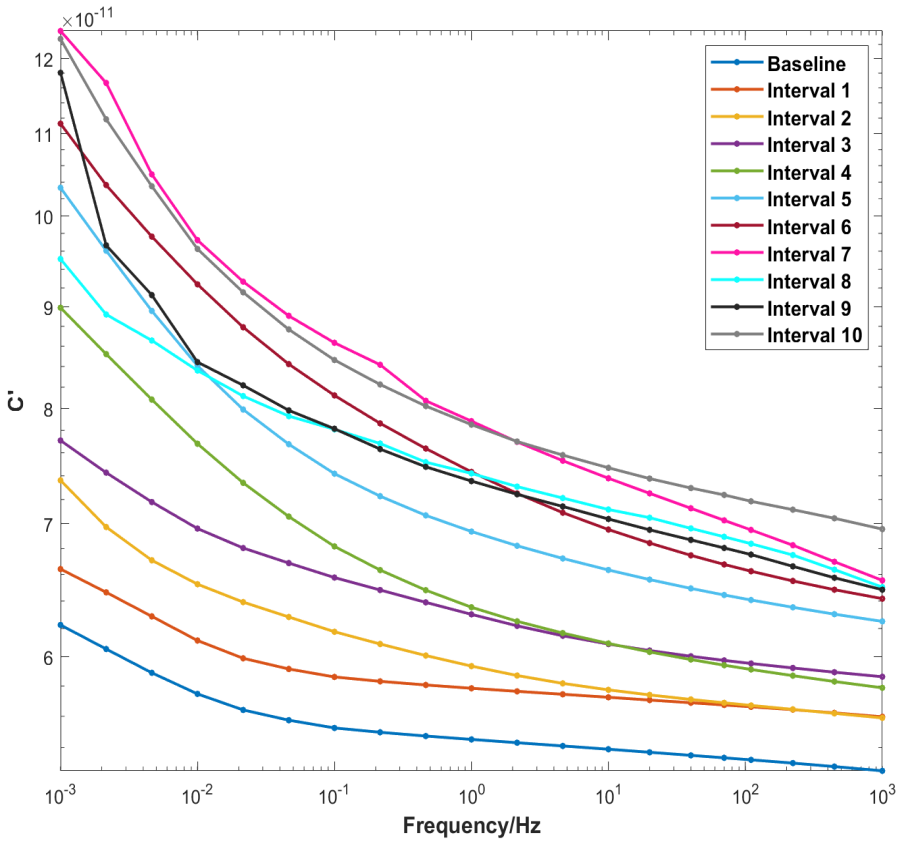

Figure 3.25: C' of EPR-OKO vs. thermal aging

Tanδ increased similarly across the entire frequency range until interval 7 with respect to interval 1. Similarly, tanδ decreased for interval 8 in comparison to interval 7 before increasing for intervals 9 and 10, moving closer to interval 7. At the lower frequency zone, slight polarization peaks were visible at intervals 1, 2, 3, and 8.

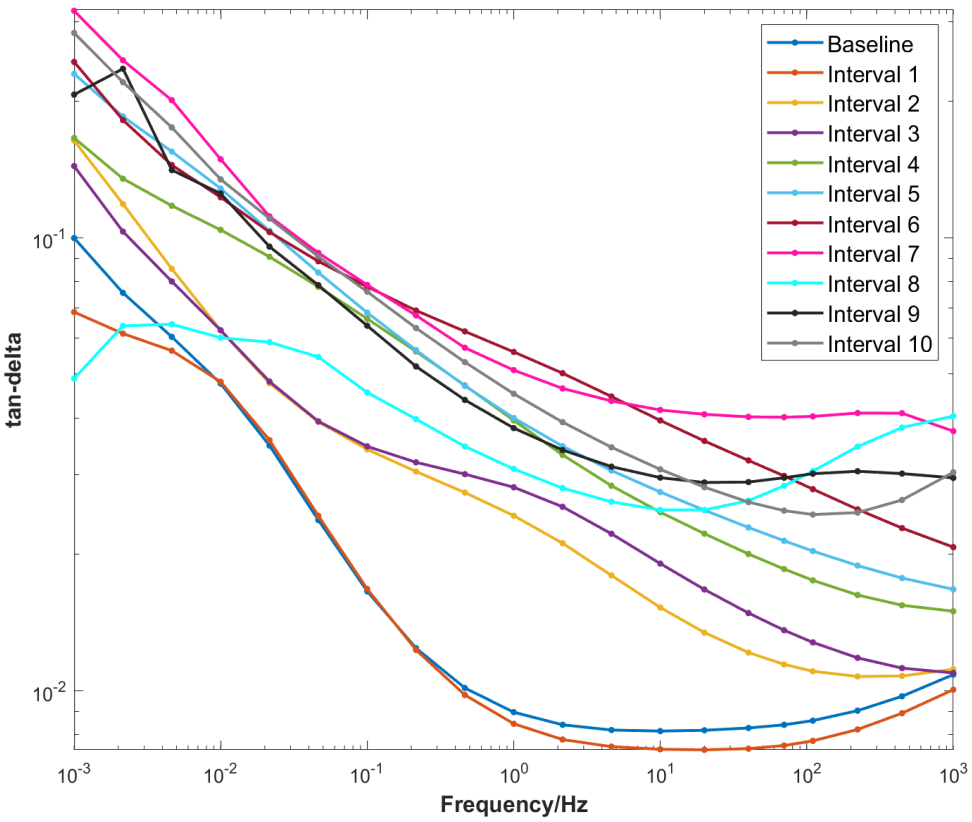

Figure 3.26: tan-delta of EPR-KER vs. thermal aging

3.4 Aging Effects on Polarization and Depolarization Current results

3.4.1 XLPE-RED

Fig.3.27 summarizes the polarization current of XLPE-RED, which demonstrated slight variations with thermal aging. More specifically, the polarization current response exhibits increasing curve shifts over the time range from 10 to 100s, although the effects are most clearly visible in specific regions. Similar curve shifts are better observed in the depolarization current response shown in Fig.3.28, most clearly in the 5s to 100s range.

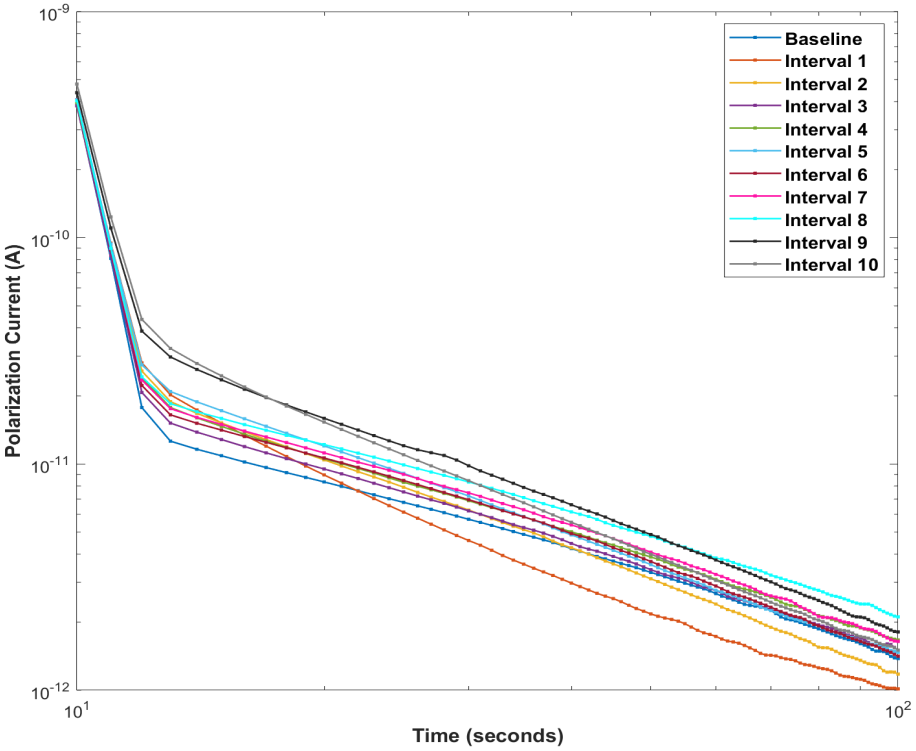

Figure 3.27: Polarization Current of XLPE-RED for 10-100 s

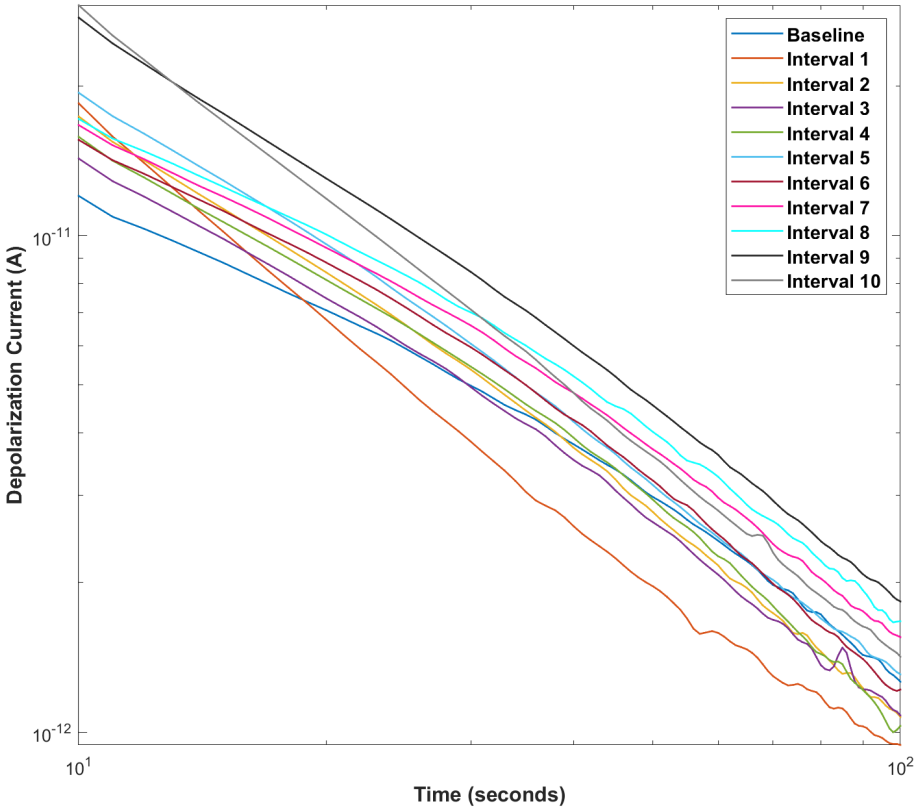

Figure 3.28: Depolarization Current of XLPE-RED for 10-100 s

3.4.2 XLPE-GREEN

Overall, an increasing trend with aging over the entire time range was observed in polarization current with respect to interval 1, as depicted in Fig.3.29. Similar to FDS results, polarization current at intervals 4 and 6 behaved differently as it decreased compared to the increasing trend of polarization current. Similar behaviour was observed in the depolarization current shown in Fig.3.30.

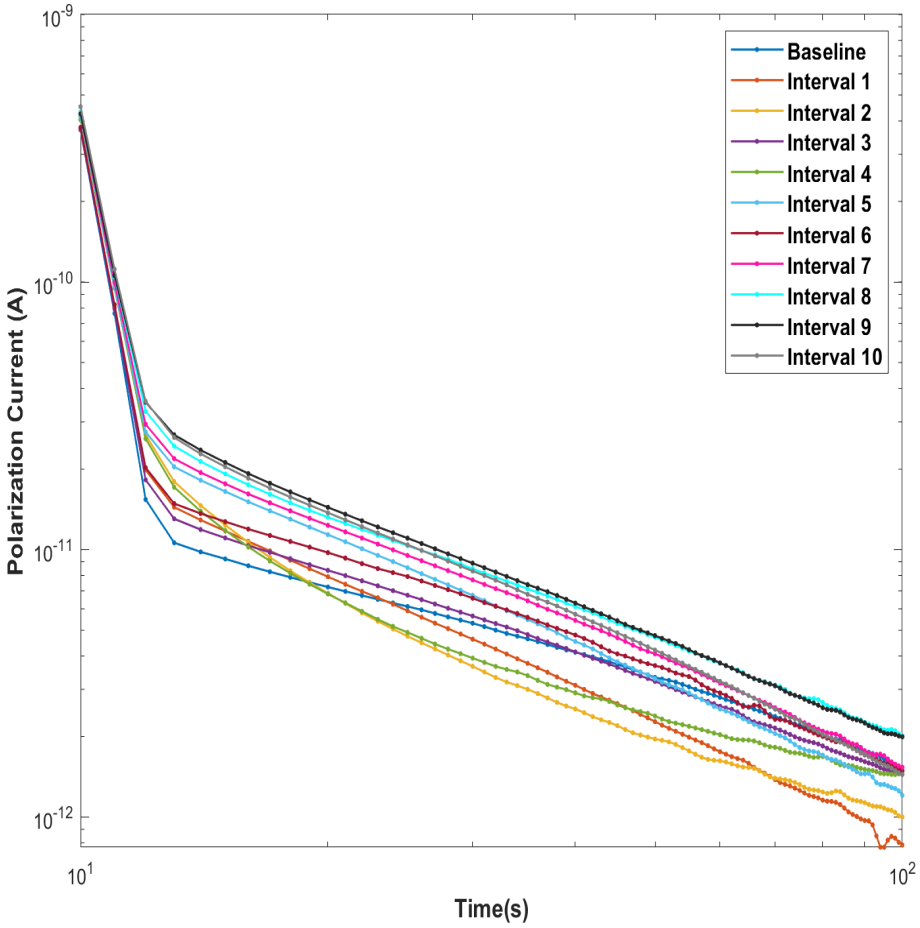

Figure 3.29: Polarization Current of XLPE-GREEN

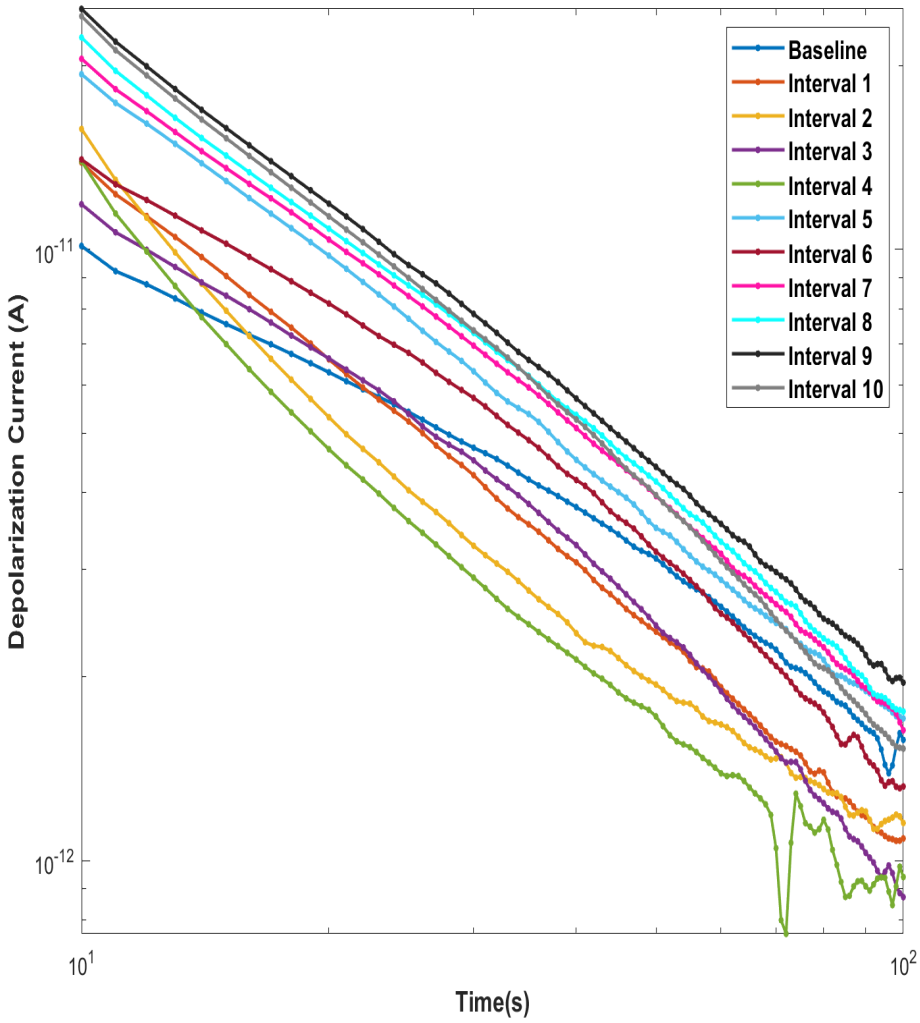

Figure 3.30: Depolarization Current of XLPE-GREEN

3.4.3 XLPE-WHITE

An overall increasing trend was observed in the polarization and depolarization currents shown in Fig.3.31, 3.32. However, the shifts are minimal as a result of thermal aging.

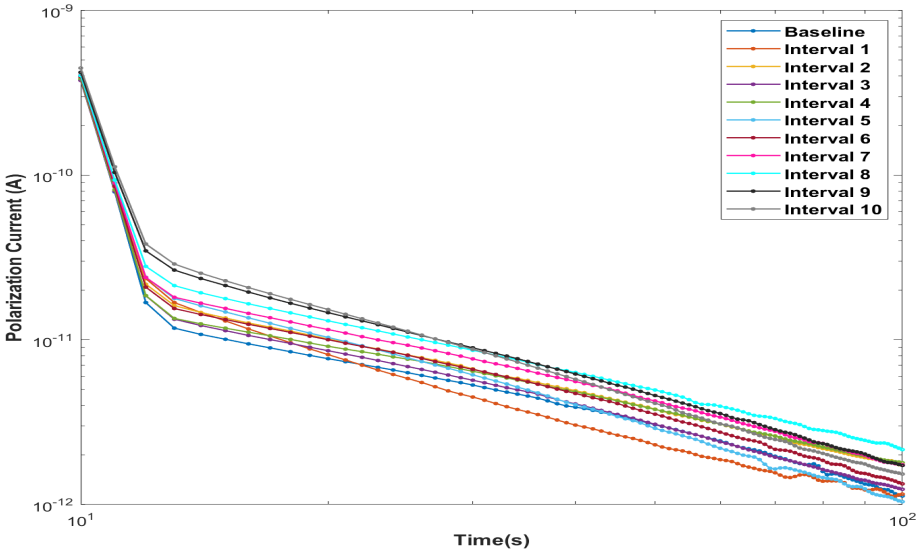

Figure 3.31: Polarization Current of XLPE-WHITE

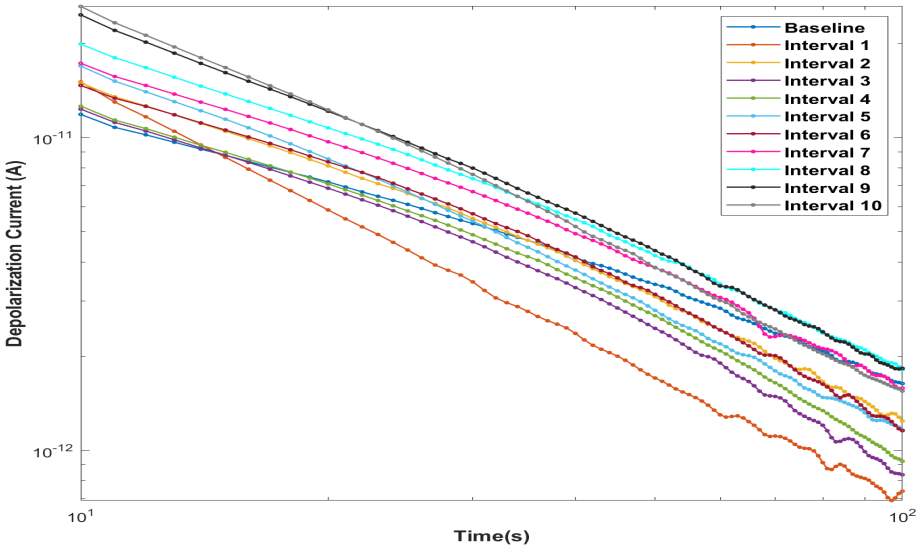

Figure 3.32: Depolarization Current of XLPE-WHITE

3.4.4 EPR-KER

The results of the polarization-depolarization measurement are depicted in Figs.3.33 and 3.34 show a clear increase with aging until interval 5, and then a decreasing trend until interval 10.

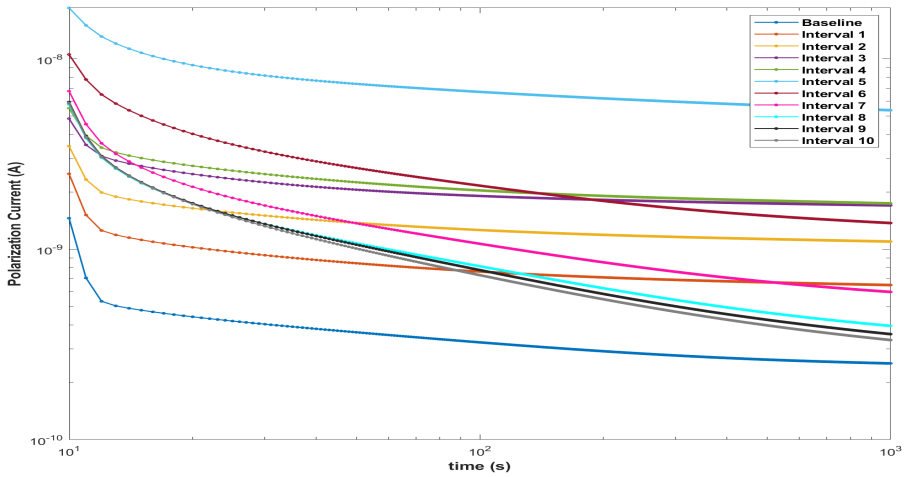

Figure 3.33: Polarization Current of EPR-KER

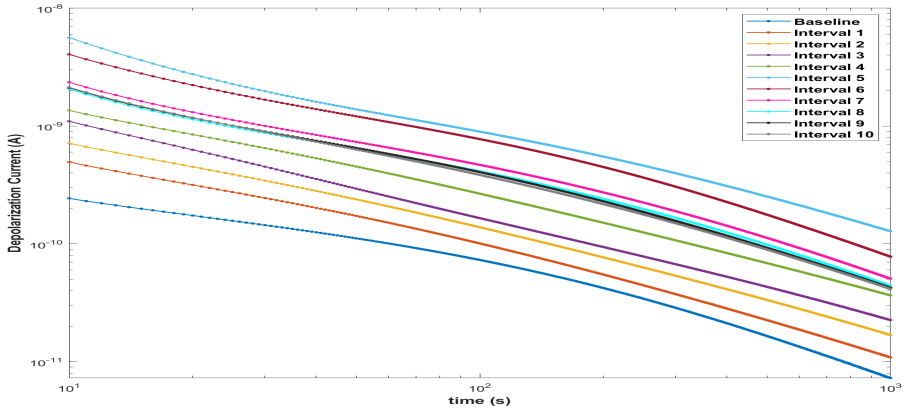

Figure 3.34: Depolarization Current of EPR-KER

3.4.5 EPR-OKO

The polarization current depicted in Fig.3.35 demonstrates an increasing trend until interval 7, then drops for the last three intervals. On the other hand, depolarization current, as depicted in Fig.3.36 has an overall increasing trend, with interval 8 showing irregular behavior.

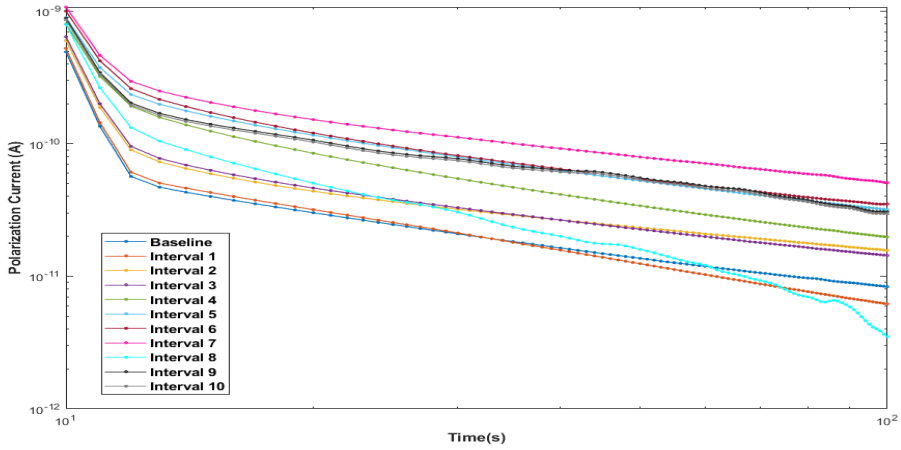

Figure 3.35: Polarization Current of EPR-OKO

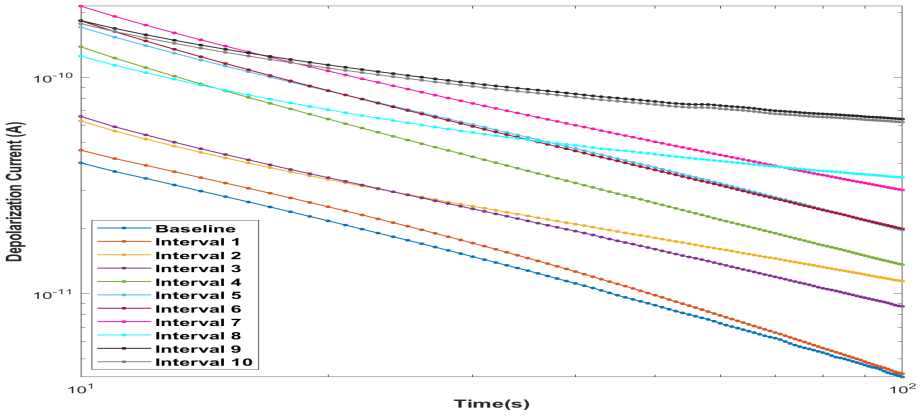

Figure 3.36: Depolarization Current of EPR-OKO

Chapter 4

Discussion

Insulation resistance, leakage current, and other electrical properties, as well as mechanical properties, are frequently used to monitor nuclear power plant cables. Elongation at break and tensile strength are widely regarded as acceptable mechanical characteristics due to their effective correlation with aging. Since aging occurs as a result of the environmental conditions and time that they have been in use, accelerated aging is commonly used to investigate the changes in a reasonable time. The literature on the relationship between accelerated aging and mechanical or chemical indicators, which are primarily destructive tests, has been extensively researched. Non-destructive approaches, on the other hand, are more advantageous and can provide greater flexibility. There is still a scarcity of literature on the effect of aging on the electrical properties of low voltage insulation, specifically variations in dielectric parameters from advanced electrical diagnostic tests.

Electrical properties were analyzed to understand the effect of thermal aging on both XLPE and EPR insulating materials, as these cables used inside nuclear power plant containment are subjected to a variety of environmental conditions, among which temperature is one of the most important parameters. Ionizing radiation is also linked to the nature of the environment, which can have an impact on the aging process. However, because this type of cable is not typically exposed to high voltages, electrical stresses are not significant in aging.

4.1 Influence of test temperature on FDS and PDC results of Pristine Cables

Test temperature has a great influence on the complex permittivity and dielectric loss. The evolution of tanδ with increasing temperature can be compared using different reference frequencies to the study the dependence. Fig.4.1 depicts the tanδ trend with increasing temperature for a variety of frequencies that could be associated with the trend. At higher frequencies, there was no massive distinction in dielectric loss between temperatures. Changes in tanδ, on the other hand, were discovered to have a distinct trend with increasing temperature in the lower frequency region.

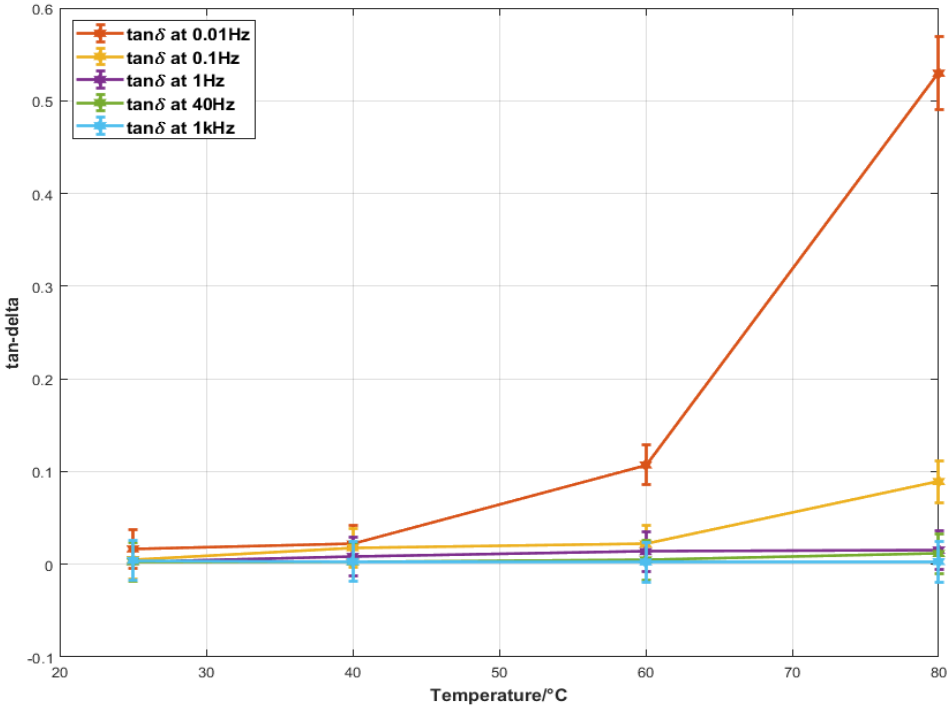

Figure 4.1: tan-delta of XLPE-RED over a wide range of frequency for increasing temperatures

Based on the trend demonstrated above, three frequencies were chosen in this case to compare the dielectric loss behaviour:

- Low-frequency region: 0.01 Hz
- Mid-frequency zone: 0.1 Hz
- High-frequency zone: 1 kHz

Figures 4.2, 4.3, 4.4, 4.5 and 4.6 show the tanδ as a function of temperature at the chosen reference frequencies, 0.01 Hz, 0.1 Hz and 1 kHz, respectively.

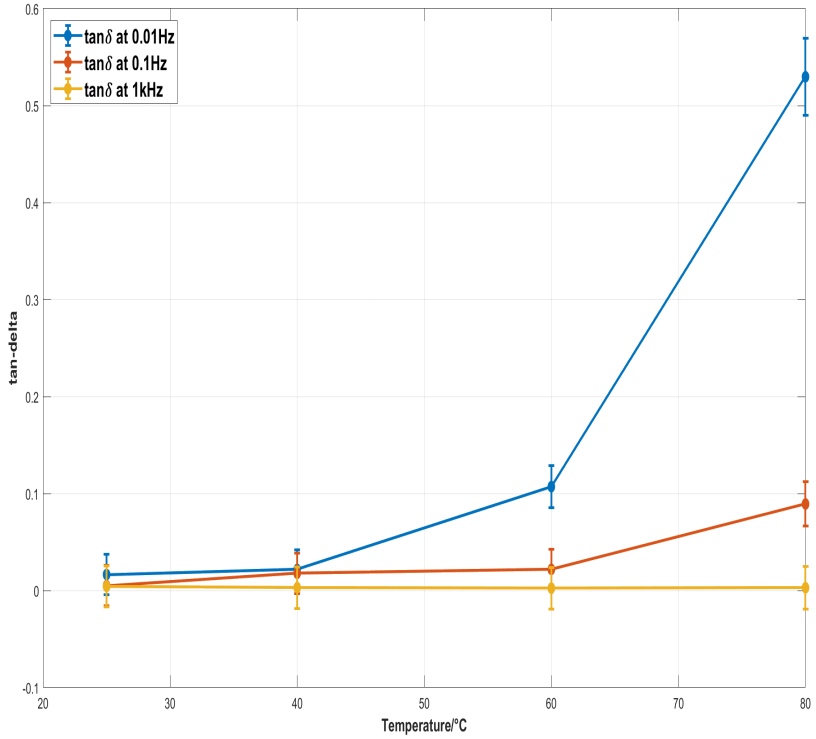

Figure 4.2: tan-delta of XLPE-RED at 0.01Hz, 0.1Hz and 1kHz

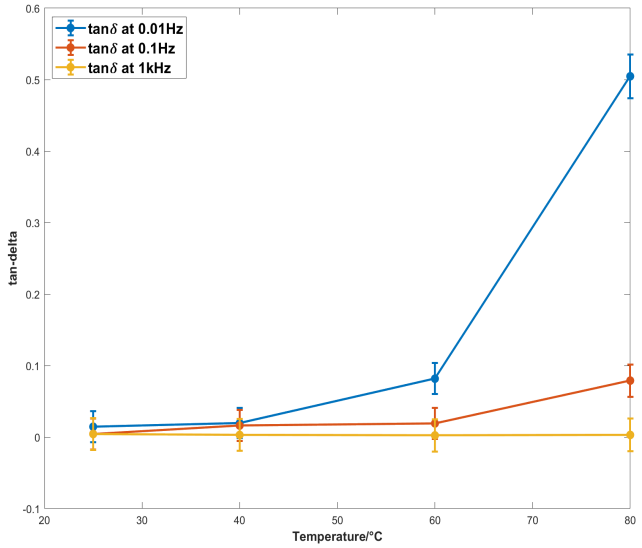

Figure 4.3: tan-delta of XLPE-GREEN at 0.01Hz, 0.1Hz and 1kHz

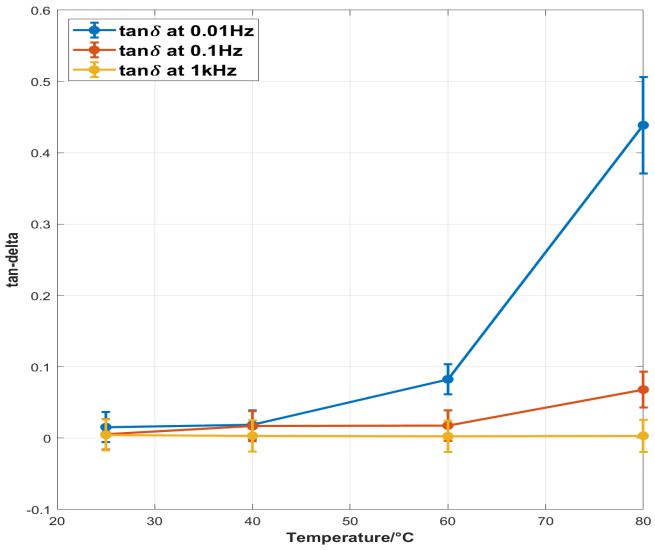

Figure 4.4: tan-delta of XLPE-WHITE at 0.01Hz, 0.1Hz and 1kHz

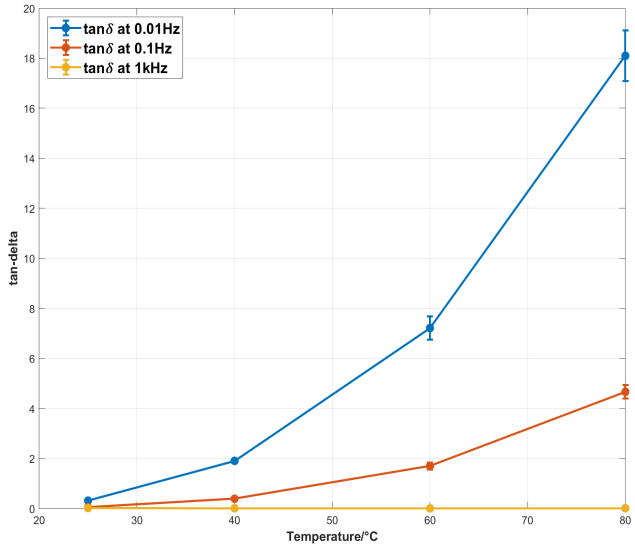

Figure 4.5: tan-delta of EPR-KER at 0.01Hz, 0.1Hz and 1kHz

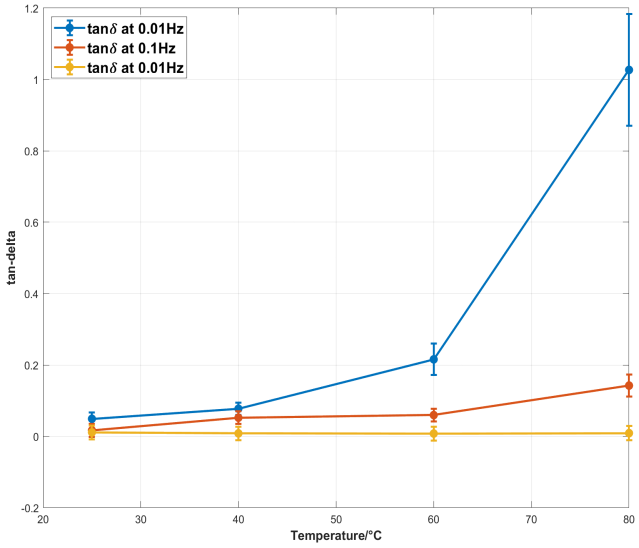

Figure 4.6: tan-delta of EPR-OKO at 0.01Hz, 0.1Hz and 1kHz

The metrics show that tanδ values at selected frequencies nearly all show an increasing trend except for that at 1000 Hz. The noted tanδ trend behavior are increased at 40°C and 60°C compared to ambient for both 0.01 and 0.1 Hz. The 80°C data also suggested a similar behavior. It should be noted that the observed trend was best defined for tanδ at lower frequencies as shown in the figures and nearly constant at the higher frequency for all the insulation types. The findings confirm that dielectric loss in the low frequency range is sensitive to temperature and rises with increasing temperature. This phenomenon could be explained by the fact that increasing temperature induces more carriers, resulting in an increase in conductivity. However, because of the low electric field frequency, carriers move slowly, accumulating near the interface between the electrode and the sample and generating electrode polarization. Because conductivity and electrode polarizability continue to rise with increasing temperature, the real and imaginary parts of the complex permittivity change more visibly with temperature, hence the changes in dielectric loss. [46] [47]

Similar to FDS results temperature dependence was noted in PDC and to better analyze changes in polarization and depolarization current and illustrate the longer time dispersion characteristics in time domain data the ratio of polarization/depolarization current over time and insulation resistance (IR) are plotted.

Figures 4.7, 4.8, 4.9, 4.10 and 4.11 shows the polarization / depolarization data ratio for each of the five specimen types. These plots also show shifts across the entire time range with increasing temperature confirming the influence of test temperature and susceptibility of current. It is noticed that the ratio of polarization-depolarization of XLPE specimens became noisy after 100s at ambient and 40°C, similar to what was observed in polarization and depolarization currents (3.2) and it is far too large to room temperature.

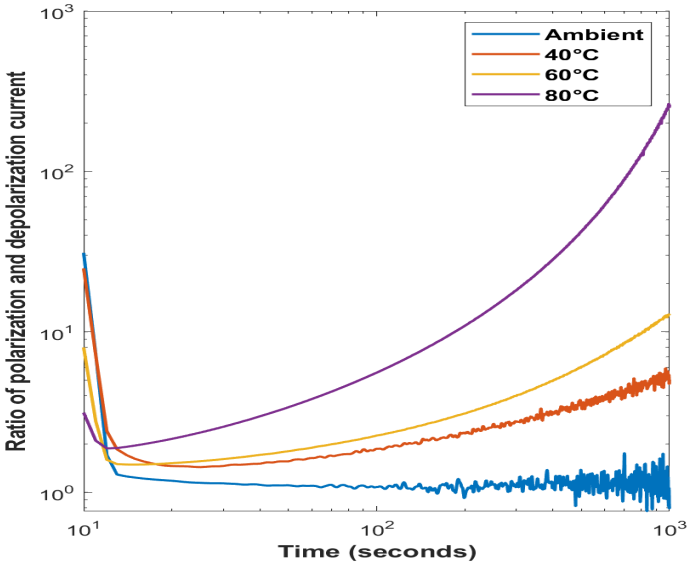

Figure 4.7: Ratio of polarization and depolarization current of XLPE-RED

Polarization current magnitude increased with temperature, as reported in Section 3.2, which is associated with current consisting of conduction and absorption current due to relaxation polarization. The conduction current increases as the temperature rises. Furthermore, as temperature rises, charge carriers migrate faster; as a result, the time required for polarization establishment decreases, and more relaxation polarization is achieved.[48]

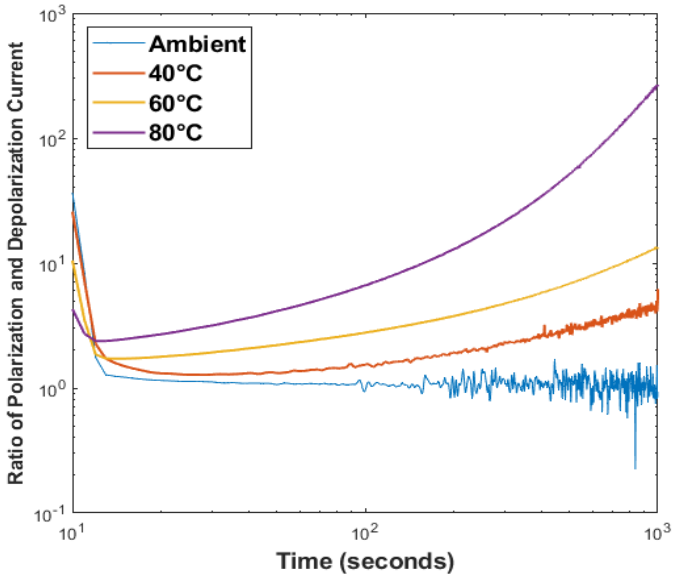

Figure 4.8: Ratio of polarization and depolarization current of XLPE-GREEN

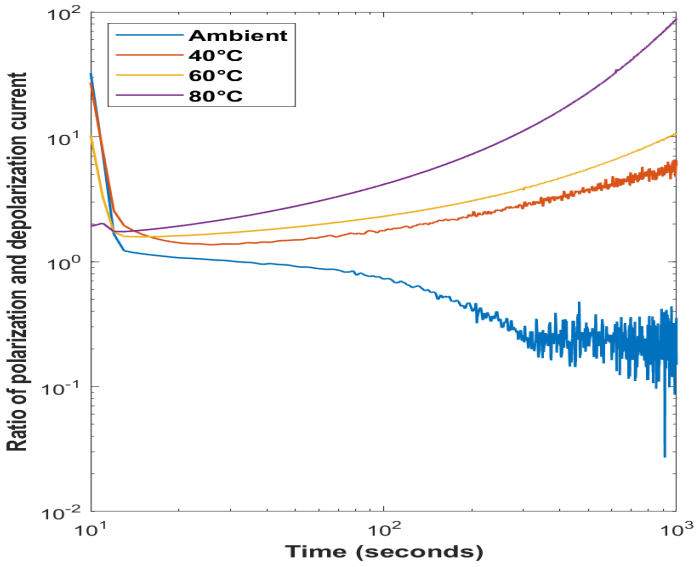

Figure 4.9: Ratio of polarization and depolarization current of XLPE-WHITE

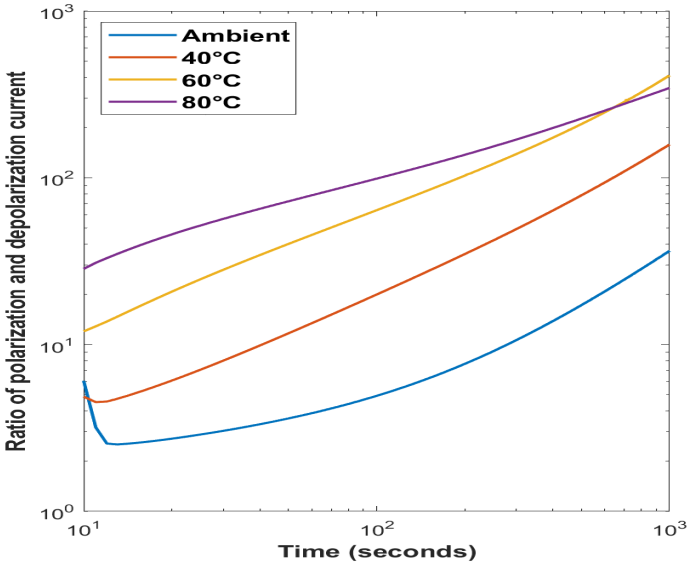

Figure 4.10: Ratio of polarization and depolarization current of EPR-KER

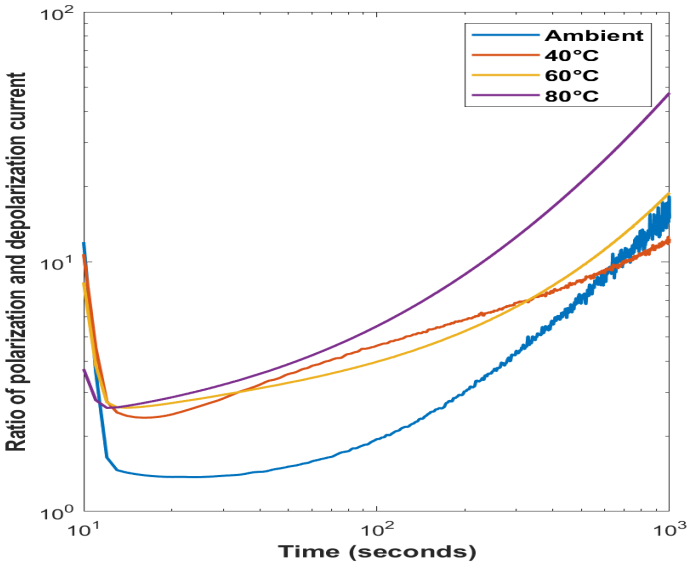

Figure 4.11: Ratio of polarization and depolarization current of EPR-OKO

Similarly, the magnitude of the depolarization current rises with temperature. In general, the polarization and depolarization currents decrease over time and eventually reach a constant value. However, as the temperature rises, the inflection point moves to a lower time, as shown by the polarization current results from 10s to 100s. The ratio of polarization and depolarization, clearly identifies the temperature dependence and lowering of the inflection point with increasing time.

IR is calculated by dividing the applied voltage (200 V) by the measured consequential current (V/ Ipol). Figures 4.7, 4.8, 4.9, 4.10 and 4.11 shows the IR data for each of the five specimen types at 60s and 600s for increasing temperature. The IR should demonstrate the opposite behavior as polarization current. In general, insulation resistance is temperature-sensitive. Insulation resistance decreases as temperature rises because as the temperature increases, the conductivity of the insulation increases, meaning a decrease in the resistance. IR at 60s and 600s for both XLPE and EPR specimens showed a decreasing trend with increasing temperature. It was also discovered that IR values at timestamps 60s and 600s converge with increasing temperature. The IR values for XLPE specimens at both timestamps are equal in magnitude at 80°C. However, there were very minor differences in the IR values at 60s and 600s across all temperatures in EPR specimens.

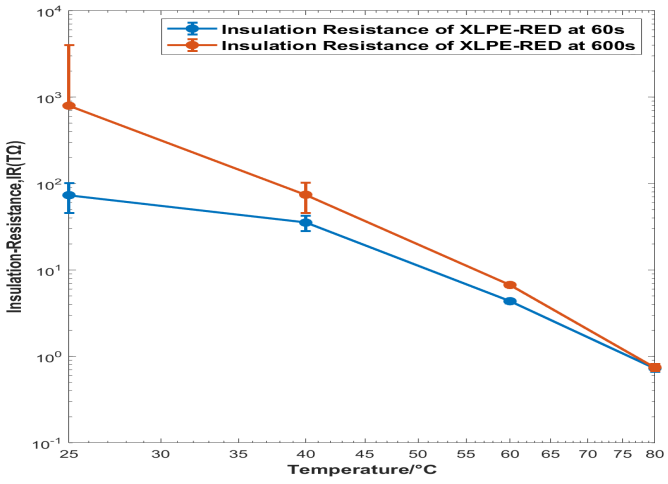

Figure 4.12: IR of XLPE-RED

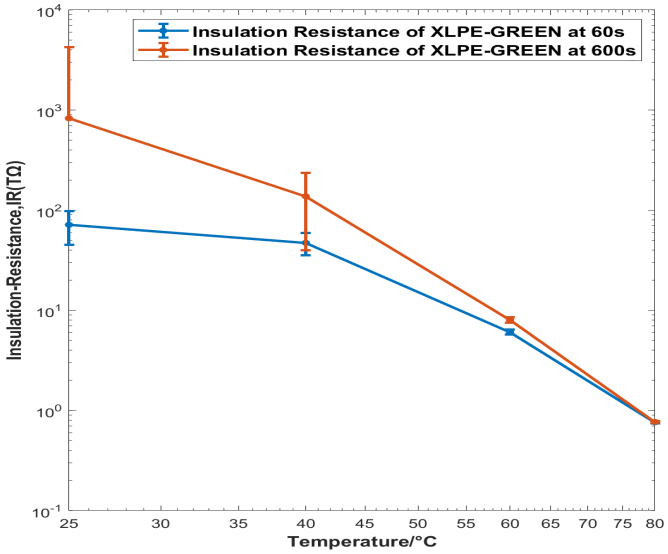

Figure 4.13: IR of XLPE-GREEN

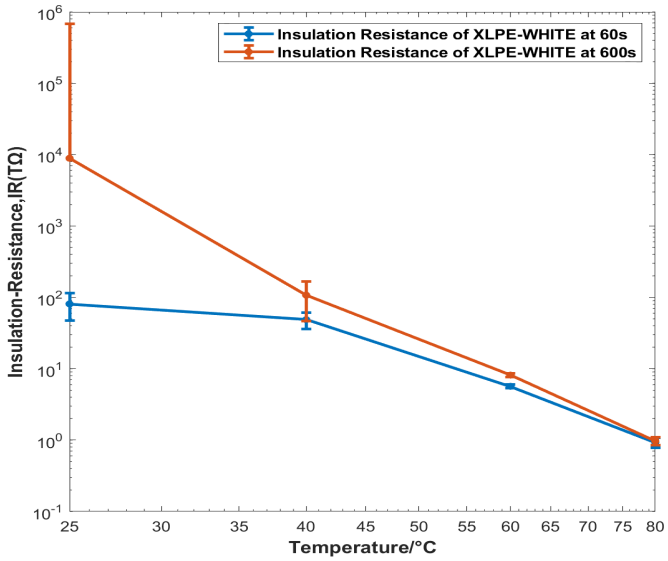

Figure 4.14: IR of XLPE-WHITE

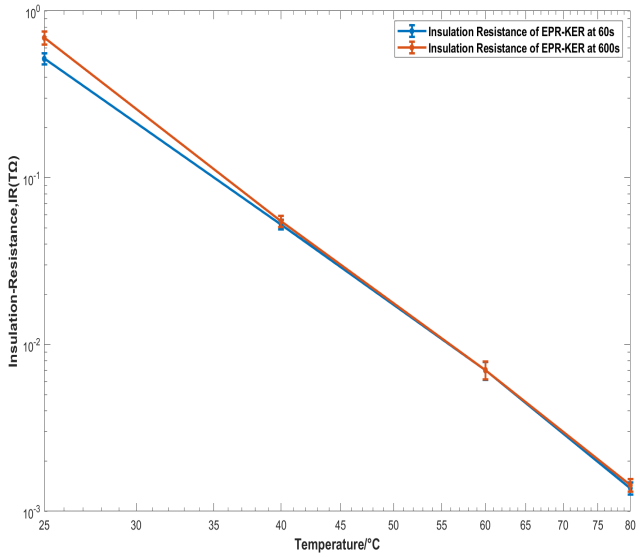

Figure 4.15: IR of EPR-KER

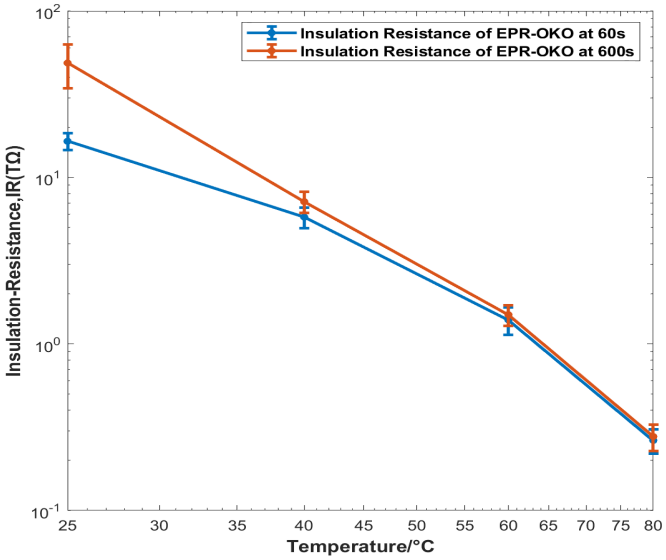

Figure 4.16: IR of EPR-OKO

4.2 Aging Effects on FDS and PDC

4.2.1 XLPE-Insulation

XLPE is a semi-crystalline polymer with linked, randomly oriented crystalline and amorphous regions. Since PE is a non-polar dielectric, its intrinsic loss is made up entirely of electron polarization and conduction loss, as well as any new polar chains or additives added during the cross-linking process. Continuous aging transforms the crystalline region into an amorphous region, which facilitates oxygen diffusion there. Chain scission processes, which are the main mechanisms of polymer chain degradation, become dominant in the amorphous area when oxygen is present. This leads to the formation of polar groups that respond to the external electric field, and an increase in the real part of permittivity is seen.[8]

Experimental results show that the change in permittivity is more pronounced at lower frequencies than at higher frequencies. A similar trend is noted in other studies as well [7] [41], which state it is related to interfacial polarization.[49] The increase in the imaginary component of permittivity with aging, particularly at lower frequencies, is due to the fact that free radicals are produced when polymers are exposed to high temperatures, as stated in [7], and they contribute to the conductivity of the material. The increase in tan-delta, particularly at lower frequencies, can be explained by the fact that dielectric loss consists of both conduction loss and relaxation loss. When the frequency decreases, the time for relaxation increases, resulting in an increase in relaxation loss.[41]

The variations observed with aging in the FDS data can be examined more closely from the tan delta values at frequencies 0.01 Hz, 0.1 Hz and 1kHz demonstrated in Fig.4.17 for **XLPE-RED**. To better understand the behaviour at the selected frequencies, the correlation coefficient for tanδ and aging hours was calculated. tanδ at 0.01 Hz had a correlation coefficient of 0.8735, indicating that tanδ at 0.01 Hz has a strong positive correlation with aging hours. This can also be seen in the plot, where as the aging hours

increased, the tanδ showed fairly an increasing trend.

At 0.1 Hz, a moderately positive correlation was deduced from the correlation coefficient of 0.5625, as can be seen in the plot that until 1200 hours of aging (interval 8) tanδ seems to be fairly consistent and then an increasing trend observed for the last two aging hours.

At 1k Hz, tanδ showed an increasing trend up to 800 hours, after which the values followed a pattern of decreasing and increasing trend for the next 4 intervals. A correlation coefficient of 0.8784 was computed.

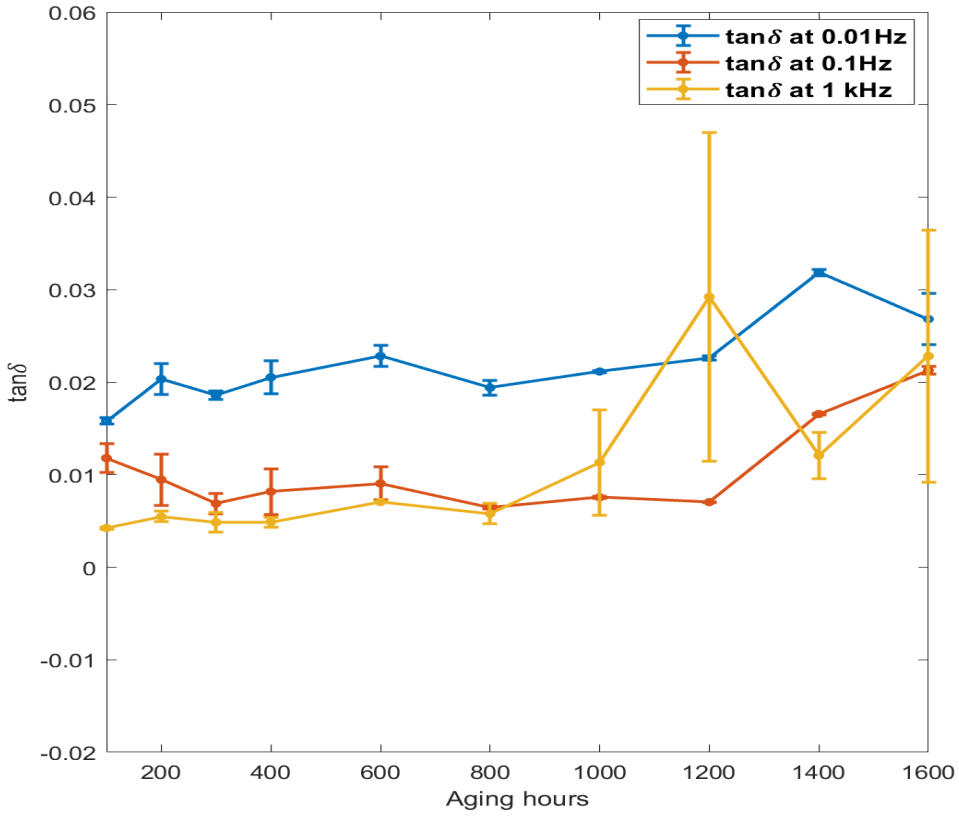

Figure 4.17: tan-delta of XLPE-RED vs. thermal aging at 0.01, 0.1 and 1000 Hz

The tan delta for **XLPE-GREEN** at frequencies of 0.01 Hz, 0.1 Hz, and 1 kHz is demonstrated in Fig.4.18. The correlation coefficient for tanδ at 0.01 Hz was 0.9464.,

indicating a strong positive correlation between tanδ at 0.01 Hz and aging hours. This can also be seen in the plot, where as the aging hours increased, the tanδ showed an overall increasing trend.

At 0.1 Hz and 1 kHz, a moderately positive correlation was deduced from the correlation coefficients of 0.6690 and 0.5165, respectively. It can be seen in the plot that starting at 800 hours of aging (interval 6), tanδ seems to demonstrate a somewhat increasing trend.

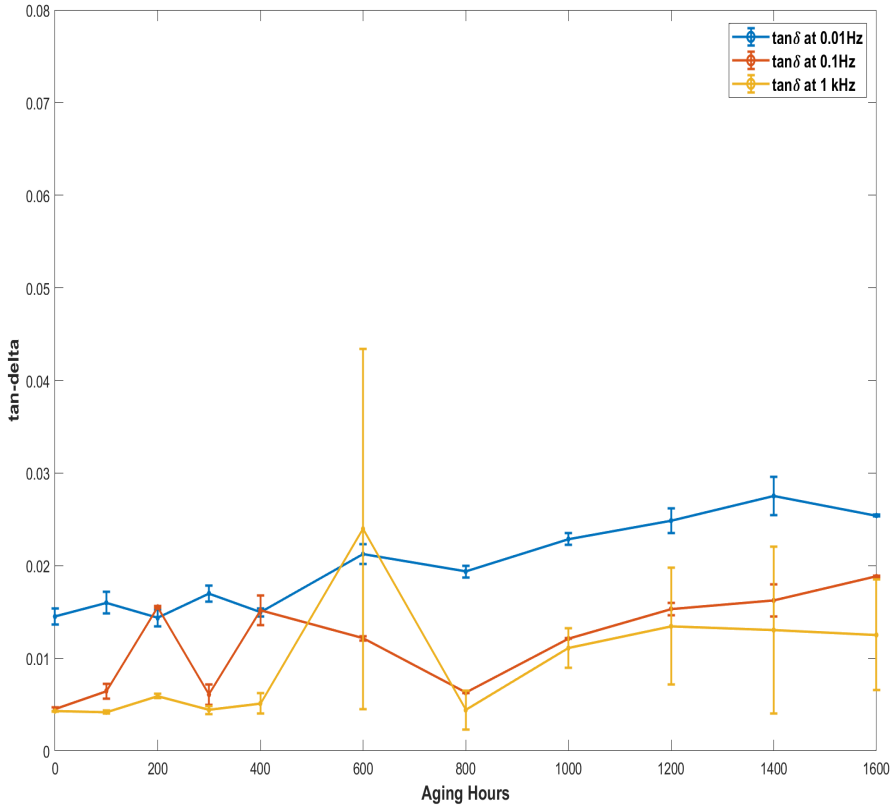

Figure 4.18: tan-delta of XLPE-GREEN vs. thermal aging at 0.01, 0.1 and 1000 Hz

The tanδ trend at frequencies 0.001 Hz, 0.01 Hz and 1kHz demonstrated in Fig.4.19 for **XLPE-WHITE** gives a closer look at how it changes with aging. The correlation coefficient of tanδ and aging hours was computed to be 0.9514 and 0.8571 respectively for 0.001 and 0.1 Hz, indicating that tanδ has a strong positive correlation with aging hours. This is also be evident in the plot, where an increasing trend can be observed. At 1 kHz, a moderately positive correlation was deduced from the correlation coefficient of 0.6470. An overall somewhat growing trend is visible with some variations in the early intervals and from 800 to 1200 hours of aging (interval 7-8).

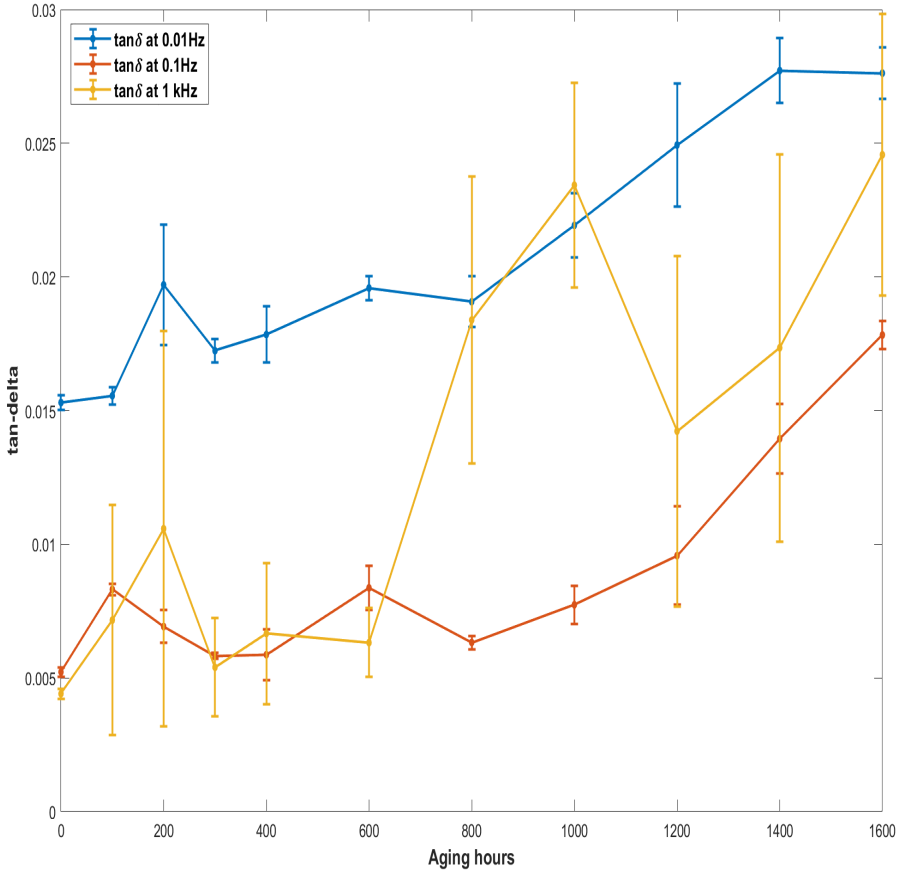

Figure 4.19: tan-delta of XLPE-WHITE vs. thermal aging at 0.01, 0.1 and 1000 Hz

There is a general tendency for polarization and depolarization currents to change more rapidly at the start which can be seen in the results (3.4). As seen in sections 3.2 and 3.4, the current is approximately separated into two parts based on the inflection point. The former section decreases rapidly and is known as the "high-frequency part," whereas the later part gradually stabilizes and is known as the "low-frequency part." Furthermore, as aging progresses, the inflection point shifts to the left, as seen in the depolarization current curves most clearly (not shown in plots in 3.4). When it reaches stability, the current value becomes relatively larger. This finding could be attributed to thermal aging, which increases the number of defects, annihilates the cross-linked structure in XLPE, and creates more charged particles and molecular groups. As a result, the discharge process is facilitated and the conductivity rises.[50]

The PDC results show that changes in insulation properties caused by thermal aging can be utilized to track aging using their characteristics, particularly the differences in polarization and depolarization responses, as well as other metrics such as polarization and depolarization ratios and insulation resistance, provides a more in-depth understanding of the underlying effects affecting the insulation.[37] [39]

The ratio of polarization/depolarization data and IR for **XLPE-RED** are provided in Figures 4.20, 4.21, and 4.22 respectively. The decaying trend is evident in the plot of the polarization to depolarization ratio as we have seen in the polarization and depolarization trends (3.4). The slight increase in the trend over aging hours noticed may be due to the fact that the conductivity increases with the time elapsed due to aging.

The IR metrics taken at 60s show an overall decreasing trend, but only a very minor change with aging. The IR exhibited almost constant behaviour at 600s.

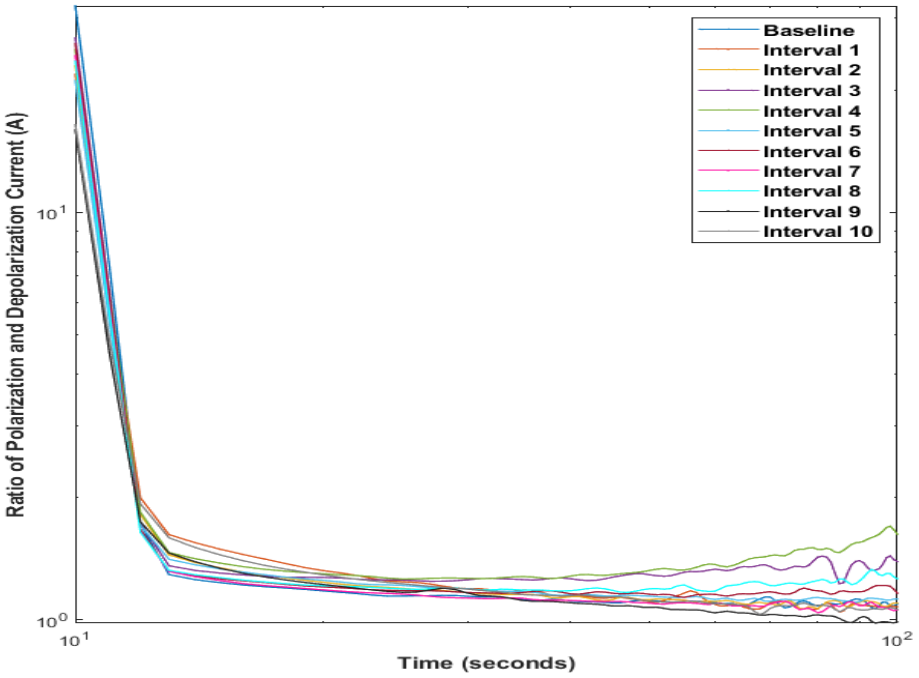

Figure 4.20: Ratio of pol/depol current of XLPE-RED for 10-100 s

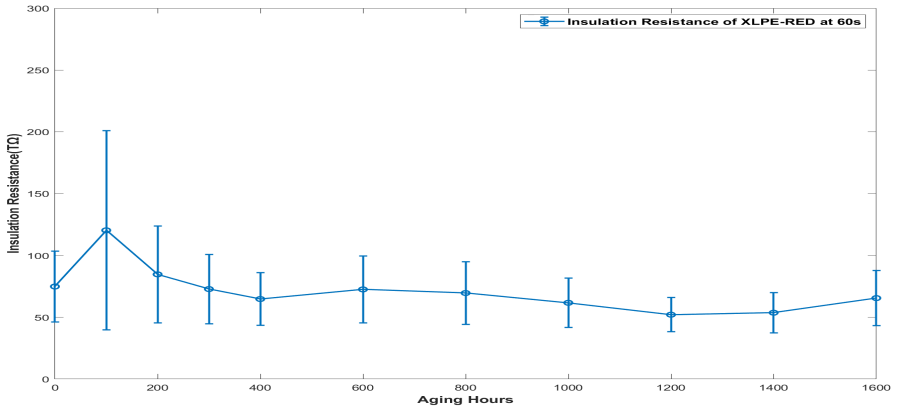

Figure 4.21: IR of XLPE-RED at 60 s

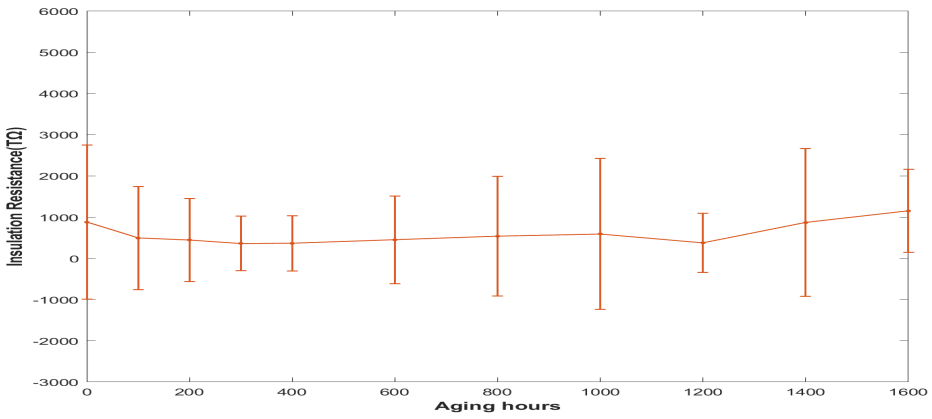

Figure 4.22: IR of XLPE-RED at 600 s

The ratio of polarization and depolarization currents of **XLPE-GREEN** is seen in Fig.4.23. Similar to FDS results, inconsistencies are observed. The ratio showed an increasing trend up to interval 4 and then a decreasing trend from interval 6 until interval 10, with interval 5 being anomalous as it dropped below interval 1 response.

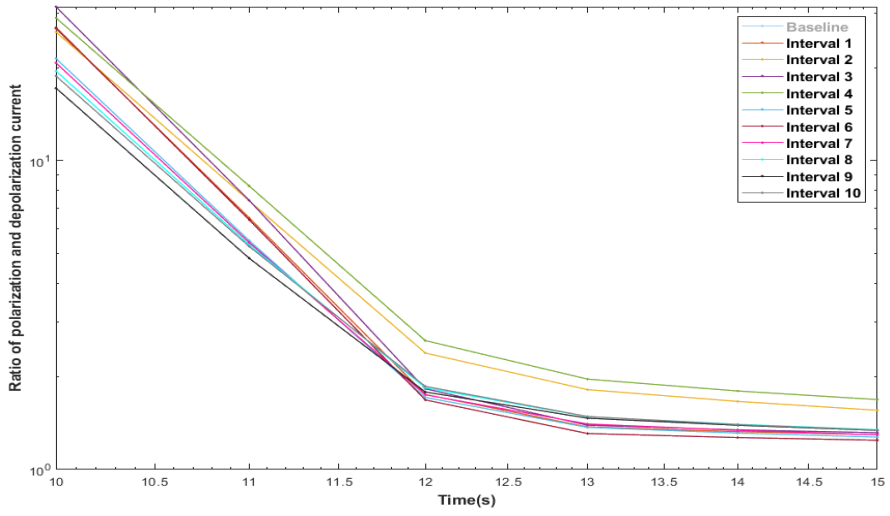

Figure 4.23: Ratio of pol/depol current of XLPE-GREEN

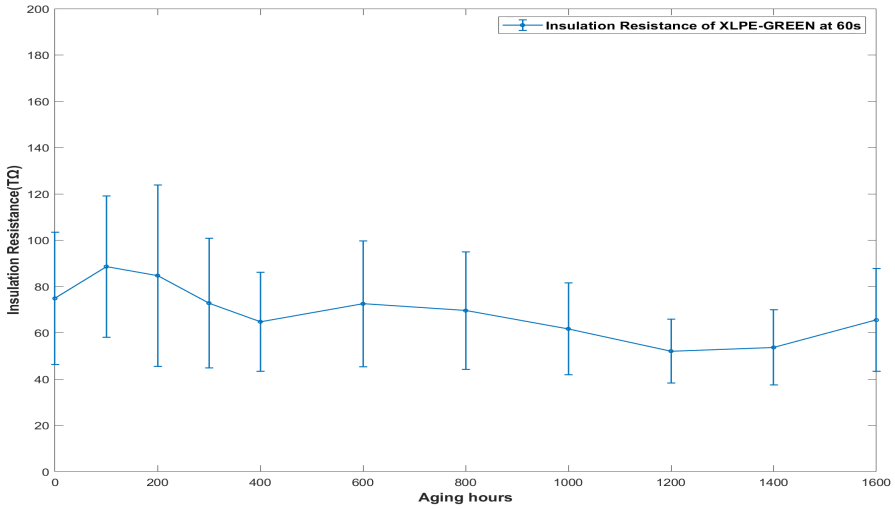

Figure 4.24: IR of XLPE-GREEN at 60s

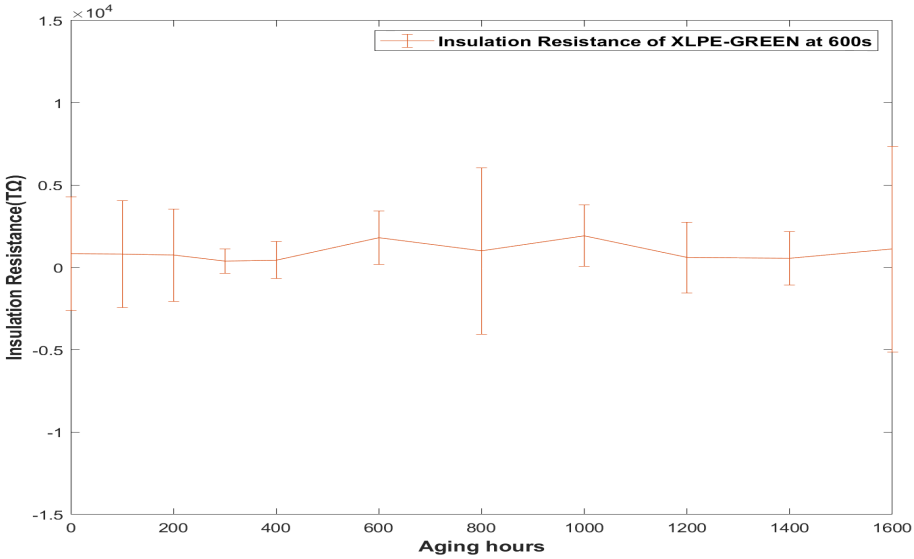

Figure 4.25: IR of XLPE-GREEN at 600s

XLPE-WHITE demonstrated a similar trend in ratio of polarization and depolarization shown in 4.26. IR metrics at 60s and 600s, as shown in Figures 4.27 and 4.28, show little change in response. At 60s, IR can be said to follow a slight decreasing trend considering the error bars.

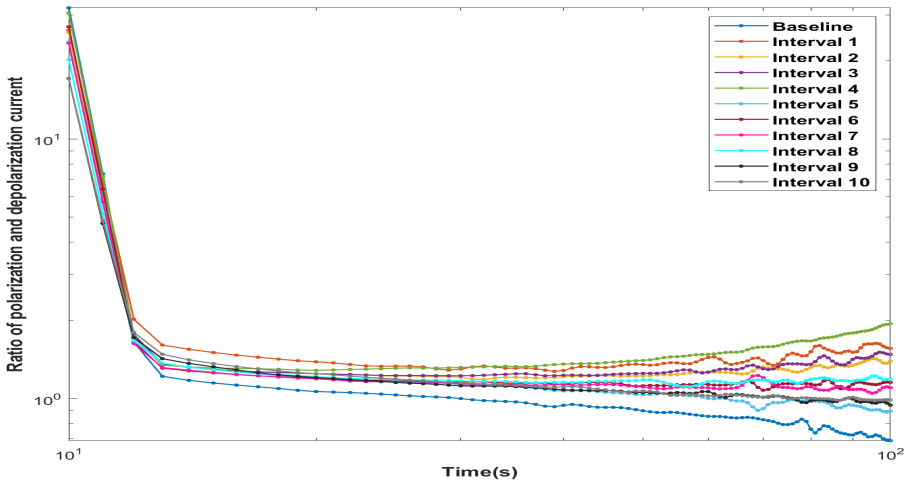

Figure 4.26: Ratio of pol/depol current of XLPE-WHITE

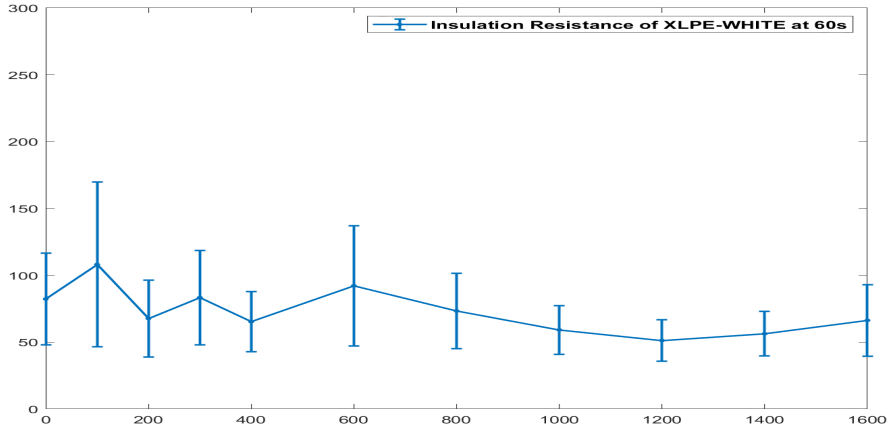

Figure 4.27: IR of XLPE-WHITE at 60s

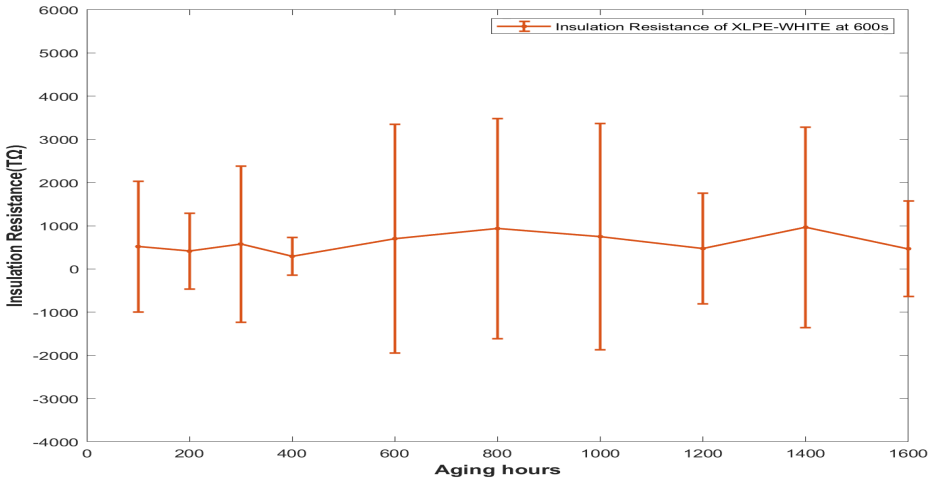

Figure 4.28: IR of XLPE-WHITE at 600s

Variations in the PDC results of the XLPE specimens may be due to differences in internal XLPE changes caused by thermal aging. Some specimens may have aged unevenly in comparison to others. Different aging processes may alter the distribution of materials that influence charge movement, such as dipole pairs and charged particles, resulting in differences in aging results.

Since the polymers are made with a variety of additives and their composition is unknown, they can have a variety of effects on the macroscopic properties of the materials. In addition, advanced analytics is required to investigate their PDC characteristics for more meaningful markers.

4.3 EPR-Insulation

EPR is a co-polymer of ethylene and propylene that has good thermal-oxidative stability due to its stable saturated main polymer chain and unsaturated side groups that promote inter-chain cross linking. As a result of this structure, inter-chain cross-linking resists degradation of a polymer main chain during thermal aging. Cross-linking processes reduce EPR permittivity, whereas chain scission increases it. [51] [52] [53] As polymer chains fragment, indicating polymer degradation and increased dipole mobility, the dissipation factor increases in value, which is evident from the experimental results in section 3.3.

Fig.4.29 shows the tanδ of **EPR-KER** as a function of the aging time at the chosen reference frequencies, 0.01 Hz, 0.1 Hz, and kHz, respectively. The property increases almost linearly with the aging time until 600 hours at frequencies of 0.01 and 0.1 Hz, followed by a decreasing trend until it saturates after 1000 hours. However, at 1 kHz, tanδ remains almost unchanged over increasing aging hours.

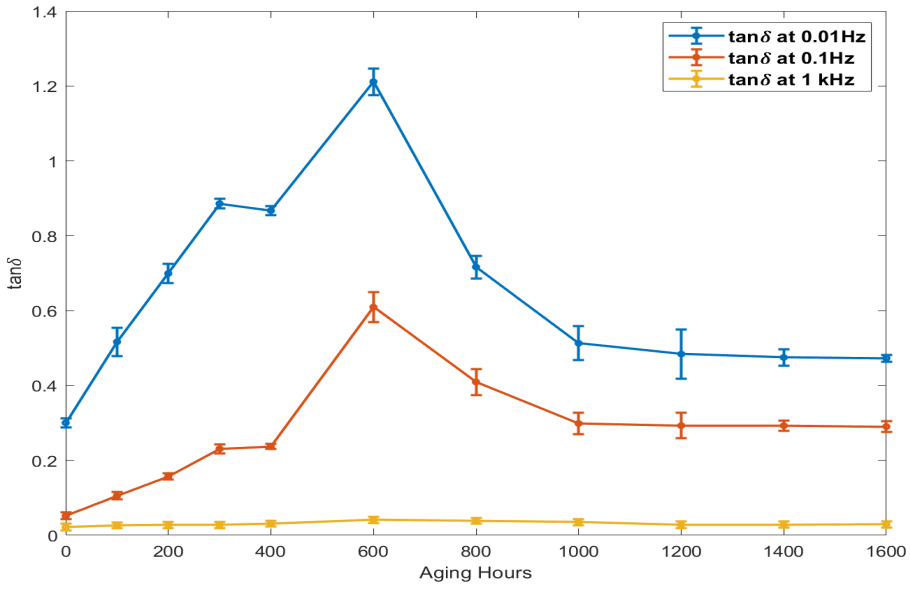

Figure 4.29: tan-delta of EPR-KER vs. thermal aging at 0.01, 0,1 and 1k Hz

EPR-OKO's tanδ trend at frequencies of 0.001 Hz, 0.01 Hz, and 1 kHz demonstrated in Fig.4.30 gives a closer look at how it changes with aging, and it is evidently seen that the response matches with C' and C" behavior. An increasing trend can be observed independent of the frequency until 1000 hours (interval 7), then dropping at 1200 hours before increasing again. The correlation coefficients of tanδ and aging hours computed (0.7426, 0.7107, and 0.8673, respectively, for 0.001, 0.1 Hz, and 1 kHz) support the increase, indicating a positive correlation.

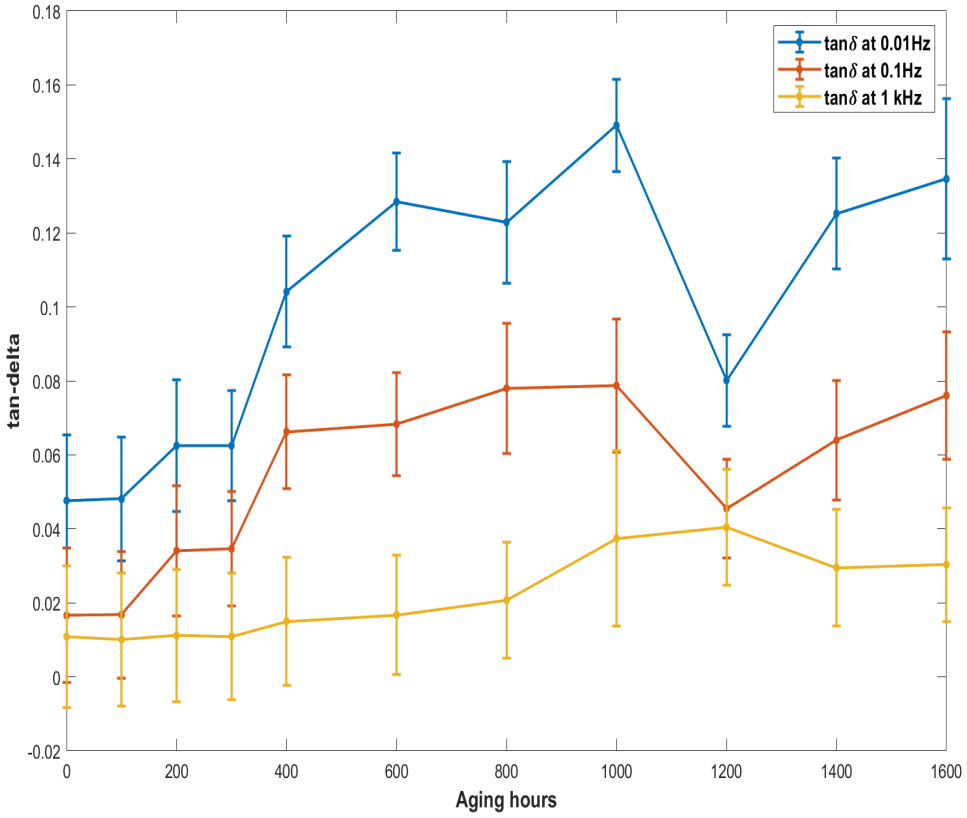

Figure 4.30: tan-delta of EPR-OKO vs. thermal aging at 0.01, 0,1 and 1k Hz

The initial significant increase in tan values for 0.01 and 0.1 Hz can be attributed to interfacial polarization, which represents the occurrence of chain scission reaction [44], which became stronger as aging times increased. According to [44], the imperfect diffusion of space charges interfacial polarization into the dielectric in the presence of an electric field. As a result, they gravitated toward the physical and chemical interfaces.

EPR-OKO showed an increase in tan-delta at 1 kHz when compared to EPR-KER. This could be due to the small voids and cracks that formed in the EPR-OKO insulation as it aged. During the aging process, they may have expanded in the presence of dipolar-natured oxygen, allowing it to penetrate the material. Because the oxygen that bonded to the radicals produced dipolar species, chain oxidation became prominent.[44]

The ratio of polarization and depolarization current of **EPR-KER** is provided in Fig.4.31. An increasing trend with aging until interval 5, and then a decreasing trend until interval 10 is seen similar to the trends noticed in its polarization and depolarization currents. The same inflection point is observed in FDS results as well.

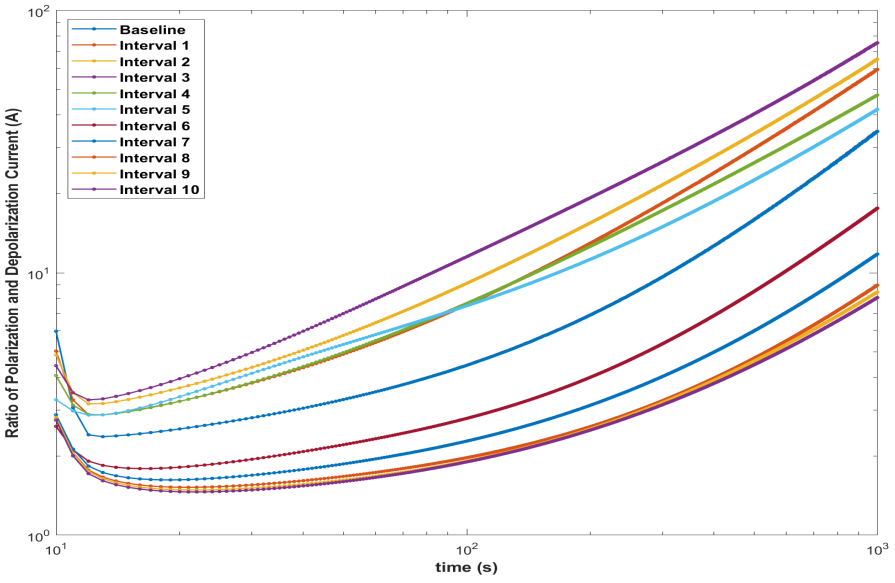

Figure 4.31: Ratio of pol/depol current of EPR-KER

The IR at 60s and 600s are provided in Fig.4.32. These plots show a decreasing trend until interval 5 and then an increasing trend until interval 10 which supports the trend pointed in polarization current.

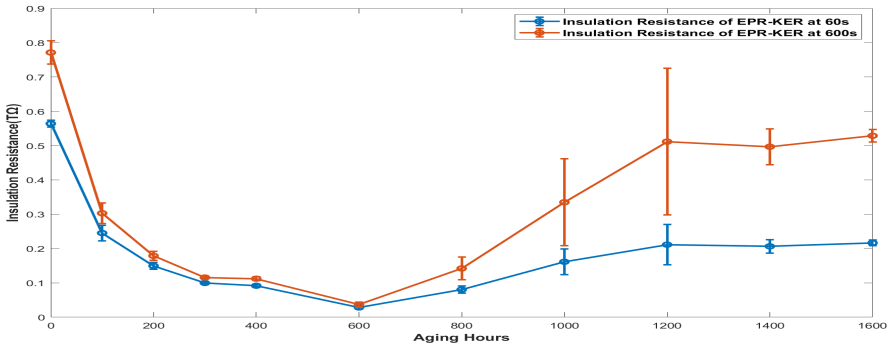

Figure 4.32: IR of EPR-KER at 60s and 600s

Similarly, an overall increasing trend is seen in the ratio of the polarization and depolarization metrics of **EPR-OKO** in Fig.4.33, although the shift can be considered to be minimal as a result of thermal aging in comparison to EPR-KER.

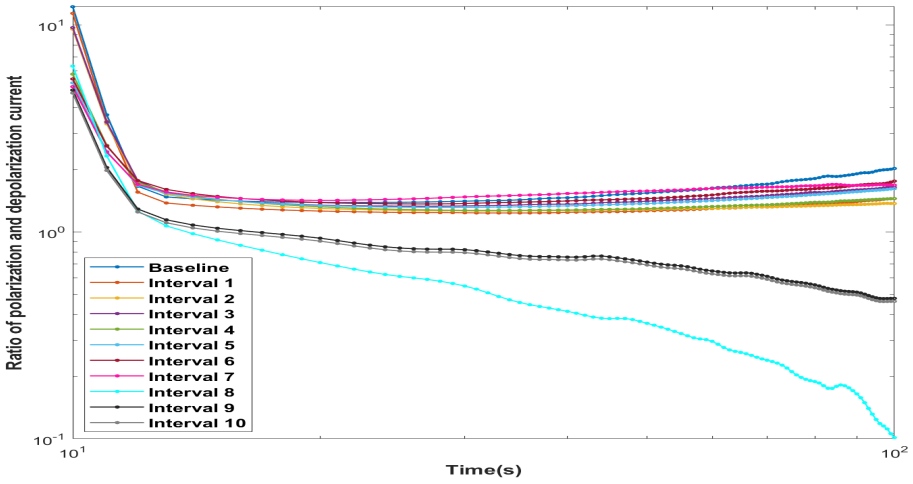

Figure 4.33: Ratio of pol/depol current of EPR-OKO

The IR at 60s and 600s, as shown in Fig.4.34 demonstrates an overall decreasing trend. It decreases until interval 7 and increased for a while at interval 8 and then follows the decreasing trend again. This aligns with the FDS results as well where the inflection point was observed too.

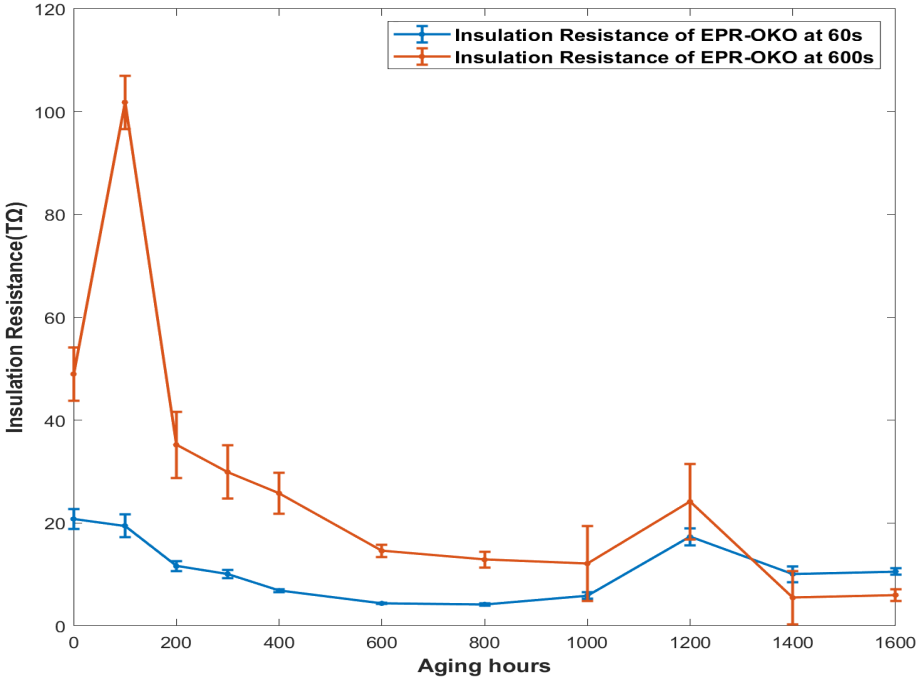

Figure 4.34: IR of EPR-OKO at 60s and 600s

As demonstrated by the results, electrical conduction effects increase, then decrease, as evidenced by an increasing trend followed by a decreasing trend in polarization current of EPR-KER.

When XLPE and EPR specimens are compared, the shifts in PDC observed in XLPE specimens are not as pronounced as a result of thermal aging as they are in EPR specimens, particularly EPR-KER.

Chapter 5

Conclusion and Future Work

Insulated low-voltage cables and their condition assessment remain a top priority, especially for the nuclear industry. This thesis focused on two distinct insulating materials, namely XLPE and EPR-based insulations which are widely used in the industry. LV cable samples were extracted and subjected to accelerated thermal aging at 130 °C in a mechanical convection oven for up to 1600 hours. Non-destructive condition monitoring techniques, dielectric spectroscopy and polarization-depolarization current measurements, were used to monitor and characterize the impact of cable aging on electrical parameters.

An effective accelerated thermal aging was achieved, as it resulted in significant changes across many measured parameters over the aging time and frequency range. Amongst properties studied, 0.01 Hz can be marked as one of the most suitable electrical aging markers as their relative variations were larger. XLPE-RED showed a good trend with respect to the hundred-hour aging interval, particularly at the lower frequency range. On the other hand, XLPE-GREEN, however, has the most inconsistent trend with respect to the hundred hours aging interval and lacks to demonstrate a definite trend. XLPE-WHITE, to quite some extent, showed a good trend with increasing aging time. EPR-KER and EPR-OKO both showed a good trend with respect to the hundred-hour aging interval. Especially EPR-KER presents a sharper and more a distinguishable trend.

In addition, a strong dependence on test temperature and behavior of dielectric properties was observed for pristine cables. Furthermore, it was clear from the experimental

results of the study that choosing a suitable reference frequency is crucial because the dielectric loss exhibited only slight aging-related fluctuations at frequencies between 50 and 60 Hz. The Arrhenius relation describes the relationship between the rate of degradation, and the aging temperature, assuming that the thermal aging mechanism decreases with temperature inverse.[6] The results show that temperature affects conductivity, and the insulation specimens exhibit Arrhenius-type temperature dependence.

In conclusion, the insulation of all XLPE specimens and EPR-KER remained visually intact throughout the aging and measurement process, while some cracks were observed on the EPR-OKO insulation samples for the last three intervals (1200, 1400, and 1600 hours). Besides that, different polymeric materials undergo different aging mechanisms, as evidenced by the XLPE and EPR specimens' distinct signature dielectric responses. An increase in the tan-delta value over the previously observed first interval of aging measurements suggested that degradation has taken place. Dielectric losses occured in both XLPE and EPR; EPR having higher losses than XLPE insulation, which was well observed in the experimental data.

It is clear that dielectric spectroscopy is a powerful method to get an insight into the aging effects on the properties of insulating materials. Due to the fact that the majority of the electrical characteristics examined in this research showed a good trend, they can be utilized to evaluate the state of the cable. The approaches have a tremendous potential to be utilized for assessing the condition of the cable and estimating its remaining life because they are nondestructive and independent of cable geometry. As insulating polymers are manufactured with a variety of additives that affect the aging mechanism and can have a variety of effects on the materials' macroscopic properties in future work, the experimental data would be studied using advanced data analytics to determine their true relationship and produce an association to evaluate the estimated remaining and absolute physical life spans for cables by evaluating "Arrhenius" relationships. Physiochemical tests on the same aged samples can be performed to corroborate the electrical property variation along with FDS and PDC measurements conducted at various temperatures, which may help obtain more insights in the PDC variations.

References

[1] M. Schmid, A. Ritter, and S. Affolter. *Determination of oxidation induction time and temperature bY DSC.* Journal of Thermal Analysis and Calorimetry, 2006.

[2] F.B. Meng, W.D. Li, A.X. Zhao, L.S. Cao, J.B. Deng, G.J. Zhang, Y.J. Zhi, and L.M. Zhang. *Development of time and Frequency Domain dielectric response testing device for power apparatus insulation.* 2016 International Conference on Condition Monitoring and Diagnosis (CMD), 2016.

[3] A. Gorji. *Sample Preparation Guideline for Low Voltage (LV) Cables used in Single-Core Enclosure Box.* 2021.

[4] World-nuclear.org. *World Energy Needs and Nuclear Power — Energy Needs — Nuclear Energy meeting Energy Needs - World Nuclear Association.* https://www.world-nuclear.org/information-library/current-and-future-generation/world-energy-needs-and-nuclear-power.aspx, 2022.

[5] U.S. Energy Information Administration EIA. *Nuclear power and the environment.* https://www.eia.gov/energyexplained/nuclear/nuclear-power-and-the-environment.php#:~:text=Nuclear%20energy%20produces%20radioactive%20waste,health%20for%20thousands%20of%20years.

[6] INTERNATIONAL ATOMIC ENERGY AGENCY. *Assessment and Management of Ageing of Major Nuclear Power Plant Components Important to Safety: In-containment Instrumentation and Control cables. Volume II.* IAEA, 2000.

[7] R. S. A. Afia, M. Ehtasham, and Z. A. Tamus. *"Electrical and Mechanical Condition Assessment of Low Voltage Unshielded Nuclear Power Cables Under Simultaneous Thermal and Mechanical Stresses: Application of Non-Destructive Test Techniques.* IEEE Access, vol. 9, pp. 4531–4541, Jan. 2021., 2021.

[8] E. Mustafa, R. S. A. Afia, and Z. A. Tamus. *""Application of Non-Destructive Condition Monitoring Techniques on Irradiated Low Voltage Unshielded Nuclear Power Cables.* IEEE Access, vol. 8, pp. 166024–166033, Sep. 2020., 2020.

[9] L. Verardi, D. Fabiani, and G. C. Montanari. *Correlation of electrical and mechanical properties in accelerated aging of LV nuclear power plant cables.* 2014 ICHVE International Conference on High Voltage Engineering and Application, 2014, pp. 1-4, 2014.

[10] Foro Nuclear. *Nuclear Power in the World.* https://www.foronuclear.org/en/nuclear-power/nuclear-power-in-the-world/, 2022.

[11] G. Harmon, T. Toll, and C. Sexton. *Development And Implementation Of An In-Situ Cable Condition Monitoring Method For Nuclear Power Plants.* 2020 IEEE Electrical Insulation Conference (EIC), 2020.

[12] T. Toll, P. Ward, C. Ferree, C. Sexton, and G. Harmon. *Application of Cable Condition Monitoring Technologies to Assess Age-Related Degradation of Industrial Cables Installed in Harsh Environments.* Nuclear Technology, vol. 207, no. 12, pp. 1889–1901, 2021.

[13] E. Linde, L. Verardi, P. Pourmand, D. Fabiani, and U. W. Gedde. *Non-destructive condition monitoring of aged ethylene-propylene copolymer cable insulation samples using dielectric spectroscopy and NMR spectroscopy.* Sep. 2015, Polymer Testing, vol. 46, no. Complete, pp. 72–78.

[14] S. V. Suraci and D. Fabiani. *Aging Modeling of Low-Voltage Cables Subjected to Radio-Chemical Aging.* IEEE Access, vol. 9, pp. 83569–83578, Jun. 2021.

[15] W. S. Zaengl. *Applications of dielectric spectroscopy in time and frequency domain for HV power equipment.* IEEE Electrical Insulation Magazine, 2003.

[16] J. M. Braun. *Condition assessment of unshielded aged power and control cables by electrical techniques.* IEEE Electrical Insulation Magazine, 1992.

[17] R. S. A. Afia, E. Mustafa, and Z. Á. Tamus. *Aging Mechanisms and Non-Destructive Aging Indicators of XLPE/CSPE Unshielded LV Nuclear Power Cables Subjected to Simultaneous Radiation-Mechanical Aging.* Polymers, 2021.

[18] F. Carpentier and M. Cornaton. *Radio-Oxidation Aging of XLPE Containing Different Additives and Filler: Effect on the Gases Emission and Consumption.* Polymers, 2021.

[19] Maléchaux A, Colombani J, Amat S, and Dupuy N Marque SRA. *Influence of Gamma Irradiation on Electric Cables Models: Study of Additive Effects by Mid-Infrared Spectroscopy.* Polymers, 2021.

[20] S. V. Suraci, D. Fabiani, A. Xu, S. Roland, and X. Colin. *Aging Assessment of XLPE LV Cables for Nuclear Applications Through Physico-Chemical and Electrical Measurements.* IEEE Access, 2020.

[21] INTERNATIONAL ATOMIC ENERGY AGENCY. *Pilot Study on the Management of Ageing of Instrumentation and Control Cables.* IAEA, 1997.

[22] R. M. Eichhorn. *A Critical Comparison of XLPE-and EPR for Use as Electrical Insulation on Underground Power Cables.* IEEE Transactions on Electrical Insulation, 1981.

[23] D. He, J. Gu, W. Wang, S. Liu, S. Song, and D. Yi. *Research on mechanical and dielectric properties of XLPE cable under accelerated electrical-thermal aging.* Polymers for Advanced Technologies, 2017.

[24] Z. Liu, J. Hao, R. Liao, Z. Gao J. Li, and Z. Liang. *Morphological, Structural, and Dielectric Properties of Thermally Aged AC 500 kV XLPE Submarine Cable Insulation Material and Its Deterioration Condition Assessment.* IEEE Access, 2019.

[25] SpecialChem. *Oxidation Induction Time.* https://polymer-additives.specialchem.com/centers/antioxidants-to-prevent-polymer-oxidation/oxidation-induction-time.

[26] B. Bartoníček, V. Hnát, and V. Plaček. *Aging Monitoring of Plastics Used in Nuclear Power Plants by DSC*. Journal of Thermal Analysis and Calorimetry, 2001.

[27] B. Bartoníček, V. Hnát, and V. Plaček. *Life-assessment technique for nuclear power plant cables*. Radiation Physics and Chemistry, 1998.

[28] Qicomposites. *FTIR Non Destructive Analysis – QIcomposites*. https://www.qicomposites.com/servizi/analisi-non-distruttive-ftir/?lang=en.

[29] A. Melo Nobrega, M. L. Barreira Martinez, and A. A. Alencar de Queiroz. *Investigation and analysis of electrical aging of XLPE insulation for medium voltage covered conductors manufactured in Brazil*. IEEE Transactions on Dielectrics and Electrical Insulation, 2013.

[30] F.-B. Meng, X. Chen, C. Dai, A. Paramane M. Zhang, L. Zheng, and Y. Tanaka. *Effect of Thermal Aging on Physico-Chemical and Electrical Properties of EHVDC XLPE Cable Insulation*. IEEE Transactions on Dielectrics and Electrical Insulation, 2021.

[31] INTERNATIONAL ATOMIC ENERGY AGENCY. *Assessing and Managing Cable Ageing in Nuclear Power Plants*. https://www.iaea.org/publications/8753/assessing-and-managing-cable-ageing-in-nuclear-power-plants, 2012.

[32] D. He, T. Zhang, M. Ma, W. Gong, W. Wang, and Q. Li. *Research on Mechanical, Physicochemical and Electrical Properties of XLPE-Insulated Cables under Electrical-Thermal Aging*. Journal of Nanomaterials, 2020.

[33] W. Wang and T. Guo. *Space Charge Accumulation Characteristics in HVDC Cable under Temperature Gradient*. Energies, 2020.

[34] G. C. Montanari. *Dielectric material properties investigated through space charge measurements*. IEEE Transactions on Dielectrics and Electrical Insulation, 2004.

[35] G. C. Montanari. *Relation between space charge and polymeric insulation Aging: cause and effect*. IEE Proceedings - Science, Measurement and Technology, 2003.

[36] U. Gafvert, L. Adeen, M. Tapper, P. Ghasemi, and B. Jonsson. *Dielectric spectroscopy in time and frequency domain applied to diagnostics of power transformers*. Proceedings of the 6th International Conference on Properties and Applications of Dielectric Materials, 2000.

[37] W. Li, X. Zhang, A. Zhao, L. Wu, Z. Ren, J. Deng, and G. Zhang. *Studies of the polarization/depolarization current characteristics of XLPE cable*. 2016 IEEE PES Asia-Pacific Power and Energy Engineering Conference (APPEEC), 2016.

[38] M. A. Dakka, A. Bulinski, and S. S. Bamji. *On-site diagnostics of medium-voltage underground cross-linked polyethylene cables*. IEEE Electrical Insulation Magazine, 2011.

[39] G. Ye, H. Li, F. Lin, J. Tong, X. Wu, and Z. Huang. *Condition assessment of XLPE insulated cables based on polarization/depolarization current method*. IEEE Transactions on Dielectrics and Electrical Insulation, 2016.

[40] A. Zhao, Y. Wang, X. Zhang, J. Deng, G. Zhang, S. Tao, and L. Wu. *Insulation status diagnosis of XLPE cable based on polarization and depolarization current (PDC)*. 2015 IEEE PES Asia-Pacific Power and Energy Engineering Conference (APPEEC), 2015.

[41] J. Liu, Y. Xu, X. Wei, and X. Li. *Research of Dielectric spectroscopy on insulation Aging assessment of XLPE cables*. 2013 Annual Report Conference on Electrical Insulation and Dielectric Phenomena, 2013.

[42] Y. Wang, A. Zhao, X. Zhang, Y. Shen, F. Yang, J. Deng, and G. Zhang. *Study of dielectric response characteristics for thermal aging of XLPE cable insulation*. 2016 International Conference on Condition Monitoring and Diagnosis (CMD), 2016.

[43] M. Celina, E. Linde, D. Brunson, A. Quintana, and N. Giron. *Overview of accelerated aging and polymer degradation kinetics for combined radiation-thermal environments*. Polymer Degradation and Stability, 2019.

[44] E. Mustafa, R. S. A. Afia, O. Nouini, and Z. Á.Tamus. *Implementation of Non-Destructive Condition Monitoring Techniques on Low-Voltage Nuclear Cables: II. Thermal Aging of EPR/CSPE Cables*. Energies, 2022.

[45] M. Anglhuber, F. Kaufmann, S. Knuetter, and O.Ried. *MINIMIZING DIELECTRIC TESTING TIME*. Semantic Scholar, 2017.

[46] Y. Du, P. Geng, J. Song, M. Tian, and D. Pang. *Influence of temperature and frequency on leakage current of XLPE cable insulation*. 2016 IEEE International Conference on High Voltage Engineering and Application (ICHVE), 2016.

[47] Z. Lei, J. Song, P. Geng, M. Tian, L. Lin, C. Xu, C. Feng, J. Zeng, and Z. Li. *Influence of temperature on dielectric properties of EPR and partial discharge behavior of spherical cavity in EPR insulation*. IEEE Transactions on Dielectrics and Electrical Insulation, 2015.

[48] Z. Ma, R. Liao, X. Zhao, Y. Wang, and L. Yang. *Influence of temperature on polarization and depolarization current of oil-paper insulation*. 2012 International Conference on High Voltage Engineering and Application, 2012.

[49] Y. Gao and B. X. Du. *Effect of gamma-ray irradiation on permittivity and dielectric loss of polymer insulating materials*. IEEE, 2012.

[50] Y. Zhang, G. Gu, J. Liu, F. Jiang, Y. Fan Y, and J. Zha. *Evaluation of Non-Uniform Thermal Aging of XLPE Cable Based on Modified Debye Model*. Frontiers in Materials, 2022.

[51] OMICRON. *Dirana*. https://www.omicronenergy.com/en/products/dirana/.

[52] D. Bouguedad, A. Mekhaldi, and O. Jbara A. Boubakeur. *Thermal ageing effects on the properties of ethylene-propylene-diene monomer (EPDM)*. Scopus, 2018.

[53] A. Sriraman, N. Bowler, S.W. Glass, and L.S. Fifield. *Dielectric and Mechanical Behavior of Thermally Aged EPR/CPE Cable Materials*. IEEE, 2018.